

Expression and Analysis of Ricin A Chain in *Saccharomyces cerevisiae*

by

MARIANNE MICHELLE BARICEVIC

A Dissertation submitted to the

Graduate School-New Brunswick

Rutgers, The State University of New Jersey

in partial fulfillment of the requirements

for the degree of

Doctor of Philosophy

Graduate Program in Microbiology and Molecular Genetics

written under the direction of

Nilgun Tumer

and approved by

New Brunswick, New Jersey

[May, 2008]

ABSTRACT OF THE DISSERTATION

Expression and Analysis of Ricin A Chain in *Saccharomyces cerevisiae*

By MARIANNE MICHELLE BARICEVIC

Dissertation Director:

Nilgun Tumer

Ricin is a ribosome inactivating protein (RIP) isolated from *ricinus communis*, the castor bean plant. RIPs catalytically depurinate an adenine residue from the highly conserved sarcin/ricin loop in the large ribosomal RNA subunit, rendering the ribosome unable to translate protein. Due to its potential use as a bioweapon, understanding how ricin gains access to and depurinates ribosomes is of high importance. There is currently no approved vaccine or treatment for ricin intoxication. Learning the residues that are critical for ricin toxicity and enzymatic activity may help to generate a potential vaccine for ricin exposure. Here, I describe an analysis of ricin A chain (RTA), the enzymatic subunit of ricin, in *Saccharomyces cerevisiae*. The results provide evidence that ricin cytotoxicity is not necessarily a result of ribosome depurination and translation inhibition, ricin utilizes components of the ER Association Degradation (ERAD) pathway to reach the cytosol from the ER and the C-terminus of RTA is essential for enzymatic activity and protein translocation across the ER membrane.

ACKNOWLEDGEMENTS

I would like to express my sincere gratitude to the people who have helped make this thesis possible. First, I would like to thank my adviser and mentor, Dr. Nilgun Tumer, who was willing to train me as an undergraduate and helped propagate my interest in molecular genetics. She has been an inspirational role model and has taught me that commitment and focus will take you far in the world of scientific research. I would also like to thank past and present members of the Tumer lab. Rong Di has been a wealth of knowledge and support. She has helped me throughout my graduate career technically, analytically and emotionally. Andrew Tortora has been extremely instrumental with technical help, and Xiao-Ping Li was essential for the generation and analysis of the random mutations discussed in Chapter 2. I would also like to acknowledge Dr. Katalin Hudak, who taught me many of the assays used in this thesis. Dr. Wendie Cohick has provided support and suggestions for my thesis and career path, and the opportunity to collaborate with her and her lab members has helped to expand my scientific knowledge and understanding.

I must thank Dr. Kathleen Scott and Susan Coletta who provided me with NSF funding for 3 years as a GK-12 fellow. The opportunity they gave me showed me that science education can be just as rewarding as scientific research. I am also especially grateful for my thesis committee, who were honest and helpful with their suggestions and constant support.

Finally, I would like to thank my friends, family and especially my parents, who have supported me through the bad and good times during my graduate career. Without their constant encouragement and love, this thesis would not be complete.

Table of Contents

Abstract.....	ii
Acknowledgements.....	iii
Table of Contents.....	iv
List of Tables.....	v
List of Figures.....	vi
Chapter 1: Introduction.....	1
Chapter 2: Ribosome depurination is not sufficient for ricin-mediated cell death in <i>Saccharomyces cerevisiae</i>	18
Chapter 3: Ricin A chain utilizes the ERAD machinery to reach the cytosol.....	36
Chapter 4: Mutations in the C-terminal hydrophobic stretch of ricin A chain inhibit retro-translocation without reducing the catalytic activity.....	57
Chapter 5: Conclusions.....	78
Materials and Methods.....	83
References.....	87
Curriculum Vitae.....	93

List of Tables

Table 2.1: Characterization of pre-RTA mutants obtained by random mutagenesis.....	21
Table 4.1: Characterizations of pre-RTA and RTA point mutations.....	60
Table 4.2: The location of the C-terminal pre-RTA mutations.....	61
Table 4.3: The location of the C-terminal RTA mutations.....	65

List of Figures

Figure 1.1: Linear schematic of the three types of RIPs.....	2
Figure 1.2: The backbone structures of RTA and PAP.....	3
Figure 1.3: The 28S ribosome indicating the location of the sarcin/ricin loop (SRL), ribosomal protein L3 (L3) and elongation factor G (EFG).....	7
Figure 1.4: A. The site of depurination in the SRL, and B. the structural model of the active site of PAP and RTA with adenine.....	8
Figure 1.5: Yeast cells expressing RTA are not viable.....	15
Figure 1.6: Analysis of rRNA depurination of RTA and pre-RTA.....	15
Figure 1.7: 0.1 µg of RTA is sufficient to depurinate animal ribosomes.....	16
Figure 2.1: The pre-RTA mutants are expressed in yeast.....	20
Figure 2.2: Viability of cells expressing pre-RTA and the mutant forms of RTA.....	24
Figure 2.3: Ribosome Depurination in yeast expressing pre-RTA and the mutant forms <i>in vivo</i>	26
Figure 2.4: Ribosome depurination by pre-RTA and mutants <i>in vitro</i>	27
Figure 2.5: Three-dimensional structure of mature RTA showing the positions of the point mutations and the α -helices and β -sheets that contain these mutations.....	31
Figure 3.1: The Sec61-32 and Sec61-41 yeast mutants reduce the cytotoxicity of pre- RTA.....	39
Figure 3.2: Sec61-32 and Sec61-41 yeast expressing pre-RTA are viable compared to wildtype yeast.....	40
Figure 3.3: Pre-RTA is stabilized in Sec61-32 and Sec61-41.....	41
Figure 3.4: RTA is not stabilized in Sec61-32 and Sec61-42.....	42
Figure 3.5: Pre-RTA ribosome depurination is reduced in Sec61-32.....	43
Figure 3.6: Kar-2 yeast mutants are more viable than wildtype yeast when expressing pre-RTA.....	44

Figure 3.7: The expression pattern of pre-RTA and pre-RTAE177K is altered in Kar-2 yeast mutants.....	45
Figure 3.8: Pre-RTA can still depurinate Kar2-1 ribosomes.....	46
Figure 3.9: Pre-RTA is stabilized in the Ubc7 mutant.....	47
Figure 3.10: RAD23 yeast mutants expressing pre-RTA are viable.....	48
Figure 3.11: Pre-RTA expression is reduced in the RAD23 mutant.....	49
Figure 3.12: Pre-RTA depurination is reduced in RAD23 yeast mutants.....	50
Figure 3.13: Pre-RTA is still toxic in the proteasome mutant.....	51
Figure 3.14: Pre-RTA _{E177K} is stabilized in the proteasome mutant.....	51
Figure 4.1: Structural comparison and sequence alignment of Shiga-toxin 2 (STX2), Pokeweed Antiviral Protein (PAP) and Ricin A chain (RTA).....	58
Figure 4.2: Viability analysis of pre-RTA C-terminal deletion and point mutations.....	61
Figure 4.3: Immunoblot analysis of pre-RTA expression.....	62
Figure 4.4 Ribosome depurination in yeast expressing pre-RTA and the mutant forms..	63
Figure 4.5: Pre-RTA mutants that don't depurinate ribosomes can translate protein.....	64
Figure 4.6: Viability analysis of mature RTA C-terminal deletion and point mutations..	66
Figure 4.7: Immunoblot analysis of mature RTA expression.....	66
Figure 4.8: Ribosome depurination in yeast expressing RTA and the mutant forms.....	67
Figure 4.9: Translation inhibition of RTA and the mutant forms.....	67
Figure 4.10: A structural comparison of the C-terminal residues of RTA.....	69
Figure 4.11: A direct comparison of the deletion mutants in pre-RTA and RTA.....	72
Figure 4.12: A direct comparison of the point mutants in pre-RTA and RTA.....	74
Figure 5.1: Model for ricin induced cell death.....	82

CHAPTER 1: INTRODUCTION

HISTORY OF RICIN

Ricin has been recognized as a toxin since the 6th century B.C., when castor beans were used in Greek and Egyptian medicine. But it wasn't until the late 1800's when a doctoral student in Estonia actually used the term ricin to describe the active protein that caused the agglutination of erythrocytes treated with extracts from *ricinus communis* seeds (1). Soon after, Paul Ehrlich used ricin and a related protein, abrin from the rosary pea plant, to establish the fundamentals of immunology (1). He showed that injecting small amounts of ricin into mice conferred immunity to the toxins. However, the mechanism of ricin toxicity, structure and cellular entry was paid little attention until the 1970s. Sjur Olsnes was the first person to recognize the subunit composition of ricin and its enzymatic action on ribosomes (1). In 1986, Yaeta Endo was able to show that the target of ricin is the highly conserved stem-loop structure of the large ribosomal RNA called the α -sarcin-ricin loop (SRL), and that ricin depurinates the SRL (2). Soon after, Jon Robertus solved the crystal structure of ricin and suggested a mechanism for catalysis (3). This mechanism consists of the enzymatic A-chain of ricin depurinating a specific adenine residue from the large ribosomal subunit, rendering the ribosome unable to translate proteins. Because of this activity, ricin belongs to a specific class of proteins called Ribosome Inactivating Proteins (RIPs), which includes proteins from plants, such as pokeweed antiviral protein (PAP) and bacteria, such as Shiga-like toxin (Stx) from *E. coli* and Shiga toxin from *Shigella*.

RTA STRUCTURE

Ricin is a type II RIP, which means it is a heterodimer consisting of an enzymatic A chain disulfide bound to a lectin binding B chain. Together, the A and B chains are considered to be the ricin holotoxin. Other type II RIPs are Shiga toxin and Shiga-like toxin isolated from *Shigella dysenteriae* and *Escherichia coli*, respectively, and abrin from *Abrus precatorius*. Most type I RIPs are single chain enzymatic proteins, such as PAP and saporin. These single chain proteins are similar to the A chain of a type II RIP, and it has been suggested that the type II RIP evolved from a fusion between a type I RIP and a lectin-binding protein (4). Because type I RIPs do not have a B-chain to bind to cells and allow for optimal cellular uptake, they are considerably less toxic than type II RIPs. The type III RIPs, such as those purified from maize and barley, are generated as a single chain protein, but must undergo proteolytic processing to become active. Figure 1.1 shows a schematic depicting the linear structures of the three types of RIPs.

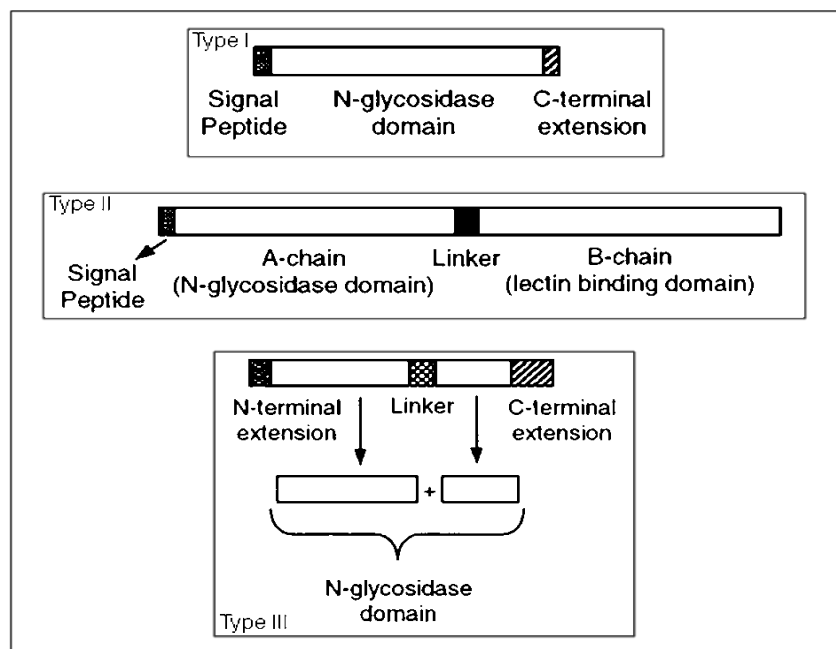


Figure 1.1: Linear schematic of the three types of RIPs

While the exact reason for the evolution of these related proteins is unknown, it is hypothesized that RIPs evolved as a defense mechanism. Interestingly, their enzymatic A chains are each approximately 30 kDa in size. A comparison between RTA and PAP show that their crystal structures are nearly superimposable (Figure 1.2), and in fact, most RIPs share very similar structures, indicating their close evolutionary background. Among the structures of these proteins, the most highly-conserved area is the centrally located active site, specifically E177, E176 and E167 in ricin, PAP and Stx, respectively (5, 6, 7) as well as their surrounding residues (Y80, Y123 and R180 in ricin).

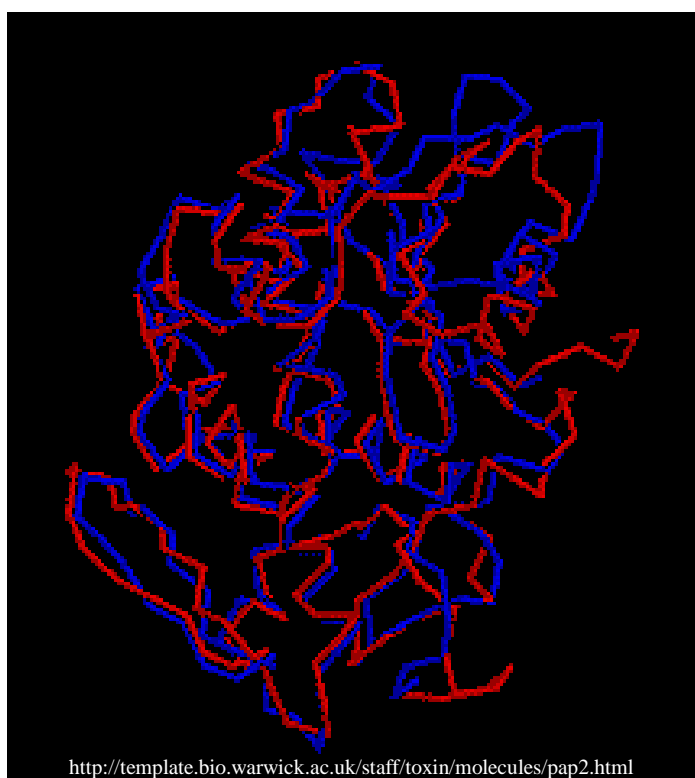


Figure 1.2: The backbone structures of RTA (red) and PAP (blue)

The ricin holotoxin is generated in the oil-storing endosperm cells of maturing seeds and accumulates in storage vacuoles (8). It is initially synthesized as a preproprotein of 576 residues. This accounts for a 35 residue N-terminal extension which includes the 26 residue signal sequence, the 267 residue A chain, a 12 residue linker and

the 262 residue B chain. After the ricin mRNA begins to undergo translation, the signal sequence directs the protein to the ER, where it is cleaved off. The proprotein is then glycosylated, the A and B chains are disulfide bonded and the protein begins to fold. Proricin is transported to the Golgi and then into vacuoles where the remaining 12 N-terminal residues are cleaved and mature ricin is stored (8).

The three-dimensional X-ray structure indicates that RTA is composed of 8 α -helices, a six stranded β -sheet and a two stranded β -sheet forming three domains (3). The amino terminal 117 residues form six α -strands and two α -helices. The central domain is made up of five helices of which the longest, helix E, runs through the center of the molecule and contains the key active site residues, Glu177 and Arg180. The third domain consists of a two-stranded antiparallel β -sheet and an α -helix, which is anchored to the first helix in the N-terminal domain. This forms part of the active site cleft and interacts with RTB in the holotoxin.

RICIN TRANSLOCATION TO THE CYTOSOL

The ricin holotoxin enters target cells when RTB binds to β -1, 4-linked galactose residues or galactose containing receptors on the cell surface. Because many types of mammalian cells have these galactose residues, ricin is able to gain entry into a wide variety of cells. Upon binding to the cell surface, ricin is endocytosed by both clathrin-dependent and clathrin-independent endocytosis (9, 10). Ricin then moves from early endosomes to late endosomes and finally to the Golgi by retrograde transport. The holotoxin then moves from the Golgi to the lumen of the ER by an unknown mechanism (11). Once inside the ER, the disulfide bond between RTA and RTB is reduced.

Once RTA and RTB are separated, it is hypothesized that RTA is exported to the cytosol by hijacking a quality control mechanism called the ER associated degradation (ERAD) pathway (12). ERAD occurs when proteins are recognized as being misfolded or non-native in the lumen of the ER. The aberrant protein is exported from the ER to the cytosol where it undergoes ubiquitination and proteolytic degradation. The main protein exporting channel in ERAD is the transmembrane Sec61 translocon, which consists of the three proteins, SEC61, SSS1 and SBH1 (13). Together, these proteins form a channel that allows co-translational protein import from active ribosomes, as well as protein export into the cytosol. Sec61 is also responsible for retrotranslocation of misfolded proteins out of the ER into the cytosol where they undergo degradation via the ubiquitin-proteasome system (14).

In the ER lumen, resident chaperones assist with proper folding of proteins. A prolonged association of a chaperone with an unfolded protein may target the protein for ERAD (15). The Hsp70 chaperone, KAR2, is one of the primary chaperones responsible for recognizing misfolded proteins and guiding them to the translocon (16). KAR2 may also act as a luminal “gate” to the Sec61 translocon and will only open when ERAD substrates are being exported. If KAR2 spends too much time attempting to fold an ER protein, the protein will be sent to undergo further modifications, such as the breaking of disulfide bonds and trimming of mannose residues, before being sent through the translocon.

There are several possible paths that an ERAD substrate can follow once it is translocated through the Sec61 channel. One pathway involves the ubiquitination of substrates during export by ubiquitin conjugating enzymes, such as UBC6 or UBC7 (16),

which is subsequently followed by degradation in the proteasome. However, ubiquitin conjugating enzymes attach ubiquitin residues to lysine residues of target proteins. Interestingly, RTA only has two lysine residues. It has been reported that even though RTA may be recognized as an ERAD substrate, its low number of lysine residues (2 lysines), may render it capable of avoiding ubiquitination, thereby avoiding proteolysis in the proteasome (17).

In addition to ubiquitin tagging, ERAD substrates must be structurally modified in order to undergo proteasomal degradation. To fit into the proteasome, sugar residues which can result from glycosylation in the ER, must be cleaved. The cytosolic protein, PNG1 is a deglycosylating enzyme. Normal ubiquitinated substrates are recognized by another protein, RAD23, which has a ubiquitin-like domain and is also capable of binding to PNG1 (18). RAD23 recognizes ubiquitinated substrates, and directs them to Png1, where they are deglycosylated. RAD23 might then bring the deglycosylated substrate to the proteasome for degradation (18).

There is also evidence for another pathway for ERAD substrate export which involves the direct association of the proteasome with the Sec61 translocon (19). This direct association may actually allow the proteasome to aid in the extraction of the misfolded protein of the ER, and to undergo direct proteasomal degradation, without the help of any other chaperones or factors.

RIBOSOME DEPURINATION

Once RTA reaches the cytosol, it enzymatically inactivates the large 28S subunit of active ribosomes. Endo et al discovered the affected molecular site by all RIPs while working with ricin in 1988 (2). They found that RIPs remove the first adenine from a

highly conserved GAGA tetraloop of the 28S ribosome (Figure 1.3). This same loop is also affected by the unrelated endoribonuclease α -sarcin, which is produced by *Aspergillus giganteus*, thereby giving the loop the name sarcin/ricin loop (SRL). The SRL is a binding site for elongation factors such as EF1 and EF2, and when altered, protein translation is inhibited (20). The fact that the SRL is targeted by RIPs as well as α -sarcin demonstrates its functional importance in basic cellular processes.

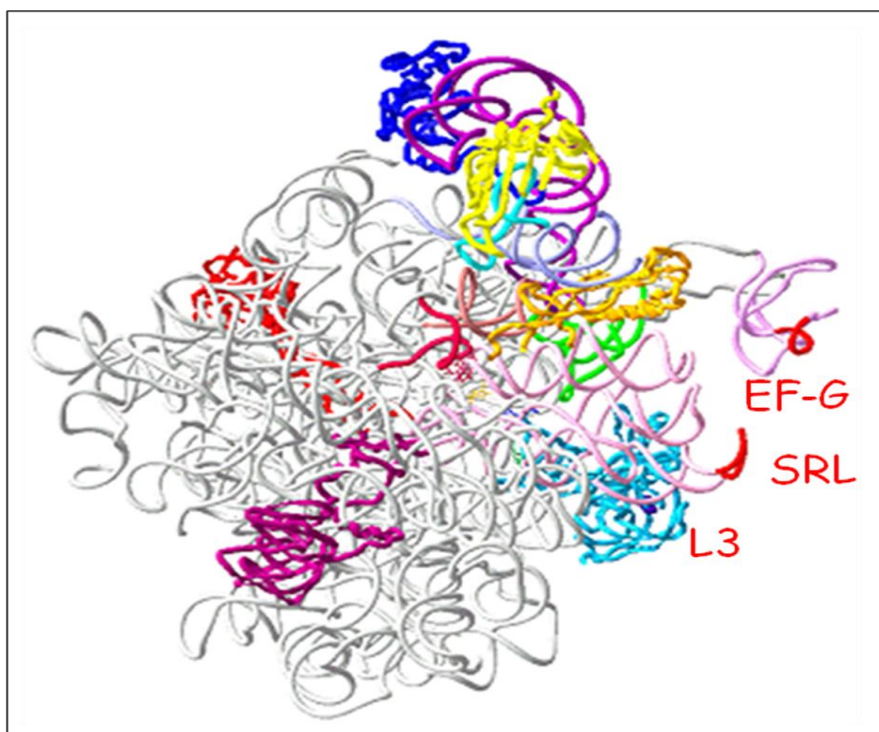


Figure 1.3: The large ribosome indicating the location of the sarcin/ricin loop (SRL), ribosomal protein L3 (L3) and elongation factor G (EF-G) (21)

In order to access this adenine residue, RIPs must be able to bind or closely associate with the ribosome. While the site of binding for other RIPs is confirmed (PAP binds to ribosomal protein L3 (22), where RTA binds on the ribosome has not been confirmed. Studies with rat ribosomes have shown that RTA can be cross-linked to ribosomal proteins P9 and P0 (23). Preliminary evidence from our lab suggests that RTA may associate with P0 *in vivo*.

Once RTA is associated with the rRNA, it enzymatically attacks the adenine residue by specifically cleaving the N-glycosidic bond between the adenine and the sugar residue (Figure 1.4A) (2). This depurination event occurs at the active site in RTA, and is conserved among all of the RIPs (2). It is expected that two tyrosine residues Tyr-80 and Tyr-123 sandwich the adenine ring of the rRNA target. Once the adenine is held in position, Arg-180 protonates the N-3 atom of the adenine, while Glu-177 stabilizes a positive oxocarbenium transition state and interacts with the ribose (Figure 1.4B) (24).

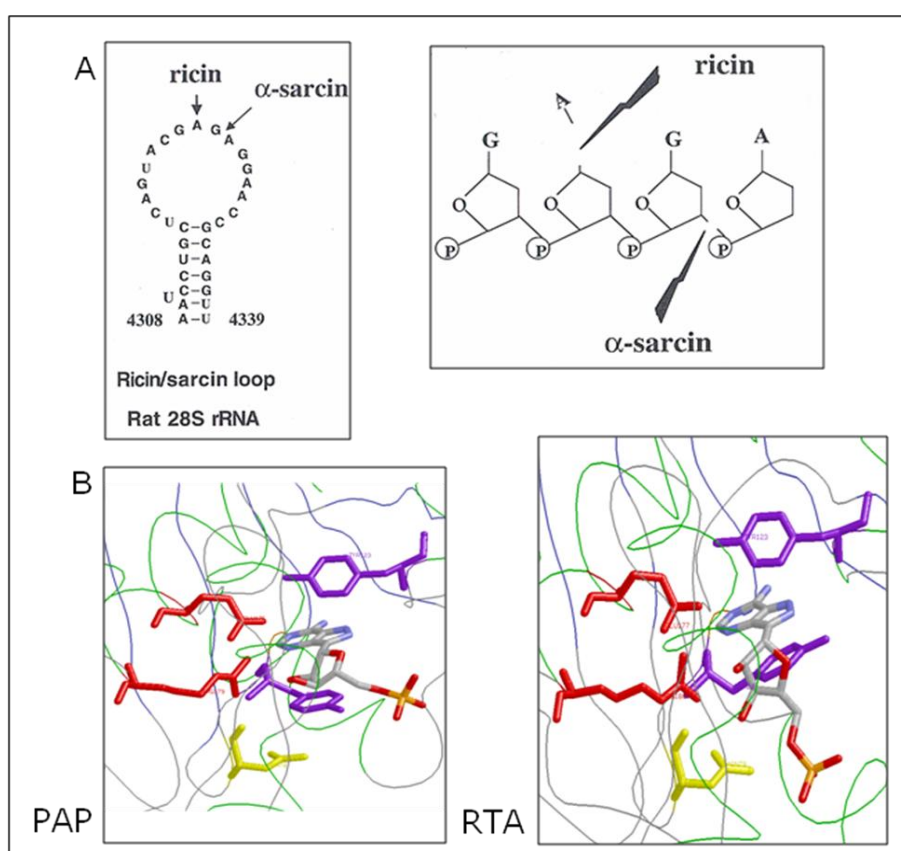


Figure 1.4: A. The site of depurination in the SRL, and B. the structural model of the active site of PAP and RTA with adenine (Parikh B, thesis 2004).

The ability of RIPs to inhibit protein synthesis was recognized in 1972 even before ribosome depurination was discovered as the underlying mechanism (1). Initially, the 60S ribosomal subunit was determined to be affected by ricin. Later, the binding site

for EF2 was specifically identified as being blocked by ricin activity (20), rendering the ribosome unable to partake in the elongation step of protein translation. Later studies by Sperti et al. also showed that the translocation step was specifically affected due to the inhibition of GTP hydrolysis and GTPase activity of EF2 (20).

RICIN CYTOTOXICITY

While it seems logical that RIP toxicity is a result of ribosome depurination, there is evidence to support that toxicity and depurination can be separated (25, 26). There are possible alternative mechanisms leading to cytotoxicity in ricin, namely the inhibition of the unfolded protein response (UPR) and ribotoxic stress.

UPR is a response mechanism that occurs when there are too many unfolded proteins in the ER. As a result of the UPR, the folding capacity of the cell is increased, the amount of new proteins translocated to the ER lumen is reduced and retrotranslocation out of the ER and degradation of ER-localized proteins is increased (27). Thus, UPR is closely linked with ER associated degradation (ERAD).

Generally, when a cell undergoes stress, the normal protein maturation process will be affected, leading to an increase in the levels of unfolded proteins. To assist with protein folding in yeast, KAR2 is recruited to help bind and fold these misfolded substrates (29). KAR2 is also necessary for other cellular processes, such as gating of the Sec61 channel. Cellular stress is indicated when the level of free KAR2 is low, which slows down protein translation initiation to prevent the further accumulation of more unfolded proteins (30). In addition, the recruitment of KAR2 to unfolded proteins may initiate the UPR pathway. KAR2 has been shown to associate with the ER luminal sensor domain of Ire1, which is a trans-membrane kinase that also has a transmembrane

domain, a cytoplasmic Ser/Thr kinase domain and an RNase L-like nuclease domain (29). Ire1 recognizes the accumulation of unfolded proteins, possibly as a result of dissociation of KAR2, and begins induction of the UPR. This entails Ire1 dimerization and activation, and cleavage of the transcription factor *HAC1* mRNA. Spliced *HAC1* mRNA binds to the unfolded protein response elements (UPRE) found in UPR-responsive genes, and helps to enhance production of their proteins. One of these genes is *KAR2*, which is upregulated to aid in proper folding of misfolded substrates. It has recently been reported that RTA prevents splicing of *HAC1* mRNA, which results in the inhibition of UPR (28). This inhibition of the UPR may be responsible for ricin-induced cytotoxicity.

Ribotoxic stress is a pathway induced by events of cellular stress and is marked by activation of cJun N^{H2}-terminal kinases (JNKs) (31). Activation of JNK leads to a cascade of various kinase pathways that either lead to cell repair and recovery, or to apoptosis. Exposure to anisomycin, an antibiotic that inhibits the eukaryotic peptidyl transferase reaction in protein translation, is known to activate JNKs (31). While inhibition of protein synthesis via anisomycin would logically be considered an event of cellular stress, and thus an activator of ribotoxic stress, it has been shown that JNK activation via anisomycin occurs even when protein synthesis is only partially affected. This indicates that the ability of anisomycin to cause ribotoxic stress does not rely entirely on its ability to inhibit protein synthesis (31). Because both RTA and anisomycin damage the ribosome and inhibit translation, it is possible that, like anisomycin, RTA induces ribotoxic stress.

Interestingly, IRE1 can also activate JNKs during the UPR (32). In addition, PERK, a transmembrane protein kinase in the ER, is activated by events that occur during

ER stress, such as accumulation of misfolded proteins. PERK also phosphorylates eIF2 α , and when PERK is overexpressed in cells *in vitro*, it can inhibit protein translation (33), which could lead to ribotoxic stress. Therefore, ricin toxicity may result from a combination of UPR inhibition, ribotoxic stress and ribosome depurination.

RICIN POISONING

Exposure to ricin can occur via inhalation, ingestion or injection of the powdered, crystallized or liquid forms of the toxin or, in the case of ingestion, consumption of the castor beans (34). The amount of ricin that results in toxicity and the resulting symptoms depends on the route of exposure. However, the epithelial cells of both the gastrointestinal tract and the respiratory pathway are the primary targets of ricin intoxication (34). The damage inflicted by RTA on the epithelial cells often results in a clinical manifestation called vascular leak syndrome (VLS), which is characterized by hypoalbuminemia and edema (35). VLS does not result from the inhibition of protein synthesis of RTA, as VLS is observed several hours before protein synthesis inhibition (35). Instead, *in vitro* evidence has shown that VLS activates apoptosis via caspase 3 (36), suggesting that death via ricin intoxication may be due to complications from the VLS activity, and not ribosome depurination.

While inhalation and injection of ricin are considerably more lethal than ingestion, the threat of ricin contamination to food, water and air supplies are most likely. Reports have shown that ingestion of as little as one half of a castor bean resulted in symptoms, and as few as two beans resulted in death (37). Symptoms begin within 4-10 hours of ingestion and are usually nonspecific, such as diarrhea, abdominal pain and heartburn. 4-36 hours after ingestion more severe symptoms, such as liver dysfunction or

low blood pressure may occur, possibly resulting in death (37). Consumption of large quantities of charcoal and cleansing of the GI tract with a cathartic may help to eliminate ricin toxicity after ingestion (38).

The dissemination of aerosolized ricin is probably the most likely way for a terror attack to occur. Ricin intoxication via inhalation is dependent on the size of the particles. The smaller the particle, the more likely it will be inhaled and lodged deep into the respiratory system (39). The lethal dose for mice for particles less than 5 μm in size was determined to be 3-5 $\mu\text{g/kg}$ of body weight. Animal studies in which ricin was inhaled showed that inflammation and necrosis of cells in the airway and lungs occurred as a result of ricin toxicity. While there are no current reports of ricin intoxication via inhalation, past studies have indicated that symptoms occur 4-8 hours after inhalation of ricin particles (34). It is expected that symptoms of ricin intoxication can occur up to 24 hours after inhalation, and that the primary cause of death is respiratory failure (34, 40).

The injection of ricin is the least likely method for a large scale terror attack, and there are no current reports of ricin intoxication via injection. However, the lethal dose for mice that were exposed to ricin parenterally was 0.7-2 $\mu\text{L/kg}$ of body weight (41). The symptoms of ricin intoxication occur 10-12 hours after injection and include fever, nausea and abdominal pain. Tissue damage at the site of injection is sometimes present (41, 42) and multisystem organ failure may eventually occur (34, 43).

RICIN TREATMENT

Development of a ricin vaccine would need to maintain the toxin's active site, and the active site of ricin is responsible for the damage to ribosomes and subsequent cell death. Therefore, the generation of mutant forms of ricin that have a functional active site, but do not result in cell death are ideal for vaccine development. While there is currently no approved ricin vaccine, there are and have been some possible candidates.

Inactivated, formaldehyde treated ricin (toxoid) has been successfully used as both an intranasal (44) and orally administered (45) vaccine in animal studies to prevent ricin intoxication. However, there is a threat of ricin toxoid reverting back to the active form. Deglycosylated RTA has also been administered in low concentrations to initiate an antibody response in mice. Although successful production of neutralizing antibodies relies on a mucosal adjuvant, which sometimes results in nasal inflammation, clinical trials are currently undergoing investigation (46).

Passive immunity against ricin intoxication was achieved in mouse studies using anti-ricin monoclonal IgG (47), but the use of a murine antibody to neutralize ricin in humans will elicit a negative immune response. More recently, a chimeric ricin antibody was generated by coupling murine antigen-binding domains to human constant domains (48). This antibody shows promise for use with clinical studies.

Most recently, RiVax, a recombinant RTA vaccine is under development. RiVax contains the point mutations Y80A, which affects substrate binding and V76M in RTA. These mutations are proposed to affect both vascular leak syndrome and the ribotoxic stress response (49), but not the depurination activity of RTA. Results from animal studies show that administration of a concentration of 1-10 μ g of RiVax via gavage or

aerosol was able to prevent ricin-induced tissue damage and death from a challenge of 10X the lethal dose (LD_{50}) of ricin (49). Human trials were carried out in which volunteers were vaccinated with varied concentrations of RiVax, and anti-RTA antibodies and ricin-neutralizing antibodies were assayed (50). The main conclusion of the study was that RiVax would protect humans against injection of 0.3-3.0 mg of ricin. Further studies need to be conducted to determine the use of RiVax to prevent intoxication of ricin inhalation or ingestion (50).

SUMMARY OF WORK TO BE PRESENTED

In order to understand the mechanisms of RTA toxicity, a yeast *Saccharomyces cerevisiae* system was implemented and optimized because this system has been successfully used to study mechanisms of cytotoxicity of another RIP, PAP. Although the ultimate goal of ricin research is often to understand how to prevent and treat ricin intoxication in humans, yeast is an excellent model to use to analyze the mechanisms of cytotoxicity of ricin since the target of ricin, the SRL, is highly conserved between yeast, plants and mammalian cells and because yeast can easily be genetically manipulated. Yeast are eukaryotic and preliminary data from our lab and the laboratory of our collaborators has shown that ricin behaves similarly in both mammalian and yeast cells. Yeast also utilize the ERAD pathway, suggesting that yeast are an ideal model for investigating the translocation of ricin through target cells. RTA is toxic to yeast cells (Figure 1.5), and both yeast and animal ribosomes are depurinated by RTA (Figure 1.6A and 1.7). The ERAD pathway in yeast has been characterized fairly well, and there is a library of yeast ERAD mutants available for analysis. Therefore, the expression of RTA

in yeast may provide information for mechanisms of RTA-induced toxicity in mammalian cells.

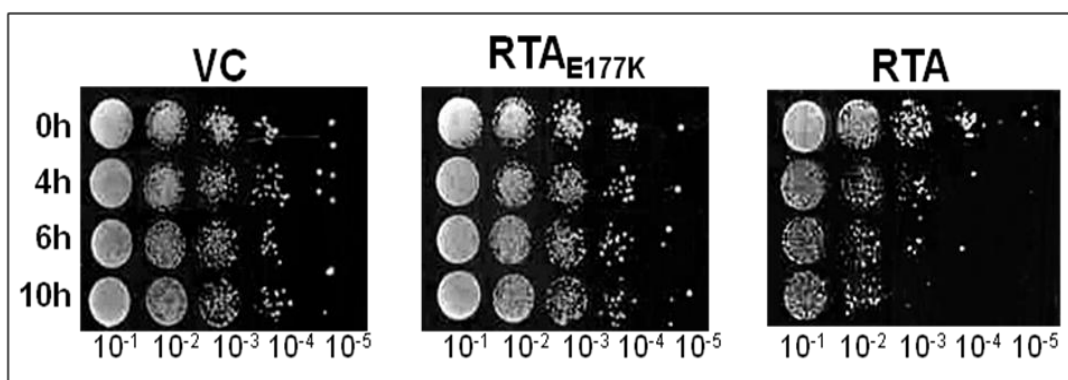


Figure 1.5: Yeast cells expressing RTA are not viable. Yeast cells expressing RTA, the active site mutant, RTA_{E177K}, or the empty vector were induced for 10 hours on SD-Leu galactose media and were then plated as serial dilutions onto SD-Leu glucose plates.

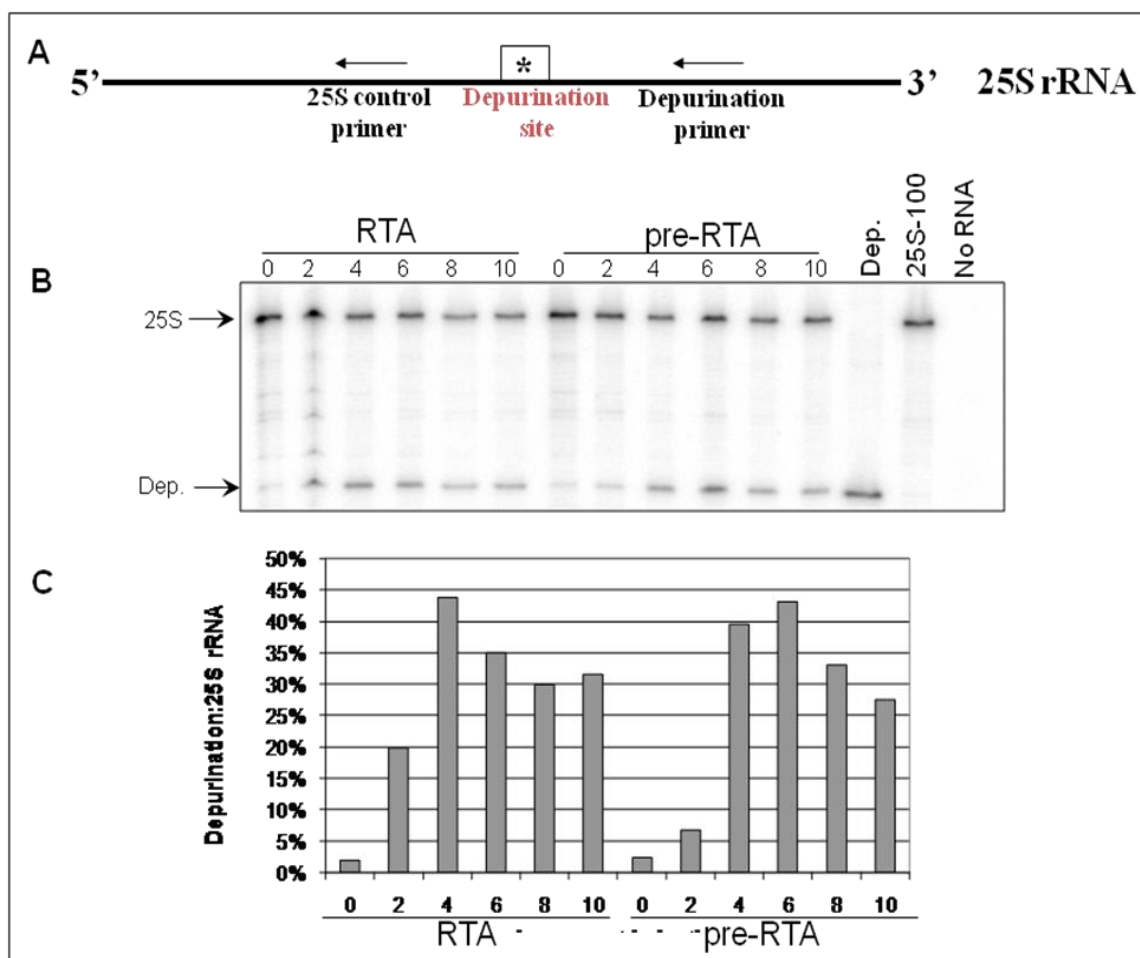


Figure 1.6: Analysis of rRNA depurination of RTA and pre-RTA. A. Schematic representation of dual-oligo primer extension assay. Two different end-labeled primers

(Depurination primer and 25S control primer) were annealed to rRNA and reverse-transcribed. The resulting fragments represent the extension products that have stopped prematurely at the depurination site and extension products that have stopped at the 5' end of the 25S rRNA. B. The primer extension products for RTA and pre-RTA representing the extent of depurination and the amount of total rRNA present at the indicated times post induction (hours). C. The extent of depurination shown in B was quantified by calculating the ratio of the depurination fragment to the 25S control fragment and was expressed as a percentage.

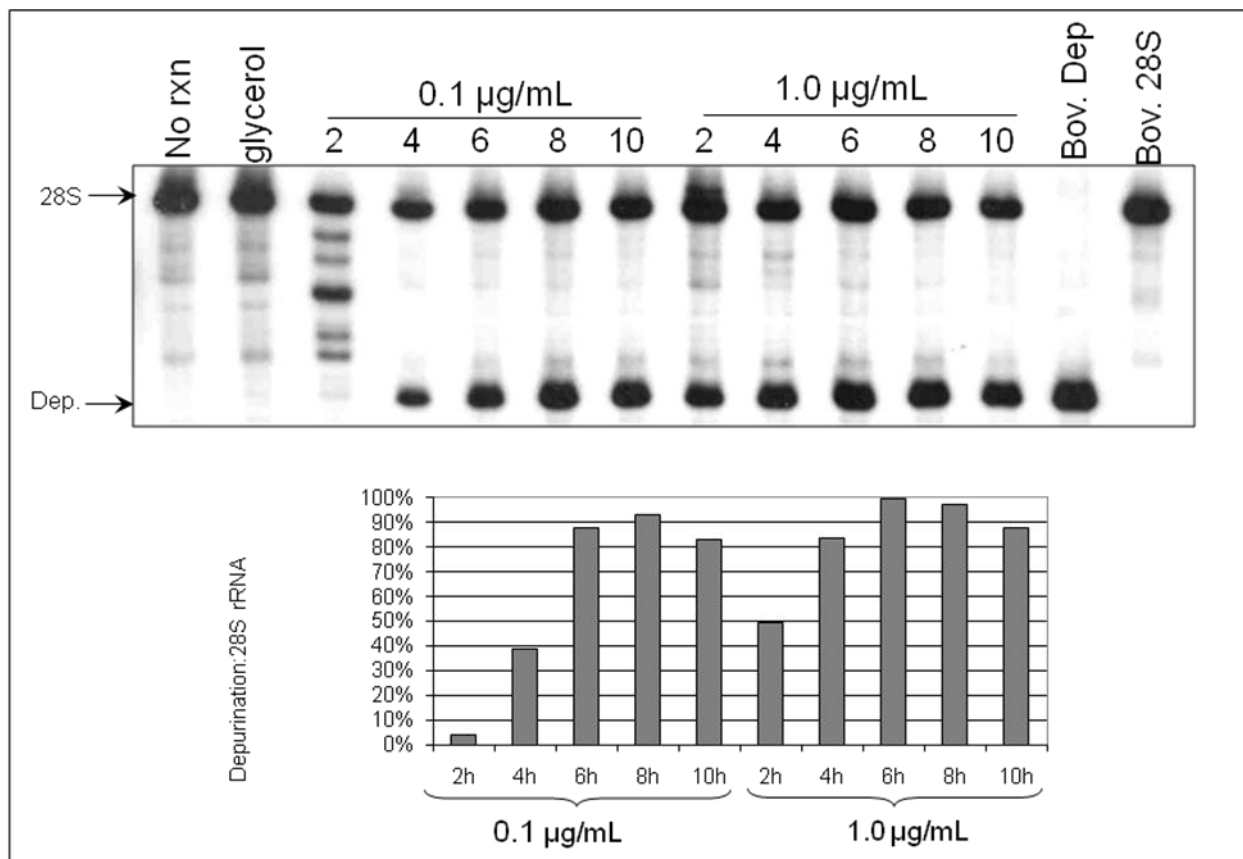


Figure 1.7: 0.1 µg/mL of RTA is sufficient to depurinate animal ribosomes. Bovine mammary epithelial cells were grown to confluence in 6-well plates. Prior to treatment, cells were serum deprived for 16 hrs. Cells were treated with 0.1 µg/ml or 1 µg/ml RTA for 2, 4, 6, 8 and 10 hrs. Total RNA was isolated using Trizol (Invitrogen) and analyzed by primer extension as described above using a depurination primer and a 28S control primer. As a vehicle control, cells were treated with the same amount of glycerol as in the 1 mg/ml treatment.

In the following chapters I will discuss new information regarding possible mechanisms for the cytotoxicity of RTA. In chapter two I will discuss the results of random mutagenesis of RTA, which demonstrate that RTA toxicity is not a direct result

of ribosome depurination and translation inhibition. Chapter three discusses how RTA uses the ERAD machinery to reach the cytosol, without undergoing complete proteosomal degradation. In the final chapter, I will discuss the results from site-directed mutagenesis of the C-terminal end of RTA, and how this may provide information regarding the driving force of RTA's utilization of the ERAD pathway. In addition to gaining a better understanding of RTA, there are several references and suggestions regarding the mechanism of other RIPs, namely PAP and Shiga-like toxin from *E. coli*, which will enhance general knowledge on the medical uses and potential treatments for exposure to these toxins.

CHAPTER 2: Ribosome depurination is not sufficient for ricin-mediated cell death in *Saccharomyces cerevisiae*

INTRODUCTION

Understanding the residues that are critical for RTA toxicity is essential for the generation of ricin vaccines or antidotes. The search for additional critical residues has previously been carried out by expressing mutated RTA in *E. coli*, followed by the subsequent analysis of *in vitro* enzymatic activity. Other researchers have passaged the plasmid containing mature RTA through an *E. coli* mutator strain and identified five different mutations in residues at the active site cleft (5), including Glu177, Trp211, Gly212 and Ser215, which are located on the same helix, and Ile252, which is located close to the C-terminal end (5). Recently, another large scale mutagenesis screen was conducted using error-prone PCR of mature RTA (51). Several new point mutations with reduced toxicity were identified. While these studies identified several residues essential for enzymatic activity, the correlation between ribosome depurination and cytotoxicity had not been addressed. Here, we conducted a large-scale mutagenesis study of pre-RTA in the yeast, *Saccharomyces cerevisiae*, and isolated RTA alleles based on their inability to kill yeast cells. The nontoxic RTA alleles were characterized with respect to their ability to depurinate ribosomes, inhibit translation and cause cell death. Several alleles depurinated ribosomes and inhibited total translation to the same level as the wild type RTA, but did not cause cell death. These results demonstrated that ribosome depurination does not account entirely for the cytotoxicity of ricin.

RESULTS

Random Mutagenesis

The full length cDNA corresponding to pre-RTA, which consists of a 35 residue N-terminal extension and the 267 residue coding sequence was cloned into the yeast expression vector downstream of the *GAL1* promoter, mutagenized using hydroxylamine and transformed into yeast. Cells were plated on media containing glucose and replica plated on galactose containing plates. Out of a total of 15,000 transformants screened, 128 (0.82%) were able to grow on galactose containing media, indicating resistance of yeast to the mutated toxin. Immunoblot analysis showed that RTA expression was detected in 87 (68%) out of 128 colonies. Of the 87 colonies that showed detectable RTA expression, 37 expressed protein at the same molecular weight as wild type RTA, and 50 expressed smaller variants of RTA. All 87 plasmids isolated were retransformed into yeast to confirm that the resistance was due to the plasmid. Nucleotide sequence analysis identified a total of 35 different mutations, which led to the loss of cytotoxicity (Table 2.1). A majority of the mutations were isolated multiple times from different plates, indicating that the mutagenesis screen was saturated. The mutants were divided into three groups: Group I contains 16 different mutations with a premature termination codon, resulting in a truncated form of the protein. Group II contained 9 different frameshift mutations. In this group, the N-termini of the proteins were the same as preRTA, but the C-termini were different depending on the position of the frameshift mutation. Additional amino acids added to the C-termini before the stop codon are indicated in Table 2.1. Group III consisted of 14 different point mutations, which

resulted in single amino acid changes in the protein. Only two mutants in this group contained double point mutations. To determine which mutation was necessary for the loss of cytotoxicity, single mutations were generated by site-directed mutagenesis. Expression of RTA containing the single mutations corresponding to each double mutation was toxic to yeast, indicating that the two different point mutations are required simultaneously for the loss of cytotoxicity.

Table 2.1 shows the number of occurrence of the base pair changes, including the silent mutations. As expected for hydroxylamine mutagenesis, C/G to T/A transitions accounted for 80% of the total base pair changes. The frequency of other base pair changes was relatively low. The frequency of the deletions or additions was around 12%. Due to the high frequency of C to T changes, 11 out of 14 glutamines encoded by CAA/G in pre-RTA were changed to stop codons (TAA/G) resulting in premature termination. Random mutagenesis work was done by Xiao Ping Li.

Table 2.1: Characterization of pre-RTA mutants obtained by random mutagenesis

Protein change	No. of occurrences	Cytotoxicity	Depurination (% of wt)	Translation (% of vector)	Doubling time (h)
pre-RTA		Yes	100	35	18
Vector control		No	2	100	6.3
Group I					
Q19 stop	1	No	5	ND	ND
Q55 stop	2	No	1	ND	ND
Q112 stop	2	No	1	ND	ND
Q128 stop	3	No	1	ND	ND
G140 stop	1	No	1	ND	ND
S149 stop	1	No	2	ND	ND
Q160 stop	3	No	12.3	ND	ND
Q173 stop	3	No	4.3	ND	ND
S176 stop	2	No	4.5	ND	ND
Q182 stop	2	No	3.4	ND	ND
W211 stop	4	No	3.7	ND	ND
Q219 stop	2	No	7.9	ND	ND
Q223 stop	3	No	4.3	ND	ND
Q231 stop	3	No	9.6	60	9
Q233 stop	6	No	6.7	59	8.7
L248 stop	2	No	15.8	58	7
Group II					
T77P + 4a	1	No	0.4	ND	ND
Y84T + 48	1	No	5.6	ND	ND
F92S + 40	1	No	2.4	ND	ND
R114D + 18	1	No	2.8	ND	ND
P202L + 1	2	No	2.3	ND	ND
R213D + 31	1	No	2.8	ND	ND
R213D +31c	1	No	3.2	ND	ND
S215F + 6	1	No	5.5	ND	ND
P250L + 1	1	No	5.1	ND	ND
Group III					
G83D	6	No	41	62	12
G140R	2	No	5	93	9.1
A147P	3	No	33	69	10
E177K	3	No	5.6	73	9.8
Δ I 184	1	No	8.2	69	9
E208K	2	No	29	58	10
G212E	9	No	19	88	6.9
S215F	2	No	110	32	15
P95L-E145K	1	No	115	41	10
P95L (by PCR)		Yes	149	34	26
E145K (by PCR)		Yes	108	27	18
P250L-A253V	1	No	5.2	100	7.7
P250L (by PCR)		Yes	158	31	20
A253V (by PCR)		Yes	175	30	24

^aThe numbers after the mutations indicate the numbers of amino acids added to the C termini before a stop codon is generated.

^bND, not determined.

^cThe amino acids added to the C terminus are different from those added for the mutation listed immediately above (26).

Wild type pre-RTA and the nontoxic mutants are expressed in yeast

Immunoblot analysis using polyclonal antibodies against RTA was used to examine protein expression in each mutant 6 h post-induction. As shown in Figure 2.1, mature RTA standard from *Ricinus communis* (Sigma) contained two bands, possibly due to different levels of glycosylation. Protein isolated from yeast harboring the pre-RTA plasmid contained two bands that co-migrated with the mature form of RTA (Figure 2.1 first two lanes), indicating that pre-RTA synthesized in yeast is processed the same way as RTA in plants.

Immunoblot analysis indicated that all 39 mutants that contained the premature termination codons (Figure 2.1A), the frameshift mutations (Figure 2.1B) or the point mutations (Figures 2.1C and 2.1D) expressed detectable levels of RTA. The blot was reprobed with antibody against dolichol-phosphate mannose synthase (Dpm1p) as a loading control. The mutant proteins migrated on SDS-PAGE according to their size, except for the double mutant, P250L-A253V, which contained larger and smaller bands, indicating possible effects on protein aggregation and breakdown. Analysis of the single mutations corresponding to this double mutant indicated that P250L mutation contributed to the observed effects. In general, yeast cells carrying the non-toxic mutations expressed higher levels of RTA than cells carrying wild type or toxic forms (P95L) of pre-RTA. These results demonstrated that the loss of cytotoxicity of the mutant alleles was not due to the loss of protein expression. Viability assays were done by Xiao Ping Li.

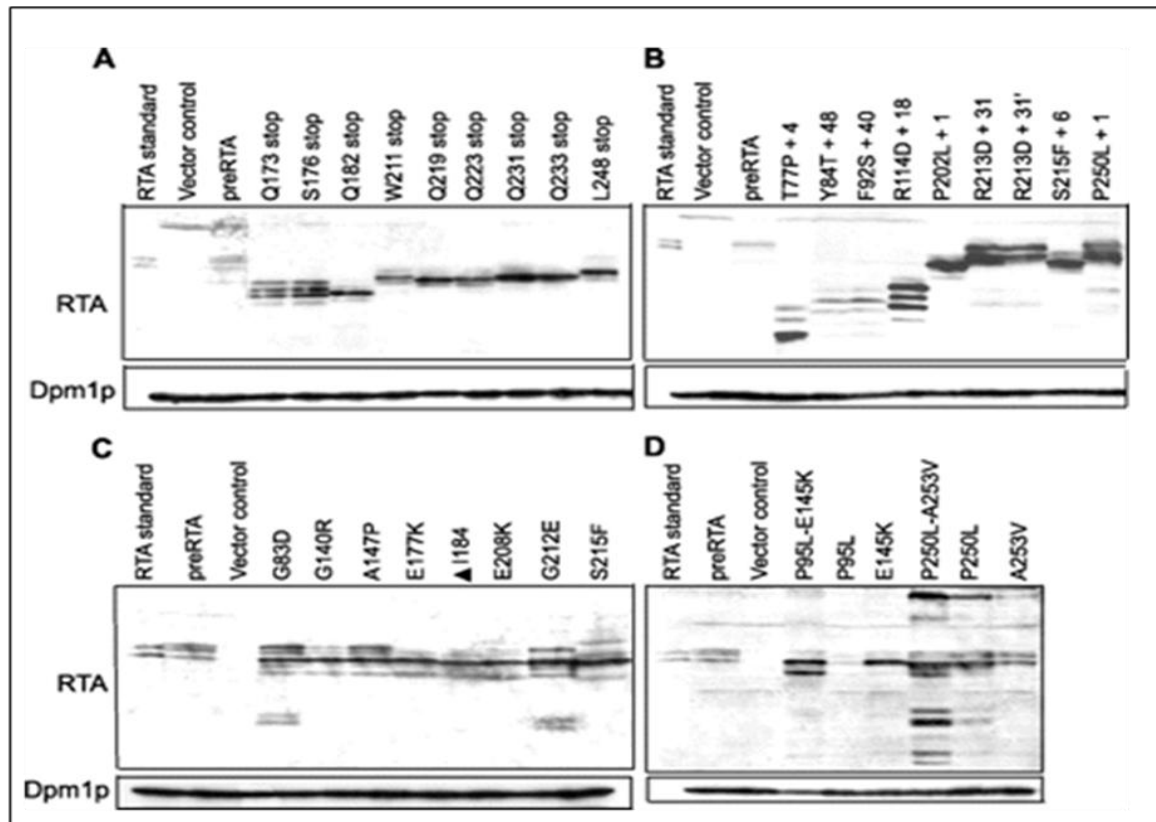


Figure 2.1: The pre-RTA mutants are expressed in yeast. Membrane fractions (15 μ g) isolated from cells expressing pre-RTA or mutants containing a premature termination codon (A), a frameshift mutation (B), a single point mutation (C), or a double point mutation (D) were separated on a 12% SDS-polyacrylamide gel and probed with polyclonal anti-RTA (1:3,000). The RTA standard (1.5 ng) was purified RTA. The blots were stripped and probed with the ER membrane marker Dpm1p as a loading control (work done by Xiao Ping Li, 26).

Pre-RTA mutants are not toxic to yeast cells

Irreversible growth inhibition was examined by conducting viability assays. As shown in Figure 2.2, cells were plated on glucose plates after induction on galactose for the indicated times. The top panel shows the yeast cells harboring either the wild type pre-RTA plasmid or the empty vector. Upon induction in yeast, the wild type RTA reduced the viability of cells by almost 3 logs at 12 h. In contrast, the nontoxic RTA mutants exhibited minimal loss of viability at 10 hours post induction (Figure 2.2). All nontoxic mutants analyzed exhibited similar viability as the cells harboring the empty

vector. Only L248* in group I and P250L+S in group II, are shown because they had the shortest deletion at their C-termini. The two double mutants, P95L-E145K and P250L-A253V were nontoxic and did not reduce viability. However, the single mutations corresponding to each double mutation (P95L, E145K and P250L, A253V) were toxic (Table 2.1 and Figure 2.2) and reduced the viability of yeast cells. Protein expression analysis was done by Xiao Ping Li.

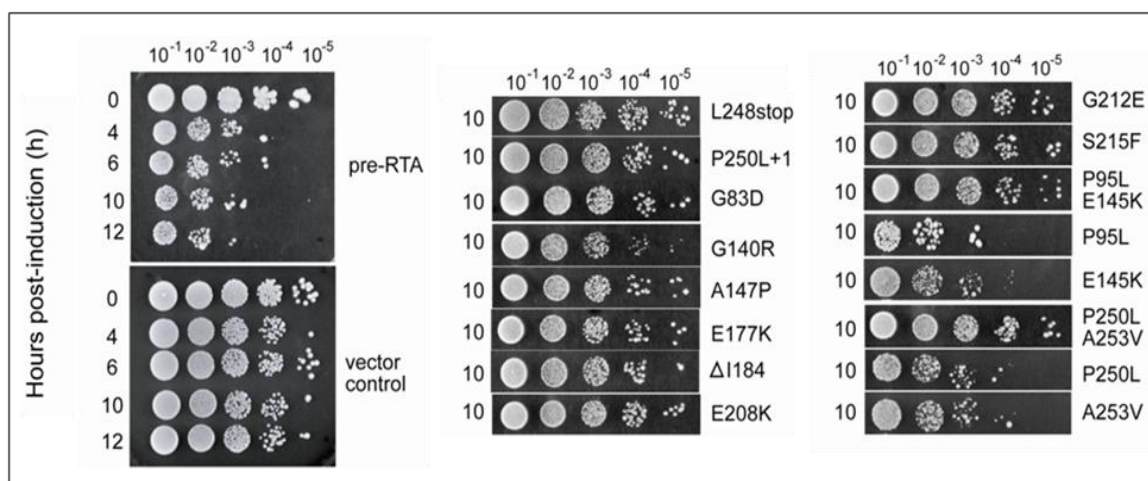


Figure 2.2: Viability of cells expressing pre-RTA and the mutant forms of RTA. Yeast cells were first grown in SD-Leu medium supplemented with 2% glucose to an optical density at 600 nm of 0.3 and then transferred to SD-Leu supplemented with 2% galactose. At the indicated hours postinduction on SD-Leu medium containing galactose (left), serial dilutions were spotted on SD-Leu plates supplemented with 2% glucose. The top two panels show the cell viability up to 12 h in cells expressing the wild-type pre-RTA or harboring the empty vector (work done by Xiao Ping Li, 26).

Nontoxic RTA mutants depurinate rRNA

To determine if the reduced toxicity of the pre-RTA mutants was due to reduced depurination of ribosomes, total RNA was isolated from each mutant and depurination of the rRNA was examined by dual primer extension at 6 h post induction. As shown in Figure 2.3, ribosomes were depurinated in cells expressing pre-RTA. Proteins that were truncated at their C-terminal end, Q231*, Q233*, and L248* showed a very weak depurination band, indicating that these mutants retained a low level of depurination

activity (Figure 2.3 A). The frameshift mutants did not show any depurination activity (Figure 2.3 B). In contrast, 5 out of 10 point mutants isolated depurinated yeast ribosomes in vivo (Figure 2.3 C). To confirm these results, the plasmids were recovered from yeast into *E. coli* and were sequenced again to confirm the mutations and transformed into yeast. The depurination assay was repeated several times with all mutants and the extent of depurination calculated from independent experiments was averaged in Table 2.1. As shown in Figure 2.3 and Table 2.1, S215F and the double mutant, P95L E145K, had at least the same level of depurination activity as the wild type preRTA in vivo, but unlike the wild type preRTA, these mutants were not toxic and did not reduce the viability of yeast cells (Figure 2.2, Figure 2.4 and Table 2.1).

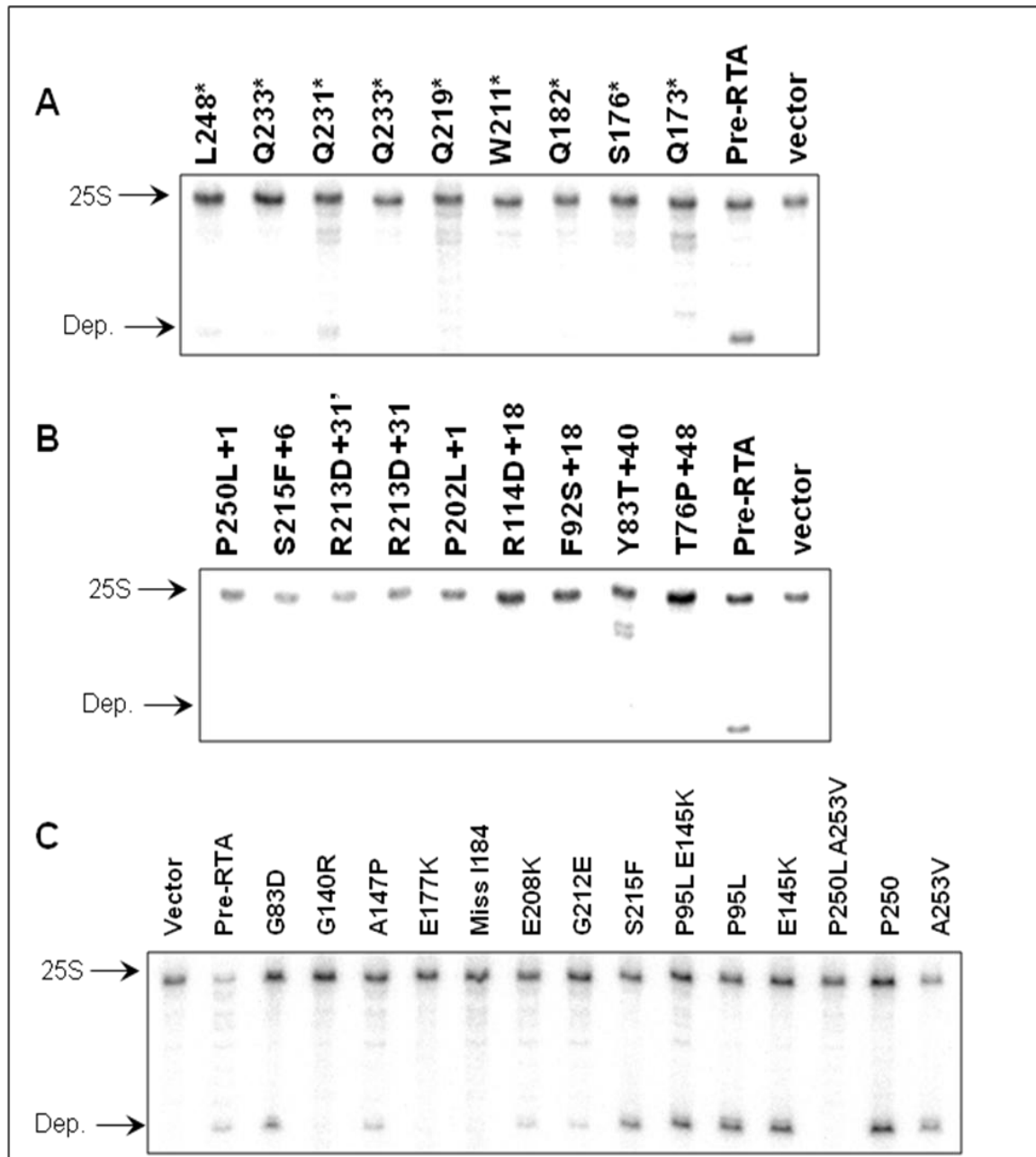


Figure 2.3: Ribosome depurination in yeast expressing pre-RTA and the mutant forms in vivo. Total RNA isolated after 6 h of growth on galactose was analyzed by dual primer extension. Primer extension analysis of the mutants with a change corresponding to a premature termination codon (A), a frameshift mutation (B), or a point mutation (C) is shown.

To determine if the mutant proteins were enzymatically active *in vitro*, we extracted the mutant proteins from yeast and examined ribosome depurination after treating purified yeast ribosomes with the wild type and the mutant proteins *in vitro*. As

shown in Figure 2.4, the wild type pre-RTA extracted from yeast depurinated yeast ribosomes *in vitro*. The S215F and the double mutant, P95L-E145K, depurinated yeast ribosomes *in vitro*, while P250L-A253V was not able to depurinate ribosomes *in vitro*. The *in vivo* depurination results were the same as those obtained with proteins isolated from yeast *in vitro* and demonstrated that S215F and P95L-E145K are catalytically active, while P250L-A253V is not.

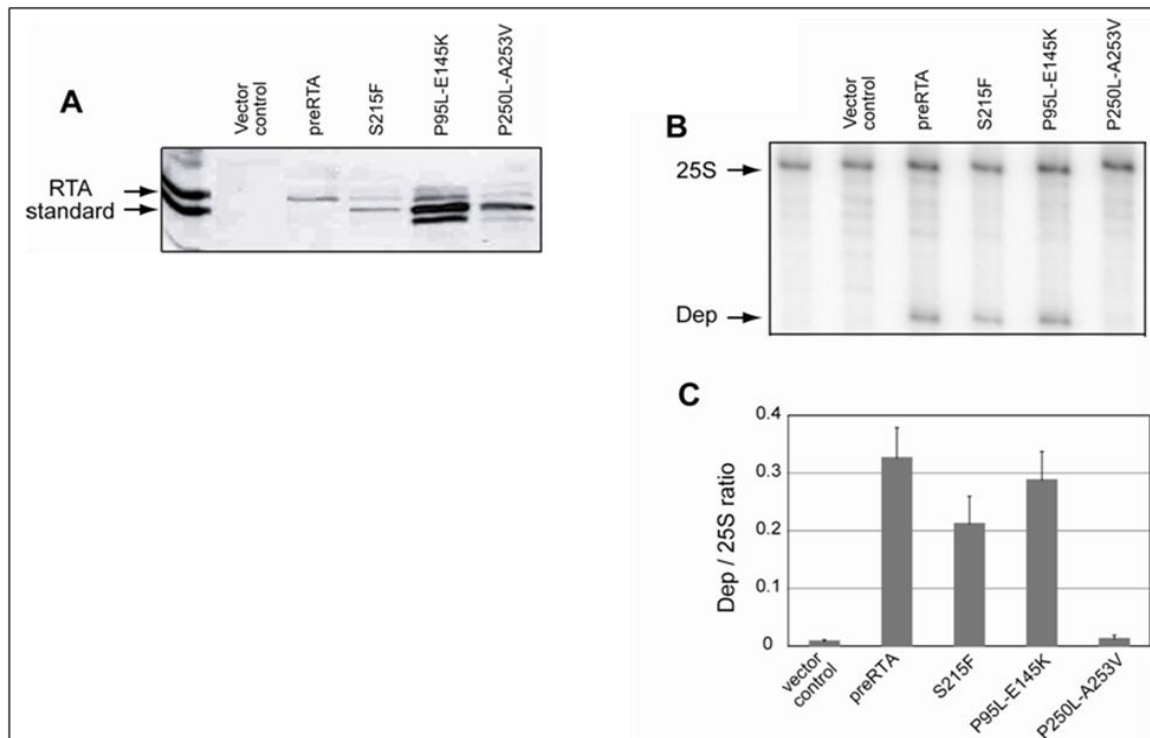


Figure 2.4: Ribosome depurination by pre-RTA and mutants *in vitro*. (A) Total protein extracted from the cytosolic fraction of 10 ml of yeast cells expressing pre-RTA or the mutants was analyzed on a 12% SDS-polyacrylamide gel and probed with polyclonal anti-RTA (1:3,000). The first lane is purified RTA standard (10 ng). (B) Ribosomes isolated from yeast cells were treated with either wild-type pre-RTA or the S215F, P95L-E145K, and P250L-A253V mutants extracted from the cytosolic fractions of yeast cells *in vitro*, and the extents of depurination were determined by dual primer extension analysis. The first lane corresponds to the untreated ribosomes, and the second lane corresponds to primer extension analysis with protein extracted from cells harboring the empty vector. (C) The extents of ribosome depurination were quantified using a PhosphorImager from three independent depurination experiments with the wild-type and mutant proteins extracted from yeast *in vitro*.

Ribosome depurination results in translation inhibition

To determine if ribosome depurination correlated with translation inhibition, we examined total translation in cells expressing pre-RTA by [³⁵S]-methionine incorporation. As shown in Table 2.1, total translation was reduced to 35% in cells expressing the wild type pre-RTA compared to total translation in cells harboring the empty vector. The wild type pre-RTA did not inhibit translation completely, indicating that some translation still occurs in the presence of RTA. Total translation was not inhibited in yeast expressing the mutants which did not depurinate ribosomes. In contrast, total translation was inhibited in S215F and in the double mutant, P95L E145K, which depurinated ribosomes (Table 2.1). These results demonstrated that translation inhibition correlated well with the extent of depurination, indicating that depurinated ribosomes are unable to translate protein.

DISCUSSION

Here, we conducted large-scale mutagenesis of pre-RTA in the yeast, *Saccharomyces cerevisiae*, and isolated nontoxic RTA mutants on the basis of their inability to kill yeast cells. The pre-RTA instead of the mature RTA was used for mutagenesis to isolate mutants defective in intracellular trafficking, protein folding, stability and interaction with ribosomes. In a recent study using PCR-based mutagenesis of the mature RTA gene, 80% of the changes observed were T to C and A to G transitions (51). In contrast, 80% of the changes observed in our study using chemical mutagenesis were either C to T or G to A transitions. The PCR-based mutagenesis and the chemical mutagenesis complement one another and generate a wide array of useful mutations. However, they each have their own limitations. It is difficult to generate only single mutations in the in the PCR-based method. Multiple mutations are often obtained

and single mutations must then be generated to identify the mutation responsible for the phenotype. In contrast, only 2 of the 35 mutants generated in our study using hydroxylamine contained double mutations (Table 2.1).

The mutants isolated here were first screened for the loss of cytotoxicity and then by protein expression. Mutants that survived when RTA was induced were characterized for expression, and only those that expressed detectable levels of RTA were further characterized by nucleotide sequence analysis. The sequencing data correlated very well with the molecular weight of each protein. The RTA-specific antibody generated using the mature RTA as an antigen was able to recognize very small RTA peptides, including an 18 amino acid N-terminal peptide with a molecular weight of 5.8 kDa (Q19 stop) (data not shown). Immunoblot analysis indicated that the nontoxic mutant forms of RTA were expressed at higher levels than the wild type or the toxic forms of RTA (Figure 2.1).

Of the nine frameshift mutations isolated, seven of them were caused by a single base pair deletion and two of them had two base pair deletions (Table 2.1). These nine frameshift mutations were isolated only once. The twenty-five mutations with stop codons or single amino acid changes were caused by single base pair changes. Most of these mutations were isolated more than twice, and some were isolated nine times from different plates, indicating that the mutation screen was saturated. Furthermore, eleven out of the fourteen glutamines in pre-RTA were changed to stop codons, providing further evidence that the mutagenesis screen was saturated. Mutations were not isolated in three glutamines, Gln5, Gln98 and Gln266. If Gln5 were changed to a stop codon, the resulting four amino acid peptide would not have been detected by immunoblot analysis. If Gln266 were changed to a stop codon, RTA would be toxic (52) and would not be

isolated by our screen. Therefore, the only mutation we did not isolate is Gln98 changed to a stop codon.

The first 26 amino acids of the 35 amino acid N-terminal extension of pre-RTA represent the signal sequence. Mature RTA does not have the signal sequence, and therefore, it does not enter the ER. Despite this, mature RTA is toxic to yeast, as shown in figure 1.5. Hydroxylamine treatment did not result in any mutations in the N-terminal extension of pre-RTA, suggesting that these mutations did not affect the toxicity of RTA. Even if a mutation in the N-terminal extension had occurred, it might disrupt the ability of preRTA to translocate into the ER without affecting its cytotoxicity, since expression of the mature RTA is toxic to yeast (51). Similarly, mutations were not recovered at Asn10 and Asn236, which are glycosylated in the mature RTA. These results provided further evidence that glycosylation does not affect the toxicity of RTA (53).

The results from three separate random mutagenesis studies and several systematic deletion experiments, indicate that there are five regions important for the function of RTA: β strand D, α helix D, E, G-H, and a hydrogen-bonded turn and β strand region (Ile249 to Val256) close to the C-terminal end of the protein (Figure 2.5) (51, 5, 52, 54). The α helix E contains the active site residues, Glu177 and Arg180. The E177K mutation was isolated several times in different studies (51, 5). Mutations in Arg180, such as R180G (51) and Ile184 (Δ I184) (54) at the beginning of helix F disrupted the enzymatic activity of RTA in vitro, emphasizing the critical nature of this region (Table 2.1). In our study, deletion of Ile184 led to loss of cytotoxicity and a significant reduction in ribosome depurination activity of RTA in vivo (Table 2.1).

Ile184 may be critical for enzymatic activity, since it contacts Phe181 and methylene carbons of Glu177, stabilizing the active center (54).

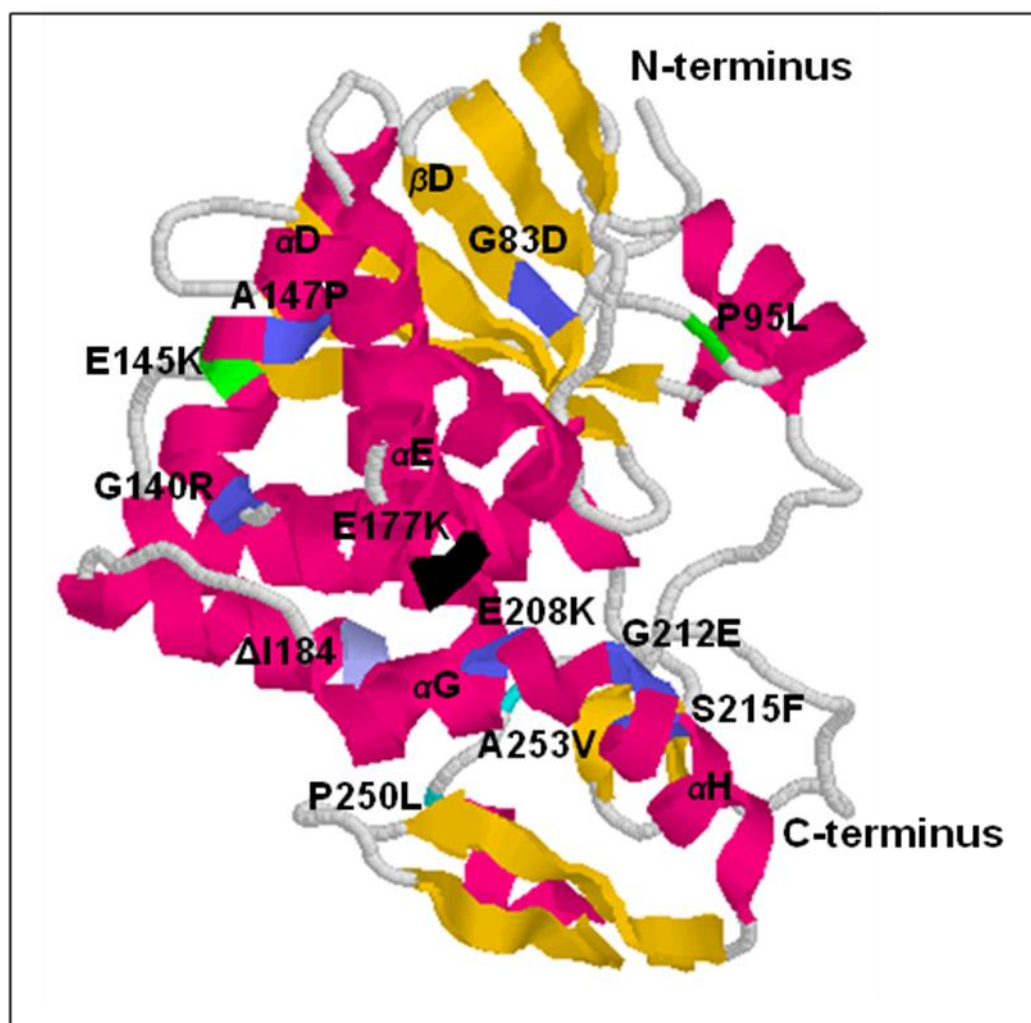


Figure 2.5: Three-dimensional structure of mature RTA showing the positions of the point mutations and the α -helices and β -sheets that contain these mutations. Coordinates of the crystal structure from the Protein Data Bank 1J1M were used in conjunction with the Protein Explorer software to create this figure. The point mutations are shown in blue. The active site mutation is shown in black. The double mutations are shown in green and cyan.

The alpha helices G to H have been the target of many different mutations, including those at Leu207, Glu208, Trp211, Gly212, Leu214 and Ser215 (55, 56, 54). Mutations in this region did not eliminate the depurination activity completely but they reduced the cytotoxicity. A mutation at Glu208 (E208K) reduced, but did not completely

eliminate the depurination activity of RTA (Table 2.1). Previous studies have shown that Glu208, which is at the bottom of the active site cleft can substitute for Glu177 in the E177A mutant (55). The E208D mutant with no change at position 177 had in vitro enzymatic activity equal to the wild type protein (54), indicating that Glu208 by itself does not play a major role in depurination.

The point mutation at Ser215 (S215F) in helix H, did not affect ribosome depurination in vivo, but significantly decreased the cytotoxicity of RTA (Table 2.1 and Figure 2.3). This mutant was enzymatically active in vitro (Figure 2.4). Previous studies showed that Ser215 can be deleted from RTA without complete loss of activity (56). Since S215F mutation led to loss of cytotoxicity without affecting ribosome depurination, the role of Ser215 in cytotoxicity can be separated from ribosome depurination. A point mutation in Gly212 in helix H (G212E) significantly reduced the depurination activity in vivo. Deletion of Gly212 led to loss of enzymatic activity of RTA in vitro (54). These results indicated that Gly212 in helix H is critical for ribosome depurination.

The α helix D crosses helix E in the middle (Figure 2.5). Each of the amino acids in helix D could be deleted, provided that the deletion does not disrupt the amphipathicity of the helix (57). Deletion of Ala147 in helix D abolished the activity of RTA in vitro, since the hydrophobic surface of helix D protects the helix E from solvent, further stabilizing the active center (54). The point mutation A147P reduced the depurination activity of RTA and led to loss of its cytotoxicity (Table 2.1). The A147P mutation likely disrupted the structure of helix D in the middle, destabilizing the active site. The point mutation at Gly140 (G140R), which is located at the beginning of helix D, resulted in the loss of both cytotoxicity and depurination (Table 2.1 and Figure 2.3). However, deletion

of this glycine did not affect the activity of RTA in vitro (54). These results indicated that the structure of RTA might be affected more when Gly140 is changed to an arginine than when it was deleted.

Mutation G83D (NT1031), which is in β strand D, eliminated the cytotoxicity of RTA in yeast cells and reduced its depurination activity (Figure 2.3). However, the G83D mutation did not completely eliminate the depurination activity of RTA in vivo. Since Gly83 is relatively distant from the active site, it is unlikely that Gly83 participates in the catalysis. Previous studies indicated that RTA lost its depurination activity when Gly83 was deleted (52, 54). These results suggested that β strand D might be important for the interaction of RTA with the ribosome, such that a mutation in this residue may affect binding of RTA to the ribosome. A point mutation in the corresponding Gly in pokeweed antiviral protein (PAP) (G75D) led to loss of depurination in vivo (25) and affected binding of PAP to ribosomes (58). In contrast to PAP, Gly83 in ricin is not sufficient for ribosome binding, since the G83D mutant retains some depurination activity in vivo.

The final important region is close to the C-terminal end of RTA. Stop codon mutations demonstrated that deleting 20 (L248 stop) amino acids from the C-terminal end of pre-RTA eliminated its cytotoxicity in yeast. The last frame shift mutation, P250L+S, which deleted 17 amino acids from the C-terminus and changed Pro250 to Leu, eliminated the depurination activity (Table I). Deletions from R258 to P262 or P263 to F267 did not affect cytotoxicity (52). However, mutations upstream of Arg258, at Ile252, Leu254 and Val256 eliminated the cytotoxicity of RTA (51, 5). The single mutations at Pro250 (P250L) and at Ala253 (A253V) had little effect on the cytotoxicity

of RTA or its ability to depurinate ribosomes. However, when they were combined (P250L-A253V), both cytotoxicity and ribosome depurination were eliminated. These results indicated that the C-terminal region of RTA is critical for ribosome depurination and cytotoxicity.

Sequence alignment analysis between RTA, a type II RIP, with mature PAP, a type I RIP, demonstrated only 30% identity. Many mutations which led to loss of cytotoxicity were in the residues which were conserved between RTA and PAP, indicating that these residues were critical for RIP activity. A majority of residues which are invariant among RIPs play an important role in the depurination reaction. The rest contribute to overall structure of the enzyme or may be critical for intracellular trafficking. Ricin has to enter the cytosol to depurinate ribosomes. Some bacterial toxins form pores in membranes. Ricin does not form pores in membranes, but may enter the cytosol from the ER using the Sec61 protein translocon (see Chapter 3). We have previously demonstrated that the C-terminal sequence of RTA is fairly homologous with the C-terminal sequence of PAP, which is critical for its transport into the cytosol (59). Since the point mutations in P250L-A253V correspond to this region, the double mutant may be unable to retrotranslocate from the ER into the cytosol. Further evidence for this is provided by the accumulation of larger forms of the protein in the ER in this mutant (Figure 2.1).

Although single mutations at Pro95 (P95L) and Glu145 (E145K) did not reduce cytotoxicity, the double mutant, P95L-E145K, was not toxic to yeast cells. The double mutant depurinated ribosomes at wild type levels (Table 2.1 and Figure 2.3), indicating that Pro95 and Glu145 were critical for cytotoxicity, but not for ribosome depurination

activity. These results and previous mutagenesis studies indicated that in some cases two amino acids must be changed simultaneously to eliminate the cytotoxicity of RTA (5). In these mutants, the first amino acid was usually located in a β strand region and the second amino acid was located in a α -helix region (L62-L129, L74-L139/T159/R193 (5) and P95-E145 in this study). The X-ray crystal structure indicated that the mutated residues in different regions of RTA do not interact with each other (Figure 2.5). Further studies will address the role of this mutant in the cytotoxicity of RTA.

Different methods for random mutagenesis have been used to isolate nontoxic RTA mutants in yeast cells (51, 5). Systematic deletion analysis has also been used to identify amino acids critical for the activity of RTA (54). We present the cytotoxicity and depurination data together and provide the first evidence that cytotoxicity of RTA is not entirely due to ribosome depurination.

CHAPTER 3: Ricin A chain utilizes the ERAD machinery to reach the cytosol

INTRODUCTION

The ricin holotoxin consists of a lectin binding B-chain and a ribosome depurinating A-chain. Upon binding to N-acetyl-galactosamine residues on target cells, ricin is taken up by endocytosis and transported to the Golgi complex. Ricin then undergoes retrograde transport to the ER where the disulfide bond between the A and B chains is reduced. RTA unfolds when the A and B chains separate allowing it to pass through the ER membrane to reach the cytosol. It must then refold to become active and depurinate ribosomes (11).

In order to reach the cytosol from the ER, RTA may utilize the Endoplasmic Reticulum-Associated Degradation (ERAD) pathway. The ERAD pathway is a quality control system that ensures that native proteins have been folded into their proper conformation before leaving the ER. If a protein is detected as misfolded or incomplete, it is removed from the ER and destroyed via the cytoplasmic ubiquitin-proteasome pathway (60). There are many proteins involved in the transport of RTA via the ERAD and proteasome pathway.

The Sec61translocon, which includes the proteins SEC61, SSS1 and SBH1 in yeast, is a protein conducting channel in the ER membrane (13). Sec61 is the primary export channel for ERAD and as such, is used to transport misfolded proteins from the ER to the tightly-associated cytosolic proteasomes where the misfolded proteins are degraded. In addition to protein export, SEC61 allows for co-translational protein import into the ER. Proteins destined to reach the ER must have an N-terminal signal which is recognized by the signal recognition particle (SRP) (30). Once this signal sequence is

translated, the actively translating ribosome must line up with the Sec61 channel (19) so that the protein may enter the Sec61 channel while it is unfolded.

The formation and function of the Sec61 complex in yeast relies on SEC63 (61), which is another integral membrane protein. The Sec63 complex is required for post-translational import of proteins into the ER and does not require the SRP. SEC63 contains a DNAJ-like domain that anchors an Hsp70 chaperone, KAR2, to the translocation channel (62). KAR2 is responsible for recognizing unfolded proteins in the ER and helping to fold them properly, and is also expected to help facilitate ERAD in yeast. KAR2 is also essential for the formation of a luminal seal during protein import into the Sec61 channel. Together, SEC63 and KAR2 allow post-translational translocation of proteins into the ER lumen (62), while SEC63, KAR2 and SEC61 are all necessary (61) for co-translational translocation.

Proteins that are destined to be degraded by the proteasome are ubiquitinated in the cytosol. Ubiquitins are attached to lysine residues of proteasome substrates via ubiquitin-conjugating enzymes (ubc's). Previous studies with ubc deletion mutants *ubc6Δ*, *ubc7Δ* and the double deletion mutant *ubc6Δ/ubc7Δ* demonstrated that the absence of these enzymes retards the ability of the cell to degrade proteasomal substrates (63). Reports have demonstrated, however, that ricin is not ubiquitinated due to the low number of lysine residues (17).

Before the ERAD substrate can be sent to the proteasome, modifications often occur. One of these modifications is deglycosylation. Long carbohydrate chains are too bulky for the proteasome (64) and are often removed in the cytosol with an N-glycanase called PNG1. PNG1 recognizes and cleaves glycosyl chains. However, in order to get

the glycosylated substrate to PNG1, RAD23 is needed. RAD23 has an N-terminal ubiquitin-like domain that is recognized by the proteasome. It also has a ubiquitin recognizing domain, and is capable of associating with PNG1. It is suspected that RAD23 recognizes and binds to ubiquitin residues of proteasome substrates, and then associates with PNG1, which subsequently cleaves the glycosyl groups. RAD23 then helps to facilitate the transfer of the ubiquitinated substrate to the proteasome via its ubiquitin-like domain.

If the pathway from the ER to the proteasome breaks down at any point, there is an opportunity for the ERAD substrate to reach the cytosol in its native and possibly active form. In this study, pre-RTA and the active site mutant pre-RTA_{E177K} were transformed into yeast with mutations in various components of the ERAD pathway. There is evidence suggesting that RTA uses Sec61 to enter the cytosol (11). However, there has been little evidence to support that RTA utilizes other proteins involved in ERAD. An initial screen was conducted in many ERAD mutants and those mutants that demonstrated either resistance to RTA or increased toxicity of RTA were analyzed further, specifically *sec61*, *kar2*, *rad23Δ*, *ubc7Δ* and *pre1-1*, *pre2-2*. The stabilization or decrease in ricin toxicity that was observed in these mutants indicates that RTA does use the ERAD pathway to reach the cytosol.

RESULTS

The cytotoxicity of pre-RTA is reduced in sec61 mutants

To determine if the Sec61 translocon is necessary for RTA cytotoxicity, yeast with a mutation in the ER luminal regions of the third and fourth transmembrane helices of SEC61 were transformed with pre-RTA or pre-RTA_{E177K}, or the mature RTA and

RTA_{E177K} (Figure 3.1 B) (65). These yeast mutants are temperature sensitive and when grown at the restrictive temperature, the ability of SEC61 to export proteins from the ER to the cytosol is inhibited, while the import function is not. Pre-RTA or RTA were cloned into a vector with a V5 epitope tag (pYES) in order to detect expression. After transformation, yeast colonies were streaked on both SD-Leu –Ura media containing glucose and SD-Leu –Ura media containing galactose (Figure 3.1 B). *Sec61-32* and *sec61-41* were able to survive better than wildtype yeast when transformed with pre-RTA, although *sec61-32* cells seemed more resistant to pre-RTA than *sec61-41*. These results show that the effect of pre-RTA cytotoxicity was reduced in these Sec61 mutants, and that a properly functioning Sec61 translocon is necessary for the cytotoxicity of pre-RTA. In addition, viability assays were conducted as previously described, and the *sec61-32* and *sec61-41* yeast cells expressing pre-RTA were more viable than wildtype cells expressing pre-RTA (Figure 3.2).

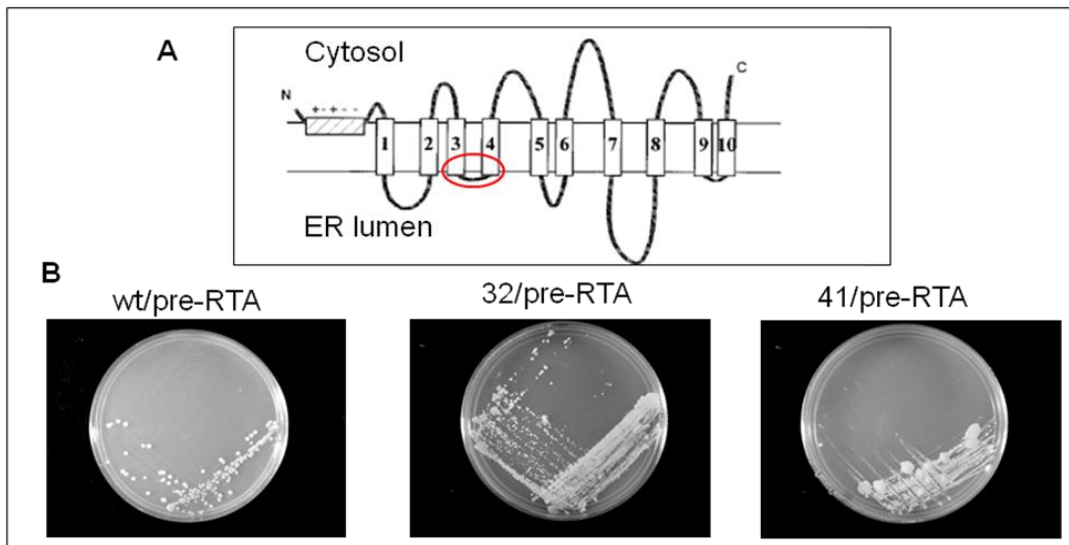


Figure 3.1: The *sec61-32* and *sec61-41* yeast mutants reduce the cytotoxicity of pre-RTA. A. The *sec61-32* and *sec61-41* mutations are located on the luminal side of transmembrane domains 3 and 4, and impair protein export from the ER to the cytosol (65). B. Yeast *sec61-32* and *sec61-41* mutants expressing pre-RTA were streaked onto SD-Leu plates containing galactose.

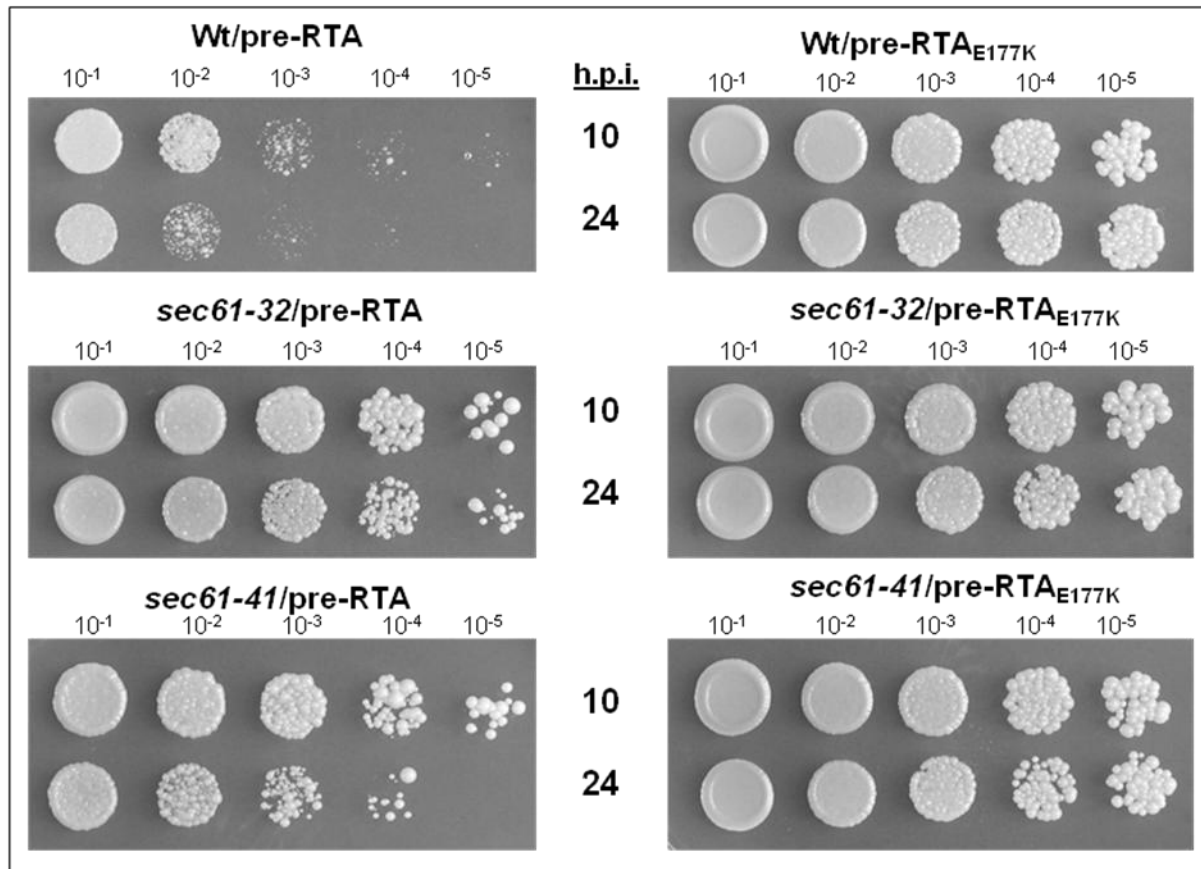


Figure 3.2: *sec61-32* and *sec61-41* yeast expressing pre-RTA are viable compared to wildtype yeast. Yeast cells expressing pre-RTA or pre-RTA_{E177K} were induced for 10 and 24 hours on SD-Leu galactose media and were then plated as serial dilutions onto SD-Leu glucose plates.

Pre-RTA is stabilized in sec61 mutants

In order to confirm that the reduction in toxicity of the Sec61 mutants was not due to a reduction in pre-RTA expression, immunoblot analysis was conducted. The transformed yeast cells were grown in SD-Leu –Ura liquid media containing glucose until they reached a cell density of approximately OD₆₀₀ 0.3. The cells were then transferred to SD-Leu –Ura containing galactose media. Aliquots of the cells were taken at 4, 6, 10 and 24 hours post-induction. The cells were lysed using a low salt buffer and the cellular components were fractionated into membrane and cytosolic proteins. The

membrane proteins were then run on a 15% SDS-PAGE gel, transferred to nitrocellulose membranes and probed with α -V5 antibodies.

The amount of pre-RTA and pre-RTA_{E177K} in the ER membrane fraction of wildtype yeast cells is destabilized over time, and at 24 hours post-induction there is very little protein associated with the ER (Figure 3.3). In contrast, in the Sec61 mutant strains, pre-RTA and pre-RTA_{E177K} are stabilized even at 24 hours post-induction. This indicates that pre-RTA is accumulating in the ER of the *sec61* yeast mutants.

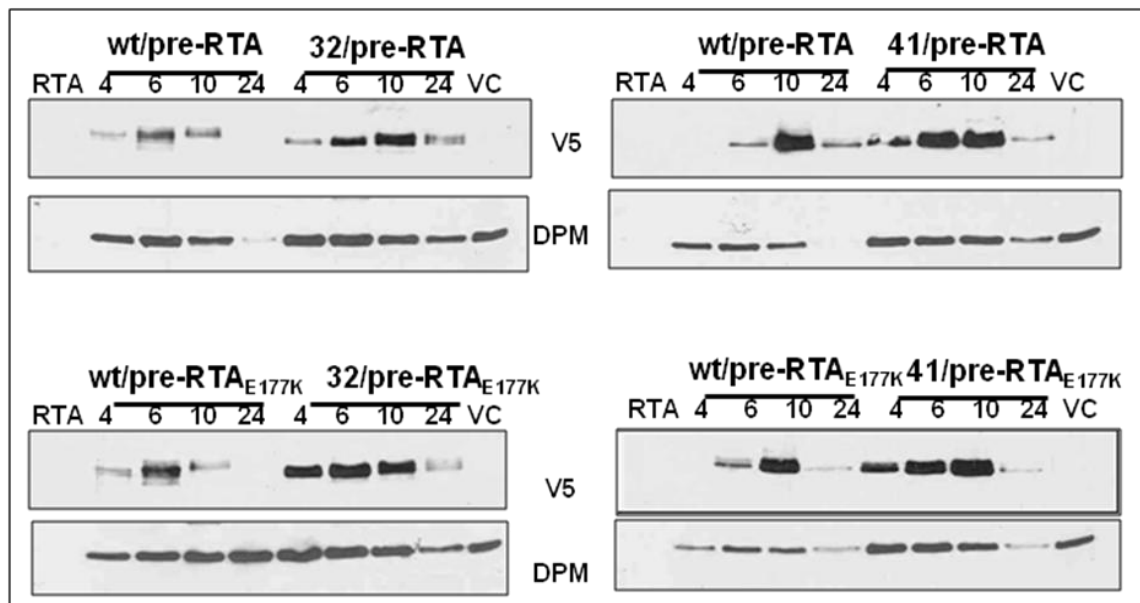


Figure 3.3: Pre-RTA is stabilized in *sec61-32* and *sec61-42*. Membrane fractions (15 μ g) isolated from Sec61 mutant yeast cells expressing pre-RTA or pre-RTA_{E177K} at 4, 6, 10 and 24 hours post-induction were separated on a 12% SDS-polyacrylamide gel and probed with anti-V5 antibody. The blots were stripped and probed with the ER membrane marker Dpm1p as a loading control.

To further confirm the use of SEC61 by pre-RTA and pre-RTA_{E177K}, mature RTA and RTA_{E177K} were transformed into the same yeast strains. RTA and RTA_{E177K} do not have the ER signal sequence and are not translocated into the ER lumen. RTA was just as toxic in the *sec61* mutants as in the wildtype yeast cells (data not shown) and there was no accumulation of protein associated with the ER fraction. However, even though these

mature proteins are not entering the ER, they are still associated with the ER, as indicated by the detection of RTA and RTA_{E177K} with the ER fraction of cell lysates (Figure 3.4).

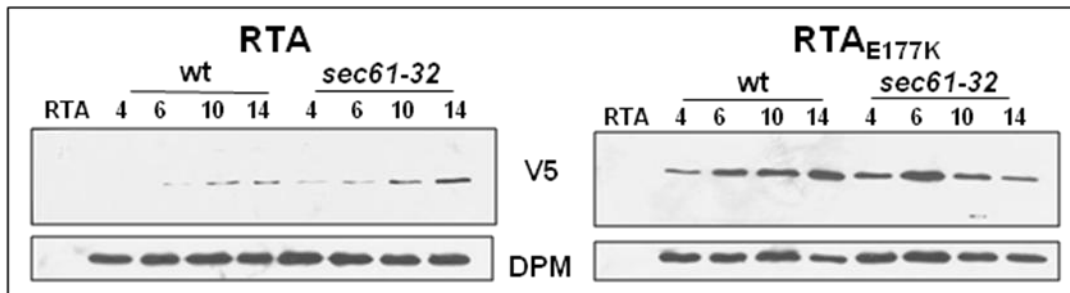


Figure 3.4: RTA is not stabilized in *sec61-32*. Membrane fractions (15 μ g) isolated from Sec61 mutant yeast cells expressing RTA or RTA_{E177K} at 4, 6, 10 and 14 hours post-induction were separated on a 12% SDS-polyacrylamide gel and probed with anti-V5 antibody. The blots were stripped and probed with the ER membrane marker Dpm1p as a loading control.

*Pre-RTA ribosome depurination is reduced in *sec61-32**

Because the *sec61* mutants exhibited reduced cytotoxicity but high levels of pre-RTA expression, it was essential to determine if the protein was still active in these yeast mutants. Yeast cells were grown as described above and induced on galactose containing media for 6 hours. Total RNA was isolated from these yeast cells and subsequently subjected to a dual primer extension assay to determine if the protein is still depurinating yeast ribosomes.

As seen in Figure 3.5, pre-RTA is capable of depurinating ribosomes of both *sec61* yeast mutants. However, the level of pre-RTA depurination is slightly reduced in *sec61-32* cells. The reduction in depurination in Sec61-32 cells is probably not due to lack of activity of pre-RTA. Instead, it is most likely a result of pre-RTA getting retained in the ER, and not accessing ribosomes in the cytosol. This may explain why *sec61-32* expressing pre-RTA grows slightly better on galactose than *sec61-41* (Figure 3.1).

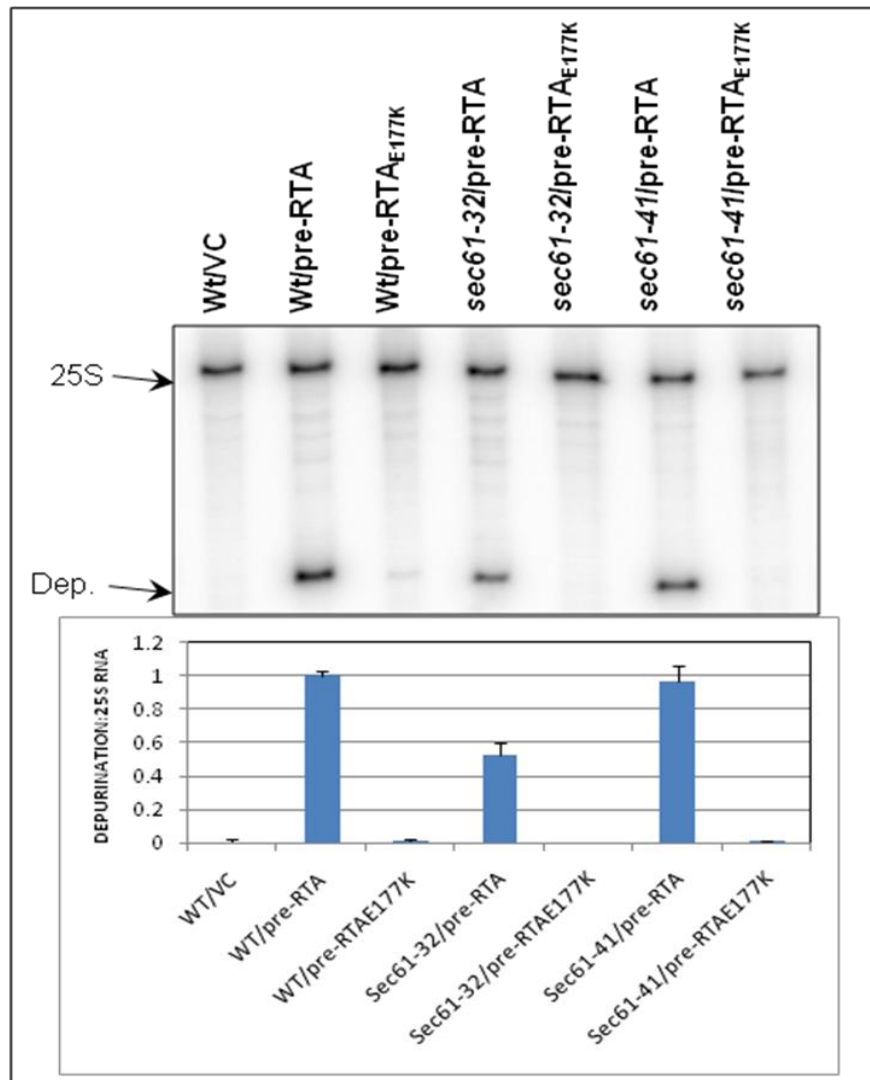


Figure 3.5: Pre-RTA ribosome depurination is reduced in *sec61-32*. Total RNA isolated from the *sec61* yeast mutants expressing pre-RTA or pre-RTA_{E177K} after 6 h of growth on galactose was analyzed by dual primer extension. The depurination bands and 25S bands were quantified and graphed as a ratio of depurination:25S.

kar2 yeast mutants expressing pre-RTA are viable

Yeast cells with a mutation in KAR2 residue P515 (*Kar2-1*), which is part of a highly conserved region of the substrate binding domain of KAR2 (29), were transformed with pre-RTA and the inactive mutant, pre-RTA_{E177K}. The *kar2-1* mutation is temperature sensitive, and at 24°C, *kar2-1* cannot recognize ERAD substrates in the ER. In addition, the *kar2-1* mutation induces the unfolded protein response when it is

expressed (29). The *kar2-1* yeast transformants were streaked on SD -Ura media containing glucose and SD -Ura media containing galactose. *Kar2-1* mutants were fairly resistant to pre-RTA expression and were able to grow on galactose containing media.

To confirm that pre-RTA is not as toxic to *kar2-1* cells as wildtype cells, a viability assay was performed. Transformed wildtype and *kar2-1* cells were grown as indicated above in liquid media. After 4 and 10 hours of growth on galactose, the cells were collected and spotted as a serial dilution onto SD-Ura plates containing glucose. After two days of growth at the permissive temperature, the plates were analyzed. Pre-RTA in the *kar2-1* yeast cells did not affect cell viability as much as in wildtype yeast cells (Figure 3.6), indicating that *Kar2-1* is necessary for pre-RTA cytotoxicity.

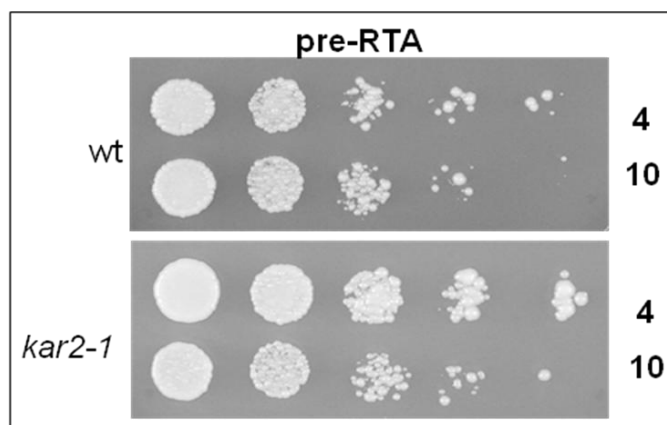


Figure 3.6: *kar2-1* yeast mutants are more viable than wildtype yeast when expressing pre-RTA. After 4 and 10 hours of growth on SD-Leu medium containing galactose, serial dilutions were spotted on SD-Leu plates supplemented with 2% glucose.

Pre-RTA is recognized as a substrate of KAR2

kar2-1 yeast cells transformed with pre-RTA and pre-RTA_{E177K} were grown as described above and were induced on galactose containing media after 4, 6, 10 and 14 hours. Cells were lysed and the membrane fraction was run on a 15% SDS-PAGE gel and probed with α -V5 antibody. Figure 3.7 shows that there are several bands migrating

slightly higher than the RTA standard, indicating the different levels of glycosylation of pre-RTA. Compared to the expression of pre-RTA in wildtype yeast cells, expression in *kar2-1* mutant cells indicates an altered level of glycosylation. Because glycosylation occurs in the ER, the amount or extent of glycosylation of pre-RTA can be used as an indication of how long the protein remained in the ER. Compared to pre-RTA expression in the wildtype cells, the *kar2-1* cells show a reduction in the glycosylated forms of pre-RTA. This suggests that the *kar2-1* mutation is affecting the amount of time that pre-RTA is retained in the ER. One of the functions of wildtype KAR2 is to bind to unfolded proteins and help to stabilize and refold them. However, because the *kar2-1* mutants are defective in their substrate binding ability, pre-RTA is most likely not recognized by *kar2-1*, and is therefore sent through the Sec61 translocon quicker than it would in wildtype cells.

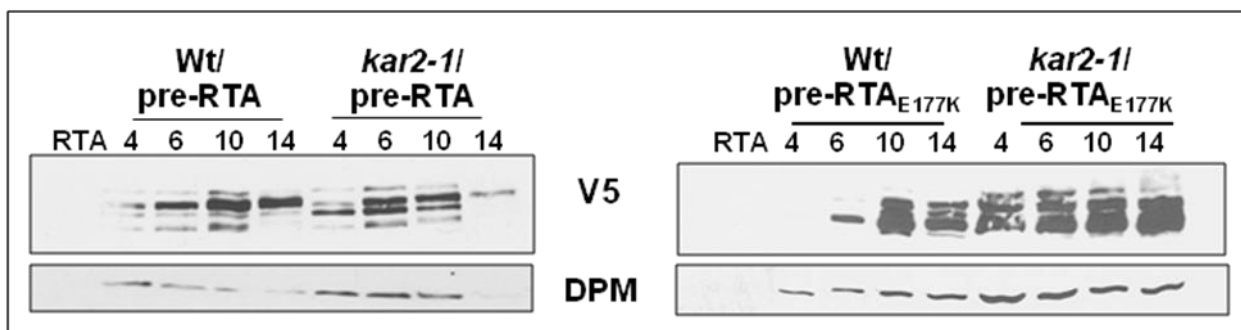


Figure 3.7: The expression pattern of pre-RTA and pre-RTA_{E177K} is altered in *kar2-1* yeast mutants. Membrane fractions (15 µg) isolated from wildtype and *kar2-1* mutant yeast cells expressing pre-RTA or pre-RTA_{E177K} at 4, 6, 10 and 14 hours post-induction were separated on a 15% SDS-polyacrylamide gel and probed with anti-V5 antibody. The blots were stripped and probed with the ER membrane marker Dpm1p as a loading control.

*Pre-RTA can still depurinate yeast ribosomes in *kar2-1* mutants*

To determine if the *kar2-1* mutation affects the enzymatic activity of pre-RTA or the complete ability of pre-RTA to reach the cytosol, primer extension analysis was used. The dual primer extension assay was performed on total RNA of wildtype and *kar2-1*

yeast cells expressing pre-RTA as described above. In both wildtype and *kar2-1* mutants, depurination occurred (Figure 3.8). This indicates that pre-RTA is still able to eventually enter the cytosol in *kar2-1* mutant cells, and that there is no effect of depurination activity in these yeast mutants.

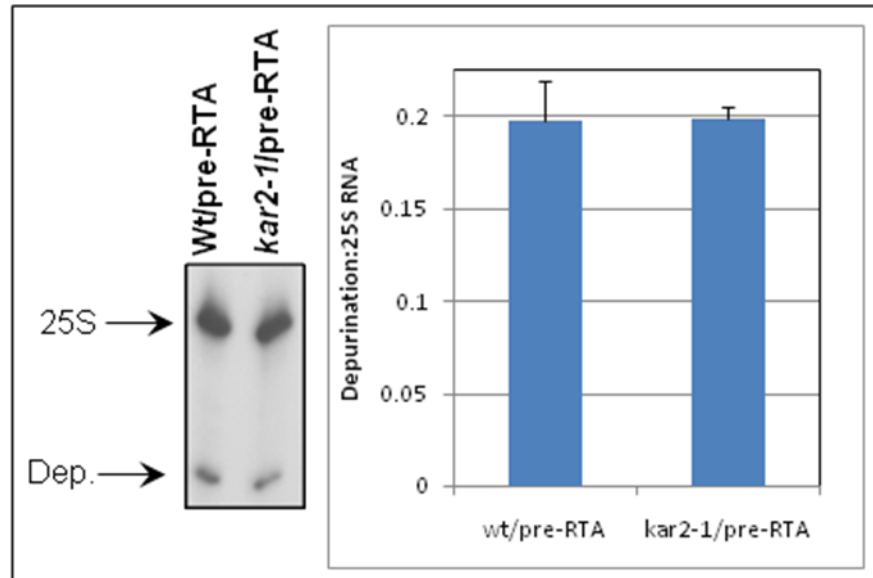


Figure 3.8: Pre-RTA can still depurinate *kar2-1* ribosomes. Total RNA isolated from wildtype and *kar2-1* yeast mutants expressing pre-RTA after 6 h of growth on galactose was analyzed by dual primer extension. The depurination bands and 25S bands were quantified and graphed as a ratio of depurination:25S.

kar2-113 has no effect on pre-RTA

Pre-RTA and pre-RTA_{E177K} were also transformed into another *kar2* mutant, *kar2-113*. This yeast mutant is deficient in the ATPase activity of KAR2 (29), which blocks the dissociation of KAR2 from IRE1, a UPR activator. In contrast to the *kar2-1* mutant, the *kar2-113* cells were still resistant to pre-RTA. The expression pattern and depurination were all similar to that of wildtype cells, indicating that the KAR2 ATPase domain is not essential for pre-RTA toxicity (data not shown).

*Pre-RTA is stabilized in the *ubc7Δ* deletion mutant*

Pre-RTA and pre-RTA_{E177K} were transformed into three different yeast strains with deletion mutations in the ubiquitin conjugating enzymes *ubc6Δ*, *ubc7Δ* or both *ubc6Δ/ubc7Δ*. Deletion of these ubiquitin conjugating enzymes generally retards the targeting of proteins for proteasomal degradation (63). When pre-RTA and pre-RTA_{E177K} were transformed into these ubiquitin mutants, there was no reduction in toxicity (data not shown). However, when the cells were induced and expression was analyzed via immunoblot analysis, protein levels of pre-RTA and pre-RTA_{E177K} was elevated in *ubc7Δ* yeast mutants compared to wildtype yeast (Figure 3.9). This indicates that the loss of UBC7 stabilizes pre-RTA and that UBC7 may play a role in pre-RTA cytotoxicity.

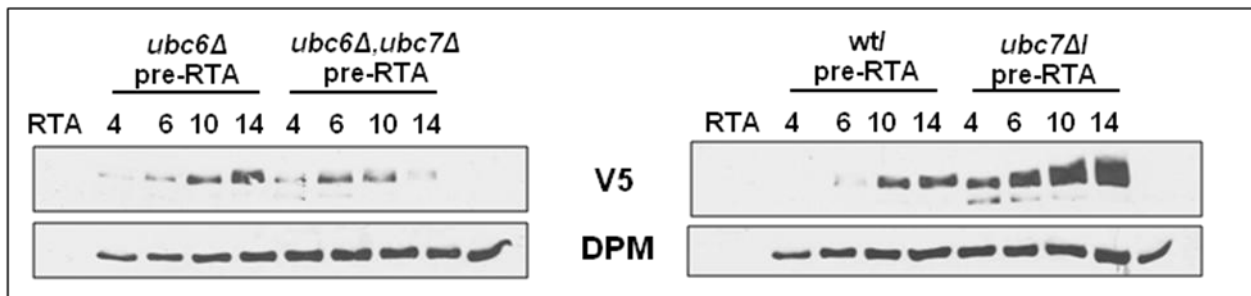


Figure 3.9: Pre-RTA is stabilized in the *ubc7Δ* mutant. Membrane fractions (15 μ g) isolated from wildtype and *ubc* mutant yeast cells expressing pre-RTA at 4, 6, 10 and 14 hours post-induction were separated on a 15% SDS-polyacrylamide gel and probed with anti-V5 antibody. The blots were stripped and probed with the ER membrane marker Dpm1p as a loading control.

rad23Δ mutants are resistant to pre-RTA

The protein RAD23 is an ERAD component that recognizes glycosylated and ubiquitinated proteins and helps to guide them to the deglycosylating enzyme, PNG1, and the proteasome (18). Yeast cells with a deletion in the *RAD23* gene were transformed with pre-RTA and pre-RTA_{E177K}. Cells were grown and assayed for viability as described above. *rad23Δ* mutant cells expressing pre-RTA were more viable than

wildtype cells (Figure 3.10), suggesting that pre-RTA toxicity relies on a function of RAD23.

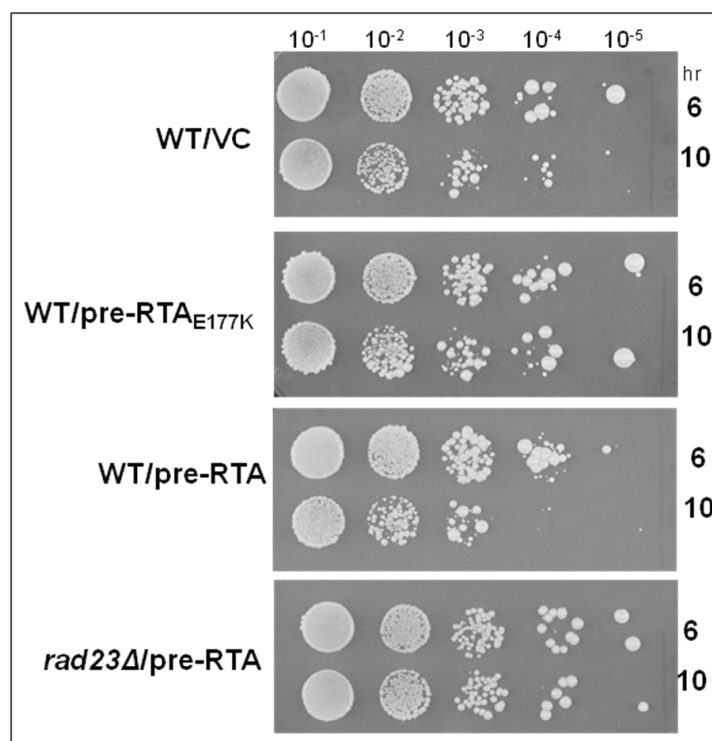


Figure 3.10: *rad23Δ* yeast mutants expressing pre-RTA are viable. After 6 and 10 hours of growth on SD-Leu medium containing galactose, serial dilutions of wildtype and *rad23Δ* mutant yeast cells expressing pre-RTA, pre-RTA_{E177K} or the empty vector control were spotted on SD-Leu plates supplemented with 2% glucose.

Pre-RTA expression is reduced by the deletion of rad23Δ

Pre-RTA expression was analyzed via a 15% SDS-PAGE and immunoblot probing as described above. Compared to wildtype cells, *rad23Δ* mutant cells expressed pre-RTA to a lower extent (Figure 3.11). This may indicate that RAD23 is one of the proteins that play a role in the stability of RTA in the cytosol. It is possible that the reduction in pre-RTA cytotoxicity (Figure 3.10) is due to a reduction in total pre-RTA accumulation. Although RAD23 seems essential for pre-RTA toxicity, as shown with the viability assay, it is possible that there are additional proteins that aid in PNG1 mediated deglycosylation. Also, because there is a destabilization of pre-RTA in the *rad23Δ*

mutant cells, RAD23 may play a role in the transfer of pre-RTA to the proteasome, where protein degradation occurs, rather than deglycosylation.

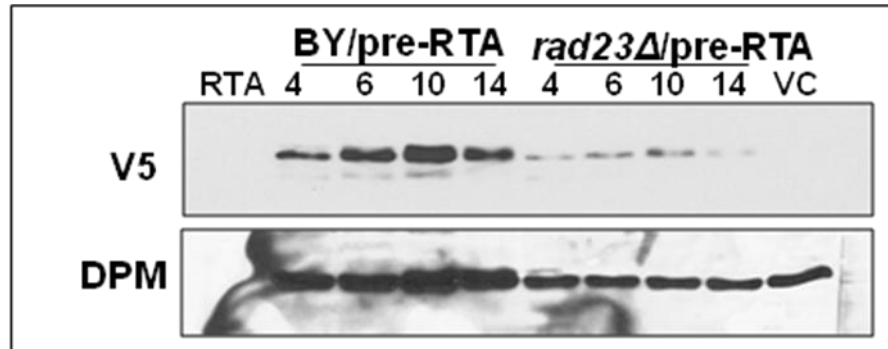


Figure 3.11: Pre-RTA expression is reduced in the *rad23Δ* mutant. Membrane fractions (15 μ g) isolated from wildtype and *rad23Δ* mutant yeast cells expressing pre-RTA at 4, 6, 10 and 14 hours post-induction were separated on a 15% SDS-polyacrylamide gel and probed with anti-V5 antibody. The blots were stripped and probed with the ER membrane marker Dpm1p as a loading control.

*Pre-RTA depurination is reduced in *rad23Δ* mutants*

To determine if the *rad23Δ* mutation affects the enzymatic activity of pre-RTA, and therefore is reducing pre-RTA mediated toxicity, primer extension analysis was performed as described above. Pre-RTA did not depurinate ribosomes in *rad23Δ* mutants to the same extent as it did in wildtype yeast cells (Figure 3.12). However, this could be a result of the decrease in total expression of pre-RTA in the *rad23Δ* mutants (Figure 3.11). The fact that there is still some depurination activity in the *rad23Δ* mutant indicates that pre-RTA is still functioning properly in the *rad23Δ* mutants.

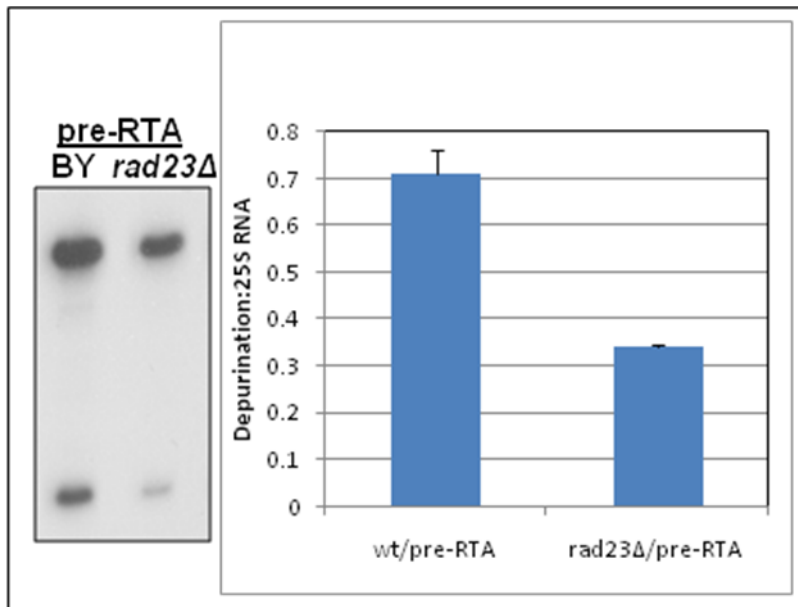


Figure 3.12: Pre-RTA depurination is reduced in *rad23Δ* yeast mutants. Total RNA isolated from wildtype and *rad23Δ* yeast mutants expressing pre-RTA after 6 h of growth on galactose was analyzed by dual primer extension. The depurination bands and 25S bands were quantified and graphed as a ratio of depurination:25S.

pre-RTA_{E177K} is stabilized in Proteasome Mutants

The yeast mutant *pre1-1*, *pre2-2* is defective in the chymotryptic-like activity of the 19S subunit of the proteasome (66). The initial phenotype that was observed when the double mutation was isolated was an accumulation of ubiquitinated substrates in the cytosol, due to the fact that these substrates were no longer degraded by the mutated proteasome. *pre1-1*, *pre2-2* cells were transformed with pre-RTA and pre-RTA_{E177K}. RTA toxicity was similar in both wildtype cells and *pre1-1*, *pre2-2* cells as confirmed by lack of growth on galactose media (Figure 3.13). Because expression of pre-RTA in the *pre1-1*, *pre2-2* cells was extremely toxic and the cells grew poorly, pre-RTA_{E177K} was used to examine protein stability in the proteasome mutants. Wildtype and *pre1-1*, *pre2-2* cells transformed with pre-RTA_{E177K} were grown and aliquoted at 4, 6, 10 and 14 hours post-induction as described above. Protein expression was analyzed by SDS-PAGE and

probed as described above. In the *pre 1-1*, *pre2-2* mutants, pre-RTA_{E177K} was stabilized up to 14 hours post induction (Figure 3.14). This indicates that the proteasome is essential for degrading pre-RTA_{E177K}. It is predicted that cytotoxicity is greater in *pre 1-1*, *pre2-2* cells expressing pre-RTA than wildtype cells expressing pre-RTA, because any pre-RTA that would normally be degraded by the proteasome is stabilized in the *pre 1-1*, *pre2-2* cells, thereby accumulating in the cytosol and inducing severe toxicity.

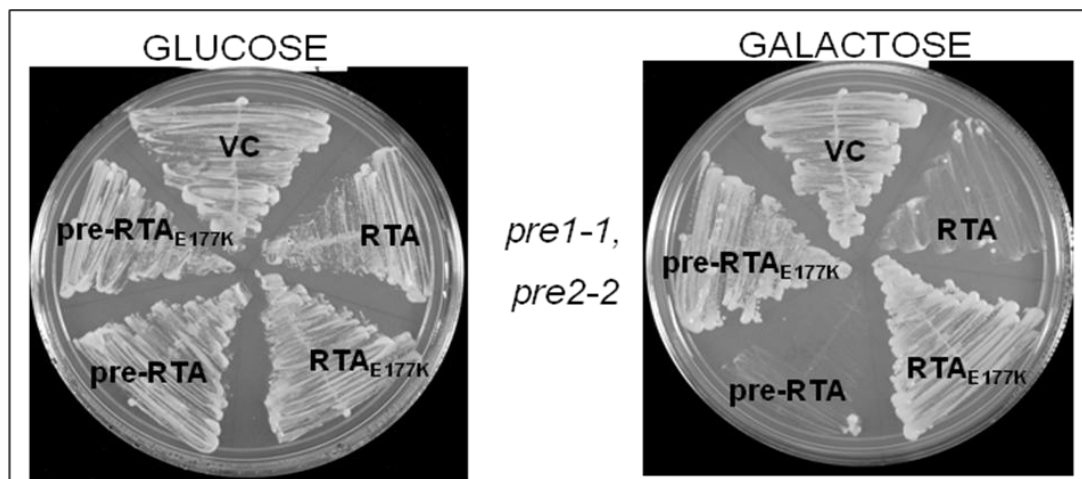


Figure 3.13: Pre-RTA is still toxic in the proteasome mutant. Proteasome mutants expressing pre-RTA, pre-RTA_{E177K}, RTA, RTA_{E177K} or the empty vector were streaked onto SD-Leu plates containing glucose and SD-Leu plates containing galactose. The plates were incubated at 30°C for 48 hours.

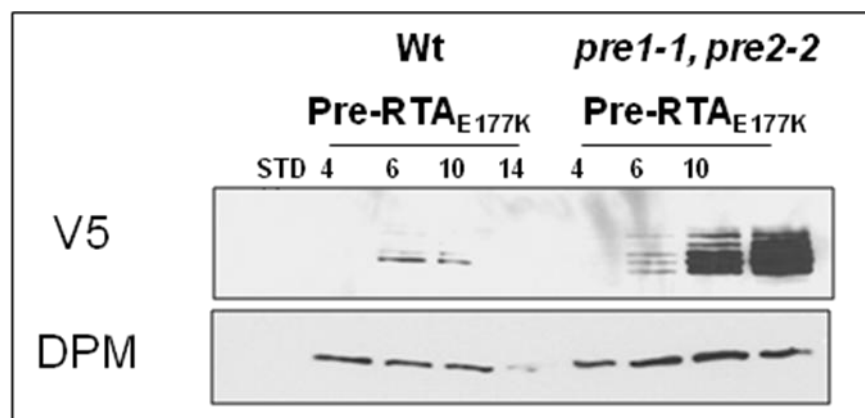


Figure 3.14: Pre-RTA_{E177K} is stabilized in the proteasome mutant. Membrane fractions (15 µg) isolated from wildtype and proteasome mutant yeast cells expressing pre-RTA_{E177K} at 4, 6, 10 and 14 hours post-induction were separated on a 15% SDS-polyacrylamide gel and probed with anti-V5 antibody. The blots were stripped and probed with the ER membrane marker Dpm1p as a loading control.

DISCUSSION

The results presented here provide evidence that pre-RTA uses the endoplasmic reticulum associated degradation pathway to reach the cytosol in yeast. Several studies have been published that support the use of ERAD by RTA. My work provided further support for this and identified the components of the ERAD pathway critical for RTA transport.

Olsnes (11) first found that RTA was associated with Sec61 by co-immunoprecipitation assays. He showed that Sec61 pulled down glycosylated, but not unglycosylated RTA. This indicates that RTA associates with SEC61 in the ER, where glycosylation occurs. Another study (67) analyzed RTA in yeast and showed that an inactive form of RTA with a Kar2 ER signal sequence, RTA_{E177D}, was stabilized in the *sec61* mutants. However, they did not analyze wildtype RTA in these *sec61* mutants.

In this study, we suggest that Sec61 is necessary for pre-RTA toxicity. By eliminating the export ability of Sec61 with the temperature sensitive mutants *sec61-32* and *sec61-42*, accumulation of pre-RTA and pre-RTA_{E177K} is increased in the ER fraction. Accordingly, the translocation of pre-RTA from the ER to the cytosol is probably affected, at least in *sec61-32*. While detection of pre-RTA and even the non-toxic pre-RTA_{E177K} in the cytosolic fraction of cell lysates is difficult, one way to determine if pre-RTA is even reaching the cytosol is to examine ribosome depurination. In the *sec61-32* cells, pre-RTA ribosome depurination is reduced in wildtype cells, indicating that pre-RTA is not reaching the cytosol as efficiently in that mutant.

Further evidence for the use of SEC61 by pre-RTA is shown by the lack of effect that the *sec61* mutants had on RTA and RTA_{E177K}. These mature proteins are in the same

yeast expression vector as pre-RTA and pre-RTA_{E177K}, but do not have the ER signal sequence. Although these mature proteins associate with the ER, as indicated by the accumulation of protein in the ER fraction of cell lysates, they are not glycosylated, indicating that they don't enter the ER lumen. As expected, toxicity of RTA in the *sec61* mutants was the same as in wildtype cells, and there was no accumulation of RTA or RTA_{E177K}.

The functions of KAR2 are of particular interest when studying RTA due to the fact that KAR2 has many roles as an ER resident chaperone. One of the functions of KAR2 is helping to fold misfolded or slowly folding proteins in the ER lumen (29). As a result of this chaperone activity, there are several possible events to follow. One possible outcome is that KAR2 will correctly stabilize and fold the protein, allowing it to continue on its route. Another possibility is that KAR2 will assist with the folding of the protein, but will take an extended amount of time. When there is a large amount of KAR2 attempting to properly fold a substrate in the ER, the cell is signaled to slow down the translation of more of these proteins, and overall protein translation is reduced. In addition, when KAR2 is recruited to these misfolded substrates, the Unfolded Protein Response (UPR) is activated (27). When the UPR is activated, the protein folding capabilities of the cell are maximized to allow the cell to begin functioning properly again.

There is little published evidence that indicates that RTA directly uses KAR2. Here, we show that a mutation in the substrate binding domain of KAR2 reduced the toxicity of and changed the amount of glycosylation of pre-RTA. It is possible that a function of *kar2-1* in pre-RTA translocation may be to help stabilize and fold the protein,

and that this assistance is necessary for sufficient amounts of pre-RTA to reach the cytosol to induce cytotoxicity. Although the ability to depurinate yeast ribosomes in both wildtype and *kar2-1* mutants was the same, it is important to realize that depurination and cytotoxicity do not always correlate in pre-RTA, as demonstrated in Chapter 2.

In addition to the *kar2-1* mutant cells, *kar2-113* cells were transformed with pre-RTA. *kar2-113* cells are mutated in the ATPase binding domain, and are expected to be defective in KAR2-mediated import into the ER (29). As previously described, protein import into the ER can occur co-translationally or post-translationally. KAR2 and SEC63 are two necessary factors for the post-translational translocation of proteins into the ER, and it is expected that KAR2 acts as a luminal gate to allow entry through the Sec61 translocon. When pre-RTA expression was induced in the *kar2-113* cells, there was no reduction of cytotoxicity. In addition, the protein expression pattern of pre-RTA in these cells was the same as in wildtype cells. Pre-RTA was also able to depurinate to the same extent in *kar2-113* cells as in wildtype cells, indicating that the mutation is not affecting the enzymatic ability of pre-RTA. These results demonstrate that KAR2 is either not essential for pre-RTA import into the ER, or that pre-RTA is translocated into the ER co-translationally and does not require the use of KAR2 for entry into the ER.

When *rad23Δ* deletion mutants were transformed with pre-RTA, cells were more viable than the pre-RTA transformed wildtype cells. However, pre-RTA was not stabilized and did not accumulate in the *rad23Δ* cells. Previous studies by Kim (18) used RTA as a substrate to better understand the interaction between RAD23 and PNG1. RAD23 recognizes and binds to ubiquitin residues of proteasomal substrates. RAD23 also binds PNG1, which deglycosylates proteasome substrates prior to delivery to the

proteasome. A model was devised which shows RAD23 binding to the ubiquitin residues of a glycosylated proteasome substrate (RTA) and then binding to PNG1. This complex then allows PNG1 access to deglycosylate RTA. RTA is subsequently transported to the proteasome via the ubiquitin-like domain of RAD23 that binds to the proteasome (18).

Of course, this model of the dependency of RTA on RAD23 is based on the fact that RTA is ubiquitinated as a result of being an ERAD substrate. However, previous studies (17) that looked at the ubiquitination of RTA suggested that RTA is not ubiquitinated. Ubiquitin residues are attached to lysine residues of proteasome substrates. RTA only has two lysine residues, and it has been postulated that this low lysine content allows RTA to escape from the ER via ERAD, but then evade degradation in the proteasome because it does not get heavily ubiquitinated (17). In order to test this hypothesis, the group expressed RTA in yeast mutants defective in ubiquitin conjugating enzymes. They found that when the ability of the cell to attach ubiquitin residues was abolished, there was little effect on the toxicity or protein stabilization of RTA. In another study, several residues in RTA were changed to lysines (68). The additional lysine residues appeared to have a reduction in cytotoxicity and an increase in proteasomal degradation. The authors therefore concluded that RTA does not get ubiquitinated and is therefore able to avoid degradation by the proteasome. However, in this study, we have found that deletion of the ubiquitin conjugating enzyme, UBC7, greatly increased the stability of pre-RTA and pre-RTA_{E177K} expression, suggesting that RTA may get ubiquitinated to some degree.

Many groups have studied the degradation of RTA via the proteasome, which is the final destination for ubiquitinated ERAD substrates. In this study, pre-RTA was so

toxic to the proteasome mutant cells and the wildtype cells that it was difficult to analyze the effect of the proteasome mutant on pre-RTA. Therefore, pre-RTA_{E177K} was transformed into the proteasome mutant cells and analyzed. As expected, pre-RTA_{E177K} was stabilized in the proteasome mutant, indicating that the proteasome does normally degrade a significant amount of RTA. As the proteasome is the endpoint for ERAD substrates, it supports the theory that RTA does normally utilize the ERAD pathway to some degree.

Taken together, the data presented here suggests that RTA exits the ER via the SEC61 translocon and utilizes the components of ERAD to reach the cytosol. Interestingly, these data indicate that RTA is both ubiquitinated and targeted to the proteasome, which should ultimately lead to its degradation. However, there must be at least a portion of RTA that escapes this degradation to access and depurinate ribosomes. The fact that the deletion mutants *ubc7Δ*, but not *ubc6Δ* or the double mutant *ubc6Δ,ubc7Δ* affected stability of pre-RTA may indicate that RTA is ubiquitinated by UBC7, but not UBC6. This may suggest that the total amount of RTA that is targeted to the proteasome is less than other proteasome substrates that normally get ubiquitinated by both UBC6 and UBC7.

CHAPTER 4: Mutations in the C-terminal hydrophobic stretch of ricin A chain inhibit retro-translocation without reducing the catalytic activity

INTRODUCTION

There is a strong similarity among several regions of the sequences of RIPs, and protein structures of several of them allow for near perfect superimposable images (Figure 4.1). One region of high sequence homology is the C-terminal domain (Figure 4.1). For several RIPs, namely Stx and PAP, there have been studies suggesting that the C-terminus is necessary for protein translocation in the cell, primarily by containing a hydrophobic membrane spanning domain (69, 70). These hydrophobic domains have been suggested to act as membrane insertion extensions that can target the RIP to specific membranes in the target cell. Studies in shiga toxin demonstrated that disruption of this hydrophobic domain via point or truncation mutations resulted in an inactive protein (71). Interestingly, there is a common critical residue in both PAP (N253) and Shiga-toxin (N241) that, when deleted along with the remaining downstream residues, results in a loss of cytotoxicity and depurination ability (69, 70). In order to determine if the C-terminus of ricin is also essential for cytotoxicity, various truncation and point mutations were generated and analyzed in both mature RTA (RTA) and RTA with its N-terminal signal sequence (pre-RTA). The results suggest that ricin, like shiga-toxin and PAP, relies on the C-terminal residues for membrane translocation and enzymatic activity.

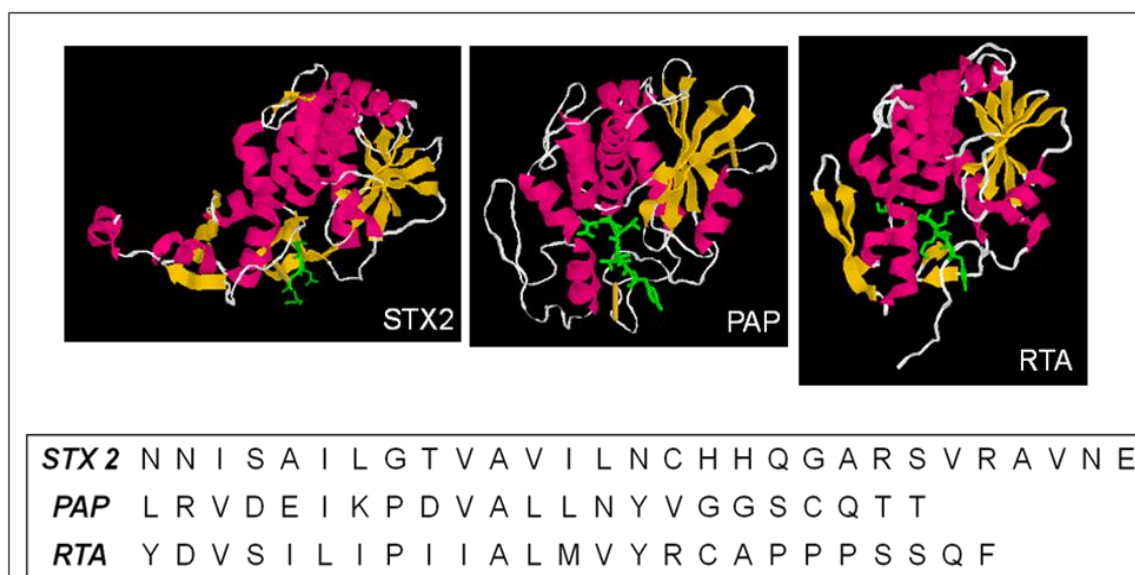


Figure 4.1: Structural comparison and sequence alignment of Shiga-toxin 2 (STX2), Pokeweed Antiviral Protein (PAP) and Ricin A chain (RTA). Protein Explorer (www.proteinexplorer.org) was used to generate the structural models using the PDB IDs 1R4P (STX2), 1PAG (PAP) and 1IFT (RTA). The green tail represents the C-terminal residues that are essential for protein toxicity.

RESULTS

The C-terminal residues of pre-RTA are essential for cytotoxicity

Stop codon mutations (*) were generated in residues I249, P250, I251, I252, A253, L254, M255, V256 and Y257 in order to truncate the C-terminus of pre-RTA (Table 4.2). Deletion of Y257 and the downstream residues did not affect the ability of pre-RTA to kill yeast cells (Figure 4.2). However, the deletion of V256 and the residues downstream resulted in a non-toxic pre-RTA mutant, suggesting that residue V256 and the downstream residues are essential for pre-RTA cytotoxicity. Deletion of further upstream residues M255, L254, A253, I252, I251, P250 and I249 also resulted in non-toxic pre-RTA variants. To determine if particular amino acids or the entire C-terminus is critical for pre-RTA mediated cytotoxicity, site-directed point mutations were also generated in these residues in order to disrupt the hydrophobicity of the C-terminus. All

of these mutations are listed in Table 4. 1. A majority of the mutations were changes to alanine or arginine, which imparts either a neutral or positive charge, respectively. The mutation V256A was non-toxic in yeast (Figure 4.2), further supporting the importance of V256 for pre-RTA cytotoxicity. In addition L254P, I252R, I251A all resulted in non-toxic mutants, suggesting that those residues are also critical for pre-RTA cytotoxicity. The double mutation, M255L V256N was generated to mimic the C-terminus of wildtype PAP. Interestingly, the sequence ALLNV in wildtype PAP is cytotoxic to yeast, but when the corresponding sequence was created in pre-RTA, the cytotoxicity of pre-RTA was abolished (Figure 4.2).

Table 4.1: Characterization of pre-RTA and RTA point mutations

Mutation	<u>pre-RTA</u>			<u>RTA</u>		
	Toxicity	% Depurination compared to wt	% Translation compared to vector	toxicity	% Depurination compared to wt	% Translation compared to vector
wildtype	Yes	100	30	Yes	100	32
I249*	No	1	120	---	---	---
P250*	No	1	97	---	---	---
I251*	No	2	100	---	---	---
I252*	No	0	120	---	---	---
A253*	No	96	52	Yes	38	42
L254*	No	0	110	No	8	102
M255*	No	0	104	No	2	91
V256*	No	0	99	No	1	108
Y257*	Yes	129	36	Yes	70	38
L248A	Yes	138	22	---	---	---
I249A	Yes	136	37	---	---	---
P250A	Yes	75	24	Yes	150	40
I251S	Yes	100	53	---	---	---
I251A	No	13	96	Yes	62	26
I252A	Yes	84	38	---	---	---
I252R	No	1	93	No	6	68
I252S	Yes	62	29	---	---	---
A253R	Yes	56	44	---	---	---
A253V	Yes	100	38	---	---	---
A253N	Yes	160	60	---	---	---
L254A	Yes	80	46	---	---	---
L254P	No	1	106	No	12	76
M255A	Yes	174	48	---	---	---
M255L	Yes	151	58	---	---	---
M255R	Yes	121	40	---	---	---
V256A	No	0	98	Yes	75	42
V256R	Yes	109	50	---	---	---
V256N	Yes	283	48	---	---	---
M255L V256N	No	2	100	Yes	64	53

246	247	248	249	250	251	252	253	254	255	256	257	258	259	260	261
S	I	L	I	P	I	I	A	L	M	V	Y	R	C	A	P
		*	*	*	*	*	*	*	*	*	*				
		A	A	A	A	A	V	A	A	A					
					S	R	R	P	R	R					
						S	N		L	N					
									L	N					

Table 4.2: The location of the C-terminal pre-RTA mutations. Non-toxic mutants are boxed in red.

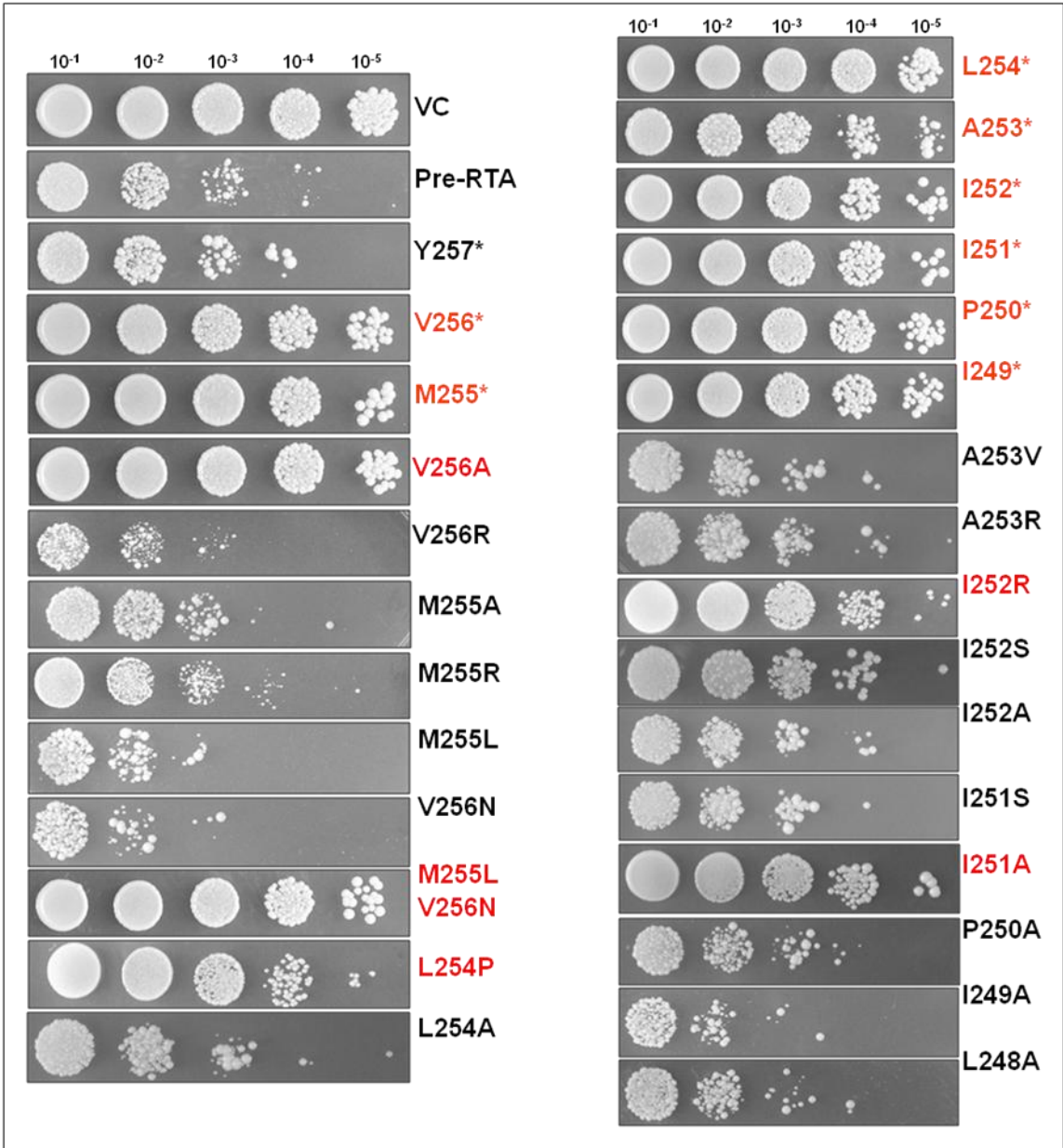


Figure 4.2: Viability analysis of pre-RTA C-terminal deletion and point mutations. Yeast cells were grown on SD-Leu containing 2% glucose to an A_{600} of 0.3 and then transferred to SD-Leu medium containing 2% galactose to induce pre-RTA expression. A serial dilution of cells was plated on SD-Leu plates containing 2% glucose for 10 h post-induction. Plates were incubated at 30°C for approximately 48 h.

The expression pattern of the pre-RTA mutants is different in non-toxic mutants

To confirm the presence of pre-RTA protein expression, 12% PAGE and immunoblot analysis was conducted. All of the mutants express pre-RTA (Figure 4.3) to varying extents. The non-toxic C-terminal deletion mutants generate a protein that has multiple lower molecular weight bands, suggesting that perhaps this protein is getting destabilized or degraded in the cell. In addition, the non-toxic point mutations generate higher levels of pre-RTA protein, probably due to the fact that the cells are not being killed by the toxin.

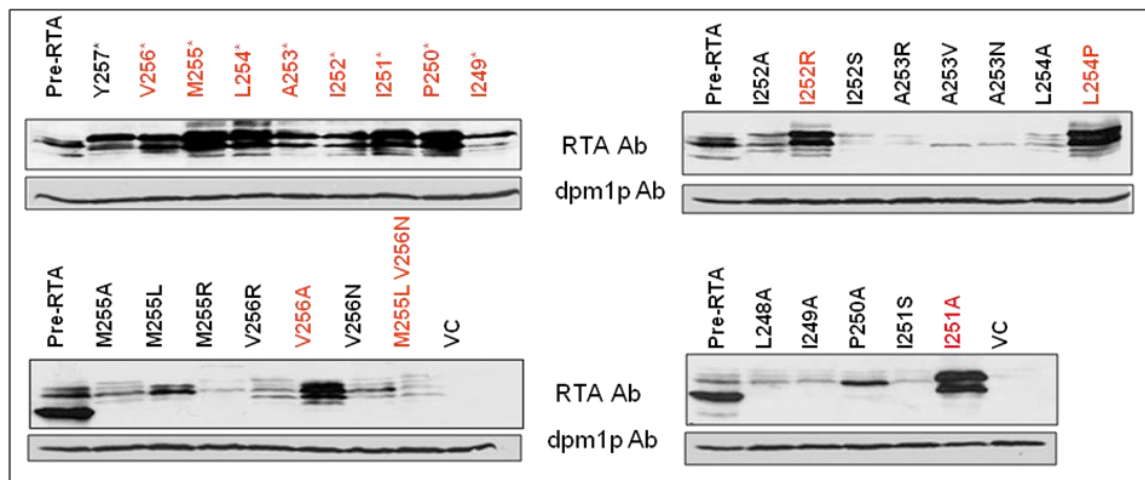


Figure 4.3: Immunoblot analysis of pre-RTA expression. Membrane fractions (15 μ g) isolated from cells expressing pre-RTA or mutants were separated on a 12% SDS-polyacrylamide gel and probed with polyclonal anti-RTA (1:5,000). The blots were stripped and probed with the ER membrane marker Dpm1p as a loading control.

The C-terminus is essential for pre-RTA depurination in yeast

To determine if the cytotoxicity of the pre-RTA mutants correlated with ribosome depurination in yeast, total RNA was isolated from yeast expressing all of the C-terminal

deletion and point mutations. The RNA was subsequently subjected to dual primer extension analysis. As expected, all of the toxic pre-RTA mutants were able to depurinate yeast ribosomes, while all of the non-toxic pre-RTA mutants were not (Figure 4.4). Interestingly, A253* was nontoxic in yeast, but was able to depurinate yeast ribosomes, although to a lesser extent than wildtype pre-RTA.

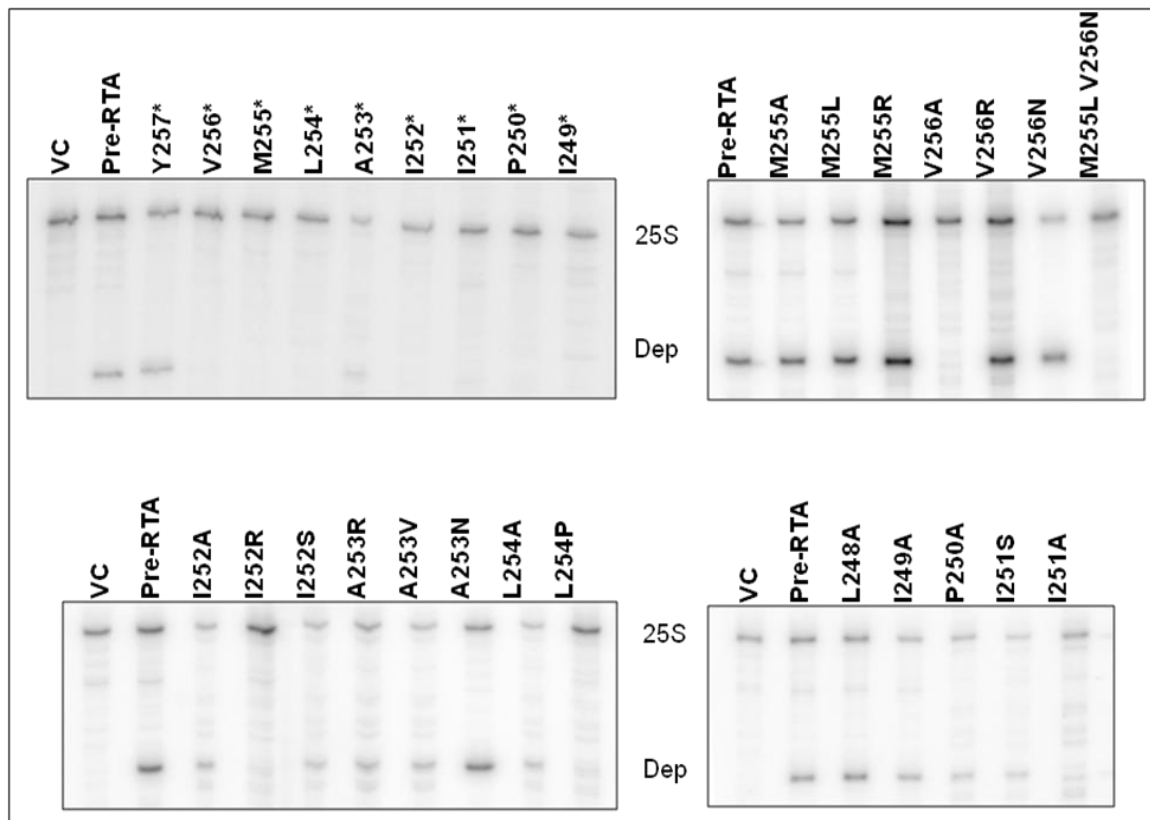


Figure 4.4 Ribosome depurination in yeast expressing pre-RTA and the mutant forms. Total RNA isolated after 6 h of growth on galactose was analyzed by dual primer extension analysis using two different end-labeled primers: the depurination primer (Dep), which was used to measure the extent of depurination, and the 25S rRNA primer (25S), which was used to measure the total amount of 25S rRNA. Primer extension analysis of cells harboring the empty vector is shown as a control.

Pre-RTA mutants that are non-toxic and not depurinating do not inhibit total translation in yeast

Ribosome depurination by pre-RTA results in inhibition of protein translation. Therefore, it is expected that the pre-RTA mutants that don't depurinate yeast ribosomes

should not inhibit translation. To confirm the ability of the pre-RTA mutants to inhibit total translation in yeast, [35 S]-methionine incorporation was assayed. As expected, the pre-RTA mutants that do not depurinate yeast ribosomes do not inhibit protein synthesis (Figure 4.5).

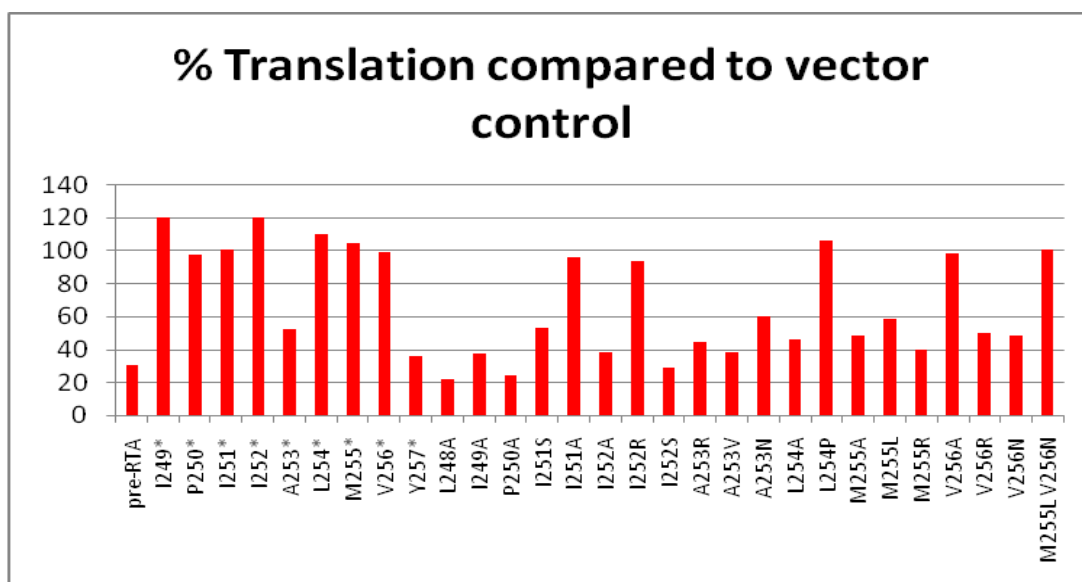


Figure 4.5: Pre-RTA mutants that don't depurinate ribosomes can translate protein. Yeast cells were grown to an A_{600} of 0.3 in SD-Leu-Met containing 2% glucose. Cells were then resuspended in SD-Leu-Met containing 2% galactose for 6 h to induce the expression of either wild-type pre-RTA or the mutant forms. At time zero, [35 S]-methionine was added to induced cells. After 30 min, 400 μ l of yeast cells was removed for growth measurements, and additional aliquots of 400 μ l were assayed for methionine incorporation in duplicate as previously described. The cpm was normalized to the A_{600} reading, and rates of translation were determined as cpm/ A_{600} /minute. Final results were displayed as percentages of total translation in yeast harboring the empty vector.

Mutations affecting the cytotoxicity of pre-RTA do not affect the toxicity of RTA

In order to determine if the C-terminus of pre-RTA plays a role in protein transport or localization in yeast, the same mutations that impaired the ability of pre-RTA to kill yeast cells were generated in mature RTA (Table 4.3) and assayed for cytotoxicity (Figure 4.6), expression (Figure 4.7), depurination (Figure 4.8) and translation inhibition (Figure 4.9). These mutations were: Y257*, V256*, M255*, L254*, A253*, V256A,

M255L V256N, L254P, I252R, I251A and P250A (Table 4.3). Because mature RTA lacks an N-terminal signal sequence, it does not enter the ER and does not undergo the same pattern of translocation as pre-RTA. Therefore, mature RTA may not rely on the same residues as pre-RTA to impart cytotoxicity. As shown in Figures 4.6 and 4.8, deletion of Y257 and the downstream residues resulted in a toxic and depurinating form of RTA, while deletion of V256, M255, L254 and A253 and the downstream residues resulted in non-toxic, non-depurinating forms of RTA. However, several point mutations that resulted in non-toxic and non-depurinating pre-RTA mutants were still toxic and depurinating when introduced in RTA. These mutations were V256A, M255L V256N and I251A. Because RTA containing any of these mutations was unable to depurinate ribosomes in pre-RTA (Figure 4.4), but could depurinate ribosomes in RTA (Figure 4.8), it is probable that these mutations do not affect the enzymatic activity of ricin, but do alter the ability of pre-RTA to exit the ER and reach the ribosomes in the cytosol. L254P and I252R RTA mutants were still non-toxic, but there was a slight increase in the amount of depurination in these mutants compared to the same mutations in pre-RTA.

246	247	248	249	250	251	252	253	254	255	256	257	258	259	260	261
S	I	L	I	P	I	I	A	L	M	V	Y	R	C	A	P
							*	*	*	*	*				
				A	A	R		P		A					
									L	N					

Table 4.3: The location of the C-terminal RTA mutations. Non-toxic mutants are boxed in red.

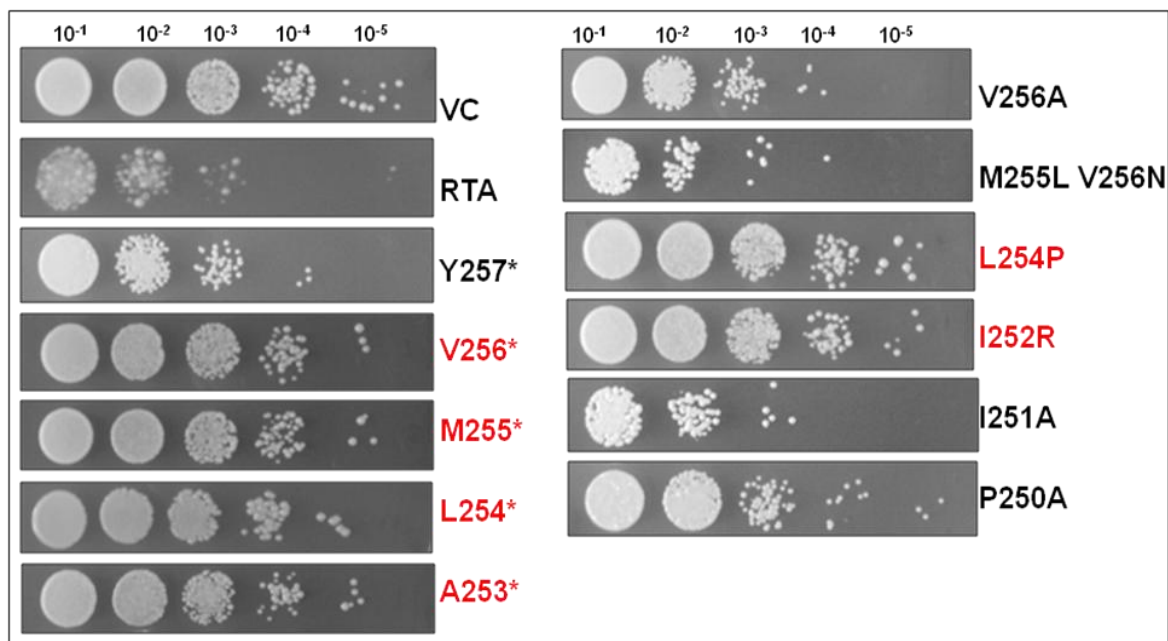


Figure 4.6: Viability analysis of mature RTA C-terminal deletion and point mutations. Yeast cells were grown on SD-Leu containing 2% glucose to an A_{600} of 0.3 and then transferred to SD-Leu medium containing 2% galactose to induce pre-RTA expression. A serial dilution of cells was plated on SD-Leu plates containing 2% glucose for 10 h post-induction. Plates were incubated at 30°C for approximately 48 h.

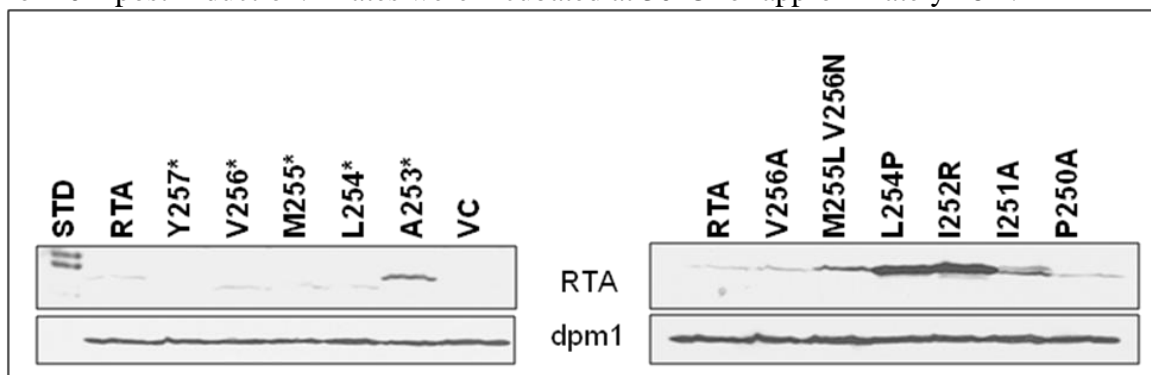


Figure 4.7: Immunoblot analysis of mature RTA expression. Membrane fractions (15 μ g) isolated from cells expressing wildtype RTA or RTA mutants were separated on a 12% SDS-polyacrylamide gel and probed with polyclonal anti-RTA (1:5,000). The blots were stripped and probed with the ER membrane marker Dpm1p as a loading control.

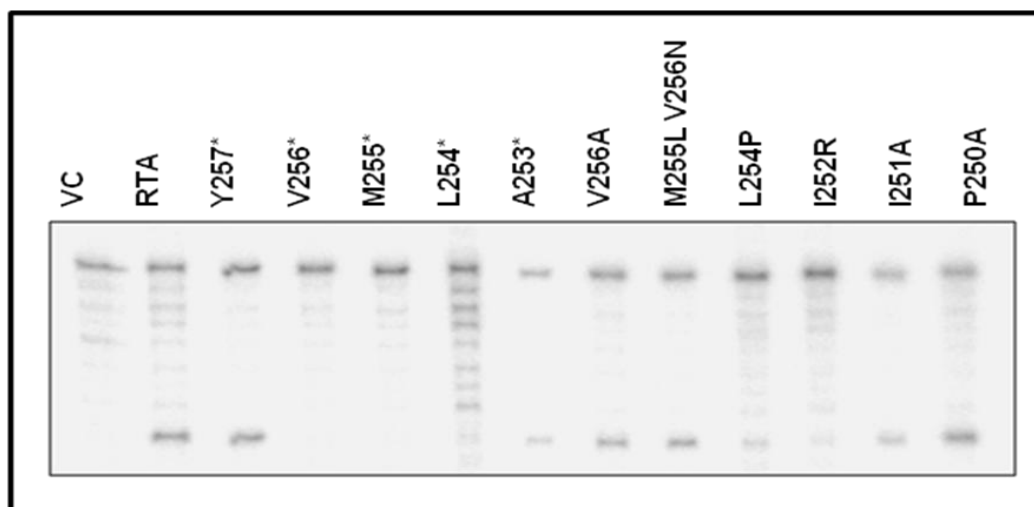


Figure 4.8: Ribosome depurination in yeast expressing RTA and the mutant forms. Total RNA isolated after 6 h of growth on galactose was analyzed by dual primer extension analysis using two different end-labeled primers: the depurination primer (Dep), which was used to measure the extent of depurination, and the 25S rRNA primer (25S), which was used to measure the total amount of 25S rRNA. Primer extension analysis of cells harboring the empty vector is shown as a control.

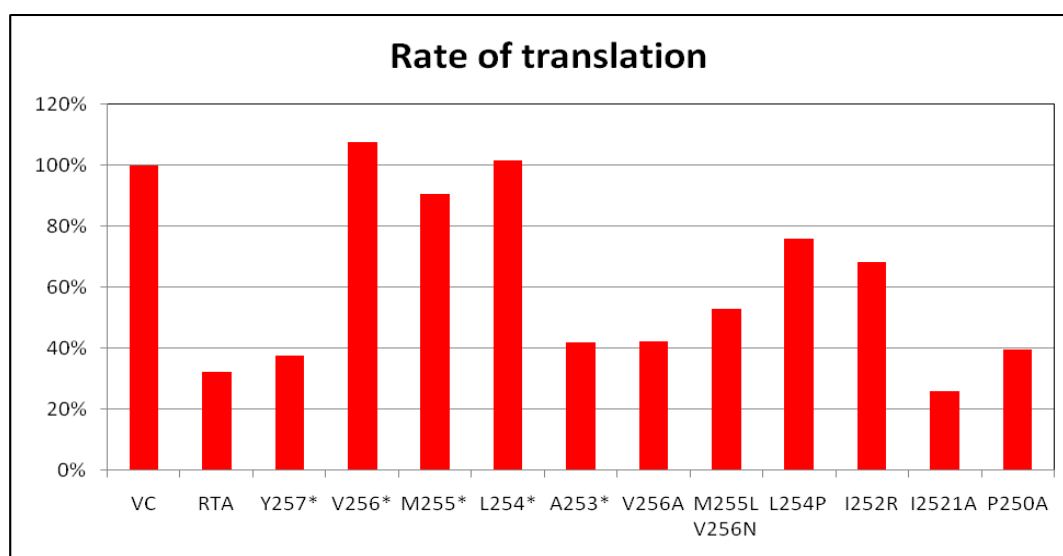


Figure 4.9: Translation inhibition of RTA and the mutant forms. Yeast cells were grown to an A_{600} of 0.3 in SD-Leu-Met containing 2% glucose. Cells were then resuspended in SD-Leu-Met containing 2% galactose for 6 h to induce the expression of either wild-type pre-RTA or the mutant forms. At time zero, [35 S]-methionine was added to induced cells. After 30 min, 400 μ l of yeast cells was removed for growth measurements, and additional aliquots of 400 μ l were assayed for methionine incorporation in duplicate as previously described. The cpm was normalized to the A_{600} reading, and rates of translation were determined as cpm/ A_{600} /minute. Final results were displayed as percentages of total translation in yeast harboring the empty vector.

DISCUSSION

The C-termini of the RIPs shiga toxin and PAP are necessary for cytotoxicity (69, 70). Protein prediction software, TMPred indicates that there is a strong putative transmembrane domain from pre-RTA residues 245-257. Studies have shown that this domain in ricin may be used for toxin localization in target cells (73). After binding to the target cell, the ricin holotoxin is endocytized and transported to the trans-Golgi network. It then undergoes retrograde transport and enters the endoplasmic reticulum. After separating from RTB, RTA is transported into the cytosol, perhaps by taking advantage of the ER-Associated Degradation (ERAD) pathway and the Sec61 translocon as discussed earlier. Upon entering the cytosol, RTA must bind to and depurinate ribosomes. The crystal structure has been solved for ricin (3). In the holotoxin, the C-terminal residues discussed in this paper are buried between RTB and RTA. After separation from RTB, the C-terminal residues of RTA are exposed and resemble a tail or extension (Figure 4.11). Since it contains a hydrophobic motif, this tail may serve to aid in localization of RTA by inserting into a target membrane. To better understand the function of this C-terminal domain in ricin, we generated deletion mutants and point mutations that either truncated the C-terminal residues of ricin or changed the composition of the hydrophobic domain (Table 4.2).



Figure 4.10: A structural comparison of the C-terminal residues of RTA. Protein Explorer (www.proteinexplorer.org) was used to generate the structural models of 1IFT (RTA). The C-terminal deleted residues are highlighted in green and demonstrate the increase in proximity to the active site of RTA as the C-terminus is deleted up to residue A253.

Initially, the deletion and point mutations were generated in the C terminus of pre-RTA. In pre-RTA, deletion of the C-terminus up to and including Y257 maintained toxicity (Figure 4.2). Protein expression showed two bands migrating at the same size as the purified RTA standard, indicating that the protein was able to enter the ER and get glycosylated (Figure 4.3). In addition, the protein was able to exit the ER and enter the cytosol, as indicated by its wildtype levels of ribosome depurination (Figure 4.3). Y257* was also able to inhibit total translation in yeast to the same extent as wildtype pre-RTA (Figure 4.4). However, deleting only one more residue upstream of Y257, V256, abolished all wildtype activities, including cytotoxicity, depurination and translation

inhibition. Accordingly, as adjacent upstream deletions were generated, almost all of the generated mutants were nontoxic and non-depurinating.

One of the deletion mutants, A253*, behaved differently from the other non-toxic mutants. While A253* was non-toxic, it was still able to depurinate yeast ribosomes, though to a lesser extent than that of wildtype pre-RTA. In addition, A253* was still able to inhibit total translation in yeast to similar levels as wildtype pre-RTA. Protein structure analysis using Protein Explorer indicates that A253 is one of the closest C-terminal residues to the active site residue of pre-RTA, residue E177 (Figure 4.11). It is possible that when the C-terminus is deleted, the remaining residues might fold improperly, blocking access of the active site to ribosomes. However, deletion of all of the residues up to and including A253 removes the entire C-terminal tail (Figure 4.10). This may open the active site cleft again, allowing it to access ribosomes. When the residues upstream of A253 are sequentially deleted (I252*, I251*, P250* and I249*), cytotoxicity and depurination activity are again abolished (Figures 4.2 and 4.3). It is possible that these upstream deletions from A253 may cause the structure of the active site cleft to become blocked again.

In addition to truncation mutations, several point mutations resulted in the loss of cytotoxicity of pre-RTA (Figure 4.2). The majority of the residues were changed to alanine to impart a neutral charge, as well as asparagine to impart a positive charge. By generating the point mutants, it was expected that the hydrophobic motif of the C-terminus of pre-RTA would be disrupted, thereby abolishing any effect the C-terminus may have for ricin translocation. In addition, we generated a double mutation to change the residues of pre-RTA to be identical to the critical residues for PAP cytotoxicity. This

indicates that while the C-terminus of RIPs is essential for cytotoxicity, the specific sequence of each may be different to perpetuate this toxicity. In pre-RTA, I251A, I252R, L254P, V256A and the double mutant M255L V256N were all non-toxic, non-depurinating mutations, indicating that they are necessary for pre-RTA toxicity and ribosome depurination in yeast.

The results of both the truncation mutants and point mutations in pre-RTA suggested two possibilities for the way that the C-terminus is used for ricin toxicity. One possibility is that the C-terminus is necessary for the enzymatic function of ricin. This hypothesis is supported by the fact that the C-terminal residues discussed here lie in fairly close proximity to the active site of RTA (Figure 4.11), especially I251, I252 and A253. Another possible function of the C-terminus of ricin could be for the promotion of translocation of the toxin out of the ER into the cytosol. To further determine the role of the C-terminus in ricin, several of the non-toxic pre-RTA mutations were generated in mature RTA and analyzed in yeast. Mature RTA does not have a signal sequence and does not enter the ER. Therefore, mutations that affect the cytotoxicity by inhibiting the translocation of pre-RTA out of the ER should not have an effect on RTA.

The deletion mutants Y257*, V256*, M255*, L254* and A253* were generated in RTA and the protein expression, toxicity, depurination and translation inhibition of each was analyzed (Figures 4.7, 4.8, 4.9, 4.10). Figure 4.11 shows a summary of these mutations in pre-RTA and RTA. Again, the Y257* mutant was toxic and caused depurination while the V256* mutant was non-toxic and non-depurinating. The upstream mutations, M255* and L254* behaved similarly in RTA as in pre-RTA. A253* also behaved the same in RTA as in pre-RTA. The fact that both pre-RTA and RTA A253* is

able to depurinate yeast ribosomes suggests that the sequential deletion of residues from the C-terminus may result in a blockage of the active site of the toxin, and that complete deletion of the C-terminus from A253 and the downstream residues re-opens the blockage so that the active site can again access ribosomes.

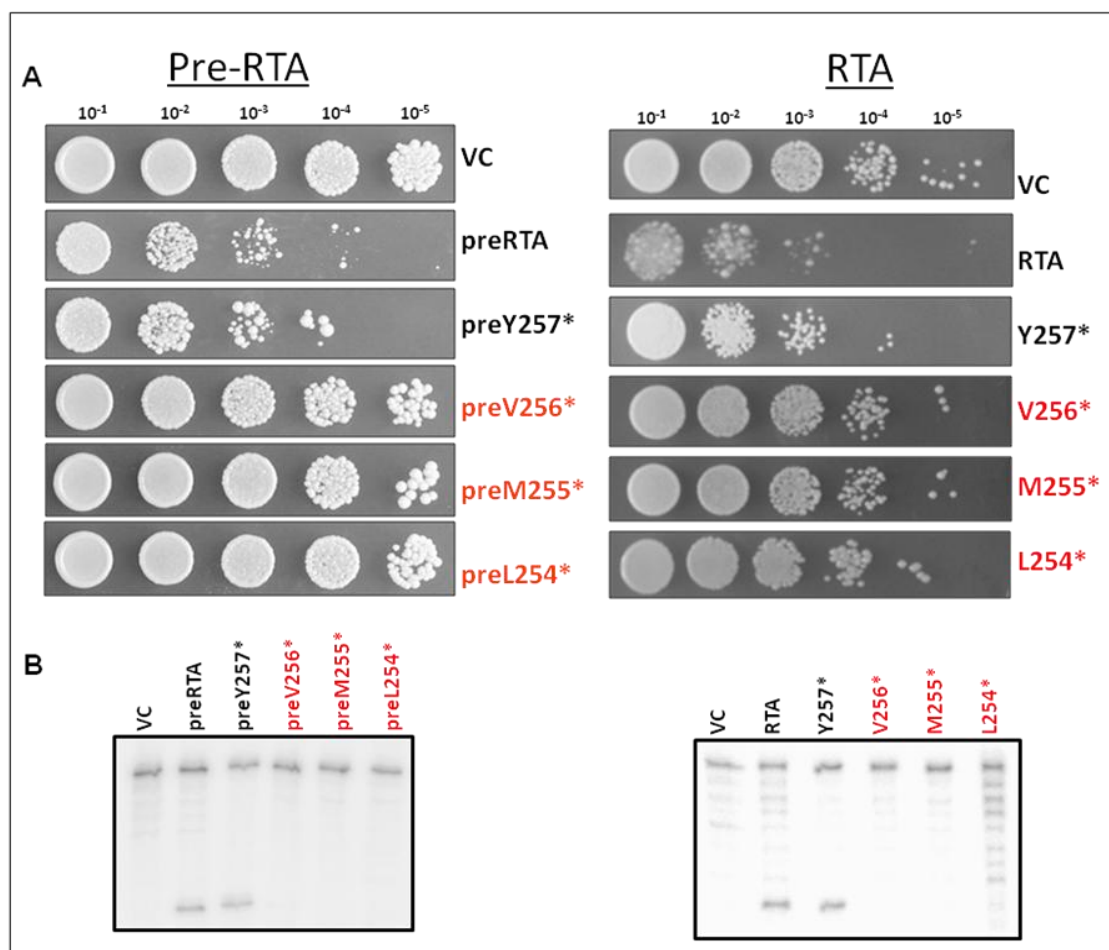


Figure 4.11: A direct comparison of the deletion mutants in pre-RTA and RTA. A. Viability assay. **B.** Depurination assay.

The point mutations that eliminated cytotoxicity and depurination in pre-RTA were generated in RTA (V256A, M255L V256N, L254P, I252R and I251A). In addition, the mutation P250A was generated due to the fact that published literature (72) suggests that this residue is important for ricin toxicity. Figure 4.12 shows a summary of these mutations in pre-RTA and RTA. The L254P and I252R RTA mutants behaved in a

similar way as in pre-RTA. Both were non-toxic and not depurinating. P250A was toxic and depurinating in both pre-RTA and RTA, suggesting that P250 is not an essential residue for ricin toxicity or depurination. However, the mutations V256A, M255L V256N and I251A were still toxic and able to depurinate yeast ribosomes when generated in RTA. To further confirm the enzymatic activity of these mutants, translation inhibition of all of the RTA mutants was performed. All of the mutants that did not depurinate yeast ribosomes did not inhibit protein translation, while those mutants that were still able to depurinate yeast ribosomes were still able to inhibit protein synthesis (Figure 4.10).

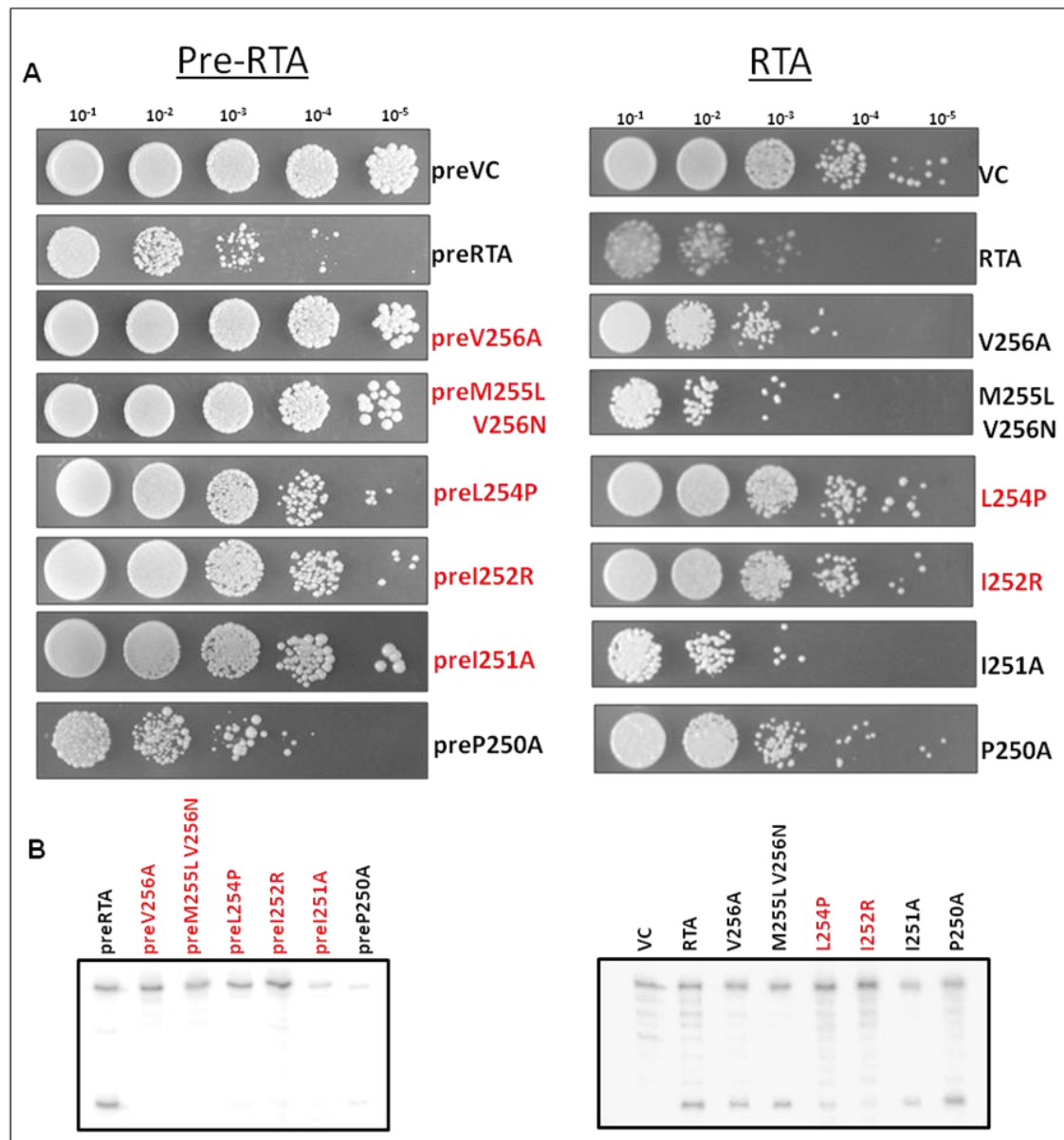


Figure 4.12: A direct comparison of the point mutants in pre-RTA and RTA. A. Viability assay. **B.** Depurination assay.

Because V256A, M255L V256N and I251A mutations in pre-RTA are unable to depurinate but do depurinate when introduced in RTA, these mutations probably do not inhibit enzymatic activity of pre-RTA or RTA, but do inhibit the translocation of pre-RTA from the ER into the cytosol. The C-terminal residues of ricin form a putative transmembrane domain, which could possibly be used as a translocation signal for entry

into the cytosol from the ER (73). The point mutations V256A, M255L V256N and I251A might disrupt this motif, thereby inhibiting the ability of the protein to translocate out of the ER to the cytosol.

Similar studies conducted in yeast expressing mature STX1 or STX1 that is targeted to enter the ER membrane (pre-STX1) yielded slightly different results (71). Leu 240 in STX1 corresponds to RTA V256 when the sequence is aligned. The truncation of pre-STX1 up to and including Leu240 (pre-STX1 L240*) resulted in a non-toxic form of the protein. However, when the same truncation was made in mature STX1 which does not go into the ER, the protein regained toxicity. Those results suggest that deleting L240 and the downstream residues from STX1 does not affect its enzymatic activity, but does inhibit retrotranslocation (71). To determine if the C-terminal sequence or only L240 is critical for retrotranslocation, mutations that changed pre-STX1 L240 to alanine, arginine, asparagine or aspartic acid were generated. None of the mutations significantly reduced the toxicity, indicating that the entire C-terminal sequence, and not just L240, is responsible for the translocation of preSTX1 from the ER to cytosol. In contrast, the truncation up to V256 in both RTA and pre-RTA resulted in non-toxic and non-depurinating proteins. These results indicate that the entire C-terminal sequence from V256 to F267 is essential for enzymatic activity, but not necessarily retrotranslocation (71).

Like RTA, PAP, a type I RIP, must also traverse an internal cellular membrane to gain access to ribosomes (74). It is thought that this membrane is the ER. Studies in yeast have indicated that the C-terminus of PAP is essential for its translocation into the cytosol (69). RTA V256 corresponds to N253 in PAP. When PAP N253 was changed to

a stop codon (N253*), the protein lost toxicity and was unable to depurinate yeast ribosomes. Immunoblots of cellular fractionation showed that the accumulation of PAP in the cytosol was dramatically reduced in N253*. Further upstream truncation mutants were generated in PAP, and when the C-terminal residues were deleted up to and including A250, which corresponds to residue L254 in RTA, PAP was still non-toxic and the protein was no longer able to reach the cytosol at all. These results indicate that A250 and the downstream residues are important for translocation of PAP into the cytosol (69). Point mutations that changed N253 to alanine (N253A) and arginine (N253R) also reduced the level of cytotoxicity of PAP and the ability to depurinate yeast ribosomes, but did not affect the ability of the protein to translocate into the cytosol. These results indicate that N253 is critical for enzymatic activity of the protein, but N253 alone is not critical for protein translocation. Interestingly, pre-RTA V256A resulted in a non-toxic non-depurinating protein, while pre-RTA V256R was still toxic and able to depurinate yeast ribosomes. Although arginine is a basic residue that should disrupt the hydrophobicity and alanine is a hydrophobic residue that should maintain the hydrophobicity of the C-terminus, it is possible that the larger size of arginine maintains an interaction with the active site, while the smaller alanine cannot.

While RIPs generally depurinate ribosomes in the same way, the critical residues that carry out the necessary steps for ribosome depurination seem to vary. However, in the three RIPs discussed here, the C-terminus plays a lead role in either protein translocation into the cytosol, enzymatic activity or both. The results of this study show that the C-terminal sequence V256-F267 in RTA is necessary for maintaining the enzymatic activity of the protein. In addition, we demonstrate that the specific residues

V256, V256 and M255 together and I251 are critical for RTA retrotranslocation from the ER into the cytosol.

CHAPTER 5: Conclusions

The threat of ricin exposure as a result of bioterrorism is a major concern as there is currently no approved vaccine or treatment available for ricin intoxication. Because wildtype ricin is highly toxic to humans, nontoxic recombinant vaccines need to be developed based on a detailed understanding of the structure and molecular mechanism of action of ricin. Ricin is toxic to yeast, and we have expressed RTA in yeast to examine the residues that are critical for translocation into the cytosol and enzymatic activity, as well as the mechanism of entry into the cytosol. Three separate analyses of pre-RTA in yeast were conducted and a summary of each of these studies is discussed below.

After the ricin holotoxin is endocytosed by the target cell, only 5% is transported to the Golgi. It then undergoes retrograde transport to the ER, and finally to the cytosol, where it can depurinate ribosomes (11). To target the most critical step of ricin translocation, which is the exit out of the ER and into the cytosol, we have cloned RTA with the N-terminal signal sequence (pre-RTA) into yeast so that the protein will translocate from the ER to the cytosol as the holotoxin does.

RTA depurinates the SRL of the large ribosomal subunit, which results in a halt in the translocation step of protein translation. While it seems that this inhibition of protein translation would result in death of the target cell, little is actually known about how ricin-induced cell death occurs. To investigate the relationship between ribosome depurination and the cytotoxicity of ricin, we conducted large-scale mutagenesis of pre-RTA in yeast and isolated nontoxic RTA mutants on the basis of their inability to kill yeast cells. A total of 35 different mutations were generated. These mutations were

classified as either an insertion of a premature stop codon, insertion of an amino acid resulting in a frameshift in the reading frame, or single or double point mutations. All of the pre-RTA mutants were expressed in yeast and the ability to kill yeast cells, depurinate yeast ribosomes and inhibit translation in yeast was analyzed. Several of the non-toxic point mutations were still able to depurinate yeast ribosomes and inhibit protein translation. This was the first report to provide evidence that ribosome depurination and translation inhibition by RTA do not lead directly to cell death. Because these mutations result in an enzymatically active toxin but do not kill cells, they show promise for use as potential ricin vaccines.

Upon binding to the surface of target cells, the ricin holotoxin is endocytized and transported to the Golgi complex. It then moves to the ER where RTA and RTB are separated. During this time, RTA must undergo at least partial unfolding so that it can pass through the ER membrane to enter the cytosol. To determine if RTA utilizes components of the ERAD pathway to exit the ER, yeast strains with mutations in ERAD proteins were transformed with pre-RTA or pre-RTA_{E177K}. The proteins involved in ERAD that had an effect on pre-RTA were SEC61, which is a protein conducting channel in the ER membrane, KAR2, which is a protein folding chaperone, UBC7, a ubiquitin-conjugating enzyme that tags proteins for proteasomal degradation, RAD23, which helps to transfer ubiquitinated substrates to the proteasome and the proteasome, which degrades proteins. When pre-RTA was expressed in *sec61* mutants defective in protein export, it was stabilized with the membrane fraction of fractionated cell lysates. This indicates that pre-RTA needs a properly functioning Sec61 translocon to exit the ER. Cytotoxicity and depurination induced by pre-RTA were not affected when expressed in yeast cells with a

mutation in KAR2. However, the expression pattern of pre-RTA in *kar2-1* yeast was altered, indicating that KAR2 plays a role in the stabilization or export of pre-RTA from the ER. Pre-RTA was stabilized in yeast cells that had a deletion in the *UBC7* gene, indicating that UBC7 may be necessary for the degradation of pre-RTA in the proteasome. In *rad23Δ* deletion mutants, cytotoxicity and depurination of pre-RTA was reduced, most likely because of a decrease in total protein expression. This suggests that RAD23 is necessary for RTA toxicity and depurination. In yeast cells with a mutation in the proteasome, pre-RTA_{E177K} was stabilized, and pre-RTA transformants were extremely toxic. This indicates that a portion of pre-RTA reaches the cytosol and is degraded by the proteasome. Taken together, the results of the SEC61, KAR2, UBC7, RAD23 and proteasome mutants provide strong evidence that pre-RTA uses the ERAD machinery to reach the cytosol.

The C terminus of RTA contains a putative transmembrane domain which could mediate toxin translocation across the ER membrane into the cytosol where it can reach ribosomes. The C-terminal residues of RTA are also in very close proximity to the active site (E177) and could potentially affect its depurination activity. To determine if the C terminal sequence is essential for RTA cytotoxicity, depurination or membrane translocation, a series of deletion and point mutations were generated in pre-RTA and RTA and the proteins were expressed in yeast. For both pre-RTA and RTA, deletion of Y257 and the downstream residues resulted in a toxic, depurinating protein, while deletion of V256 and the downstream residues abolished both cytotoxicity and depurination. This indicates that V256 and the downstream residues are essential for the enzymatic activity of RTA. When point mutations V256A, M255L V256N and I252A

were introduced in pre-RTA, the resulting proteins were non-toxic and non-depurinating in pre-RTA. However, the same mutations in RTA resulted in proteins that were toxic and depurinated. This suggests that these mutations do not affect the enzymatic activity, but do inhibit the ability of pre-RTA to translocate from the ER into the cytosol. These studies indicate that the C-terminal sequence of RTA is important for its enzymatic activity, and that there are specific residues that are critical for translocation of the toxin across the ER membrane into the cytosol.

SUMMARY

In summary, the results presented here suggest that 1) depurination and translation inhibition of RTA does not always result in cytotoxicity and cell death, 2) RTA utilizes several components of the ERAD pathway to exit the ER and 3) residues in the C-terminus of RTA are essential for enzymatic activity and protein translocation. These results have identified specific residues of RTA as well as cellular proteins and components that can potentially be used as targets for the generation of treatments of ricin intoxication. RTA mutants that are able to depurinate ribosomes but are not toxic to yeast, such as S215F and P95L E145K have a functional active site, but are non-toxic to yeast cells. These two mutants may prove to be good candidates for vaccine development as the active site will still initiate an immune response, but the toxin itself may not induce cell death in the host organism.

The *rad23Δ* deletion mutant inhibited both the expression and depurination levels of pre-RTA in yeast. If RAD23 can be inhibited in humans with little or no deleterious effects, it could be used as a potential target to prevent ricin intoxication. Alternatively, when the proteasome cannot function properly, pre-RTA_{E177K} is stabilized to very high

levels. Perhaps an increase in the level of proteasome expression could help to degrade excess RTA in the event of ricin exposure.

Because ribosome depurination does not account entirely for the cytotoxicity of RTA, there must be another mechanism employed by ricin to induce cell death. A recent publication has shown that RTA inhibits the UPR (28). The UPR increases the transcription of many genes that express ERAD proteins to aid in the translocation of misfolded proteins out of the ER and, ultimately, to the proteasome. If the UPR is not regulated, cell death will eventually occur (75), as the cell will become overwhelmed by the high concentration of misfolded proteins. It is possible that the inactivation of the UPR by RTA is necessary for RTA to avoid degradation via ERAD. A model could therefore be generated in which the cytotoxicity caused by RTA is a combination of both inhibition of the UPR and translation inhibition as a result of ribosome depurination (Figure 5.1).

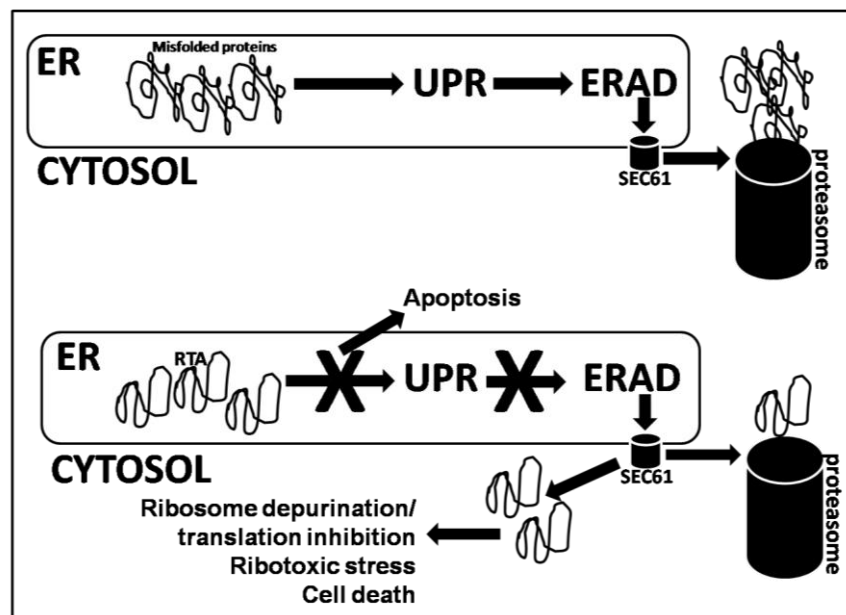


Figure 5.1: Model for ricin induced cell death. Normal misfolded proteins activate the UPR, which leads to upregulation of ERAD components and protein degradation in the proteasome. RTA inhibits the UPR, thereby limiting ERAD and allowing at least some RTA to escape proteasomal degradation and reach the cytosol.

MATERIALS AND METHODS

Yeast expression vector

The pre-RTA cDNA was constructed in our laboratory as previously described (26). The pre-RTA and RTA cDNA was cloned into the yeast expression vector YEp351 downstream of the galactose-inducible *GAL1* promoter (58) or into the pYES vector. The pre-RTA plasmid was transformed into *Saccharomyces cerevisiae* strain W303 (*MATa ade2-1 trp1-1 ura3-1 leu2-3,112 his3-11,15 can1-100* [from B. Thomas, Columbia University, New York, NY]), and transformants were selected on SD-Leu medium containing 2% glucose.

Analysis of pre-RTA or RTA expression

Yeast cells harboring the pre-RTA or RTA plasmids were grown on selective media containing 2% glucose to an A_{600} of 0.3. Cells were pelleted at $2,000 \times g$ for 5 min, resuspended in selective medium containing 2% galactose, and grown for 6 h to induce RTA expression. For immunoblot analysis, ER membrane fractions were isolated as previously described (74). The membrane fraction was dissolved in sodium dodecyl sulfate (SDS) buffer and heated at 37°C for 10 min before loading onto a 12% SDS-polyacrylamide gel. The blots were probed using polyclonal anti-RTA antibodies (1:5,000) produced in rabbits (Covance Research Products, Denver, PA) or monoclonal V5 antibodies. The blots were then stripped for 30 min with 8 M guanidine hydrochloride and reprobed with antibody to dolichol-phosphate mannosyl transferase (Dpm1p; Invitrogen,

Carlsbad, CA) (1:4,000). Purified RTA standard was obtained from Sigma Aldrich (St. Louis, MO).

Cell viability analysis

Yeast cells expressing pre-RTA or RTA were grown on selective media containing 2% glucose to an A_{600} of 0.3 and then transferred to selective medium containing 2% galactose to induce pre-RTA expression. A serial dilution of cells was plated onto plates containing 2% glucose at the indicated times post induction. Plates were incubated at 30°C for approximately 48 h.

rRNA depurination assay

Dual primer extension analysis was conducted to quantify rRNA depurination. 2 µg of total yeast RNA from cells expressing pre-RTA or RTA was hybridized with 10^6 cpm of end-labeled depurination primer (5'-AGCGGATGGTGCTTCGCGGCAATG-3'). The second primer hybridized upstream of the depurination site close to the 5' end of the 25S rRNA. To quantify the extent of depurination, the target RNA was initially hybridized in the presence of excess amounts (700 pmol) of the two [γ - 32 P]ATP-end-labeled negative-strand primers. The depurination primer described above annealed 73 nucleotides (nt) 3' of the depurination site (A_{3137}) on the 25S rRNA. The 25S control primer (5'-TTCACCTCGCCGTTACTAAGG-3') annealed 100 nt 3' of the 25S rRNA 5' end. To allow for accurate quantification, the labeled 25S control primer was diluted 1:4 with unlabeled 25S control primer. Superscript II reverse transcriptase was used to extend the primer product. Extension products for the control and depurination fragments (100 nt

and 73 nt, respectively) were separated on a 7 M urea-5% polyacrylamide denaturing gel and visualized and quantified on a PhosphorImager (Molecular Dynamics, Sunnyvale, CA). The amount of total yeast RNA used was previously determined to be in the linear range of detection.

In vivo [³⁵S]methionine incorporation

Translation inhibition was measured by in vivo [³⁵S]methionine incorporation. Yeast cells were grown to an A_{600} of 0.3 in selective –Met media containing 2% glucose. Cells were then resuspended in selective -Met media containing 2% galactose for 6 h to induce the expression of pre-RTA or RTA. At time zero, [³⁵S]methionine was added to induced cells. After 30 min, 400 μ l of yeast cells was removed for growth measurements, and additional aliquots of 400 μ l were assayed for methionine incorporation in duplicate. The cpm was normalized to the A_{600} reading, and rates of translation were determined as cpm/ A_{600} /minute. Final results were displayed as percentages of total translation in yeast harboring the empty vector.

Extraction of proteins from yeast and in vitro depurination assay

Yeast cells (50 ml) containing pre-RTA were induced on galactose for 6 h. Cells were resuspended in 1 \times low-salt buffer (20 mM HEPES-KOH, pH 7.6, 100 mM potassium acetate, 5 mM magnesium acetate, 1 mM EDTA, 2 mM dithiothreitol, and 0.1 mM phenylmethylsulfonyl fluoride) and lysed using glass beads. Samples were centrifuged briefly to remove cell debris and glass beads. The supernatant was transferred to a new tube and centrifuged at 100,000 \times g for 30 min to remove cell membranes and ribosomes. The resulting supernatant (100 μ l) was collected. Yeast ribosomes (15 μ l) were incubated

with RTA protein extracted from yeast (10 μ l) in 10 \times RIP buffer (600 mM KCl, 100 mM Tris-HCl, pH 7.4, and 100 mM MgCl₂) at 30°C for 30 min. One hundred microliters of 2 \times extraction buffer (240 mM NaCl, 50 mM Tris-HCl, pH 8.8, 20 mM EDTA, and 2% SDS) was added, and rRNA was extracted with phenol:chloroform and precipitated with ethanol. The rRNA was analyzed using the dual primer extension assay as described above.

Site-directed mutagenesis

The Quikchange Site-Directed Mutagenesis Kit (Stratagene) was used to generate the point mutations in pre-RTA or RTA according to manufacturer instructions.

Structural Analysis of RTA structure

Coordinates from the crystal structures from the Protein Data Bank of PAP (1PAG), STX2 (14RP) and RTA (1IFT) were analyzed using Protein Explorer software (Proteinexplorer.org).

References

1. Olsnes S. The history of ricin, abrin and related toxins. *Toxicon*. 2004 Sep 15;44(4):361-70.
2. Endo Y, Tsurugi K. Mechanism of action of ricin and related toxic lectins on eukaryotic ribosomes. *Nucleic Acids Symp Ser*. 1986;(17)(17):187-90.
3. Mlsna D, Monzingo AF, Katzin BJ, Ernst S, Robertus JD. Structure of recombinant ricin A chain at 2.3 Å. *Protein Sci*. 1993 Mar;2(3):429-35.
4. Van Damme EJ, Roy S, Barre A, Rouge P, Van Leuven F, Peumans WJ. The major elderberry (*sambucus nigra*) fruit protein is a lectin derived from a truncated type 2 ribosome-inactivating protein. *Plant J*. 1997 Dec;12(6):1251-60.
5. Frankel A, Schlossman D, Welsh P, Hertler A, Withers D, Johnston S. Selection and characterization of ricin toxin A-chain mutations in *saccharomyces cerevisiae*. *Mol Cell Biol*. 1989 Feb;9(2):415-20.
6. Hur Y, Hwang DJ, Zoubenko O, Coetzer C, Uckun FM, Tumer NE. Isolation and characterization of pokeweed antiviral protein mutations in *saccharomyces cerevisiae*: Identification of residues important for toxicity. *Proc Natl Acad Sci U S A*. 1995 Aug 29;92(18):8448-52.
7. Hovde CJ, Calderwood SB, Mekalanos JJ, Collier RJ. Evidence that glutamic acid 167 is an active-site residue of shiga-like toxin I. *Proc Natl Acad Sci U S A*. 1988 Apr;85(8):2568-72.
8. Lord JM, Roberts LM, Robertus JD. Ricin: Structure, mode of action, and some current applications. *FASEB J*. 1994 Feb;8(2):201-8.
9. van Deurs B, Pedersen LR, Sundan A, Olsnes S, Sandvig K. Receptor-mediated endocytosis of a ricin-colloidal gold conjugate in vero cells. intracellular routing to vacuolar and tubulo-vesicular portions of the endosomal system. *Exp Cell Res*. 1985 Aug;159(2):287-304.
10. Moya M, Dautry-Varsat A, Goud B, Louvard D, Boquet P. Inhibition of coated pit formation in Hep2 cells blocks the cytotoxicity of diphtheria toxin but not that of ricin toxin. *J Cell Biol*. 1985 Aug;101(2):548-59.
11. Wesche J, Rapak A, Olsnes S. Dependence of ricin toxicity on translocation of the toxin A-chain from the endoplasmic reticulum to the cytosol. *J Biol Chem*. 1999 Nov 26;274(48):34443-9.
12. Lord JM, Roberts LM, Lencer WI. Entry of protein toxins into mammalian cells by crossing the endoplasmic reticulum membrane: Co-opting basic mechanisms of

endoplasmic reticulum-associated degradation. *Curr Top Microbiol Immunol*. 2005;300:149-68.

13. Zhou M, Schekman R. The engagement of Sec61p in the ER dislocation process. *Mol Cell*. 1999 Dec;4(6):925-34.

14. Pilon M, Schekman R, Romisch K. Sec61p mediates export of a misfolded secretory protein from the endoplasmic reticulum to the cytosol for degradation. *EMBO J*. 1997 Aug 1;16(15):4540-8.

15. van Laar T, van der Eb AJ, Terleth C. Mif1: A missing link between the unfolded protein response pathway and ER-associated protein degradation? *Curr Protein Pept Sci*. 2001 Jun;2(2):169-90.

16. Romisch K. Endoplasmic reticulum-associated degradation. *Annu Rev Cell Dev Biol*. 2005;21:435-56.

17. Deeks ED, Cook JP, Day PJ, Smith DC, Roberts LM, Lord JM. The low lysine content of ricin A chain reduces the risk of proteolytic degradation after translocation from the endoplasmic reticulum to the cytosol. *Biochemistry*. 2002 Mar 12;41(10):3405-13.

18. Kim I, Ahn J, Liu C, Tanabe K, Apodaca J, Suzuki T, et al. The Png1-Rad23 complex regulates glycoprotein turnover. *J Cell Biol*. 2006 Jan 16;172(2):211-9.

19. Ng W, Sergeyenko T, Zeng N, Brown JD, Romisch K. Characterization of the proteasome interaction with the Sec61 channel in the endoplasmic reticulum. *J Cell Sci*. 2007 Feb 15;120(Pt 4):682-91.

20. Brigotti M, Rambelli F, Zamboni M, Montanaro L, Sperti S. Effect of alpha-sarcin and ribosome-inactivating proteins on the interaction of elongation factors with ribosomes. *Biochem J*. 1989 Feb 1;257(3):723-7.

21. Ban N, Nissen P, Hansen J, Moore PB, Steitz TA. The complete atomic structure of the large ribosomal subunit at 2.4 Å resolution. *Science*. 2000 Aug 11;289(5481):905-20.

22. Hudak KA, Dinman JD, Tumer NE. Pokeweed antiviral protein accesses ribosomes by binding to L3. *J Biol Chem*. 1999 Feb 5;274(6):3859-64.

23. Vater CA, Bartle LM, Leszyk JD, Lambert JM, Goldmacher VS. Ricin A chain can be chemically cross-linked to the mammalian ribosomal proteins L9 and L10e. *J Biol Chem*. 1995 May 26;270(21):12933-40.

24. Kim Y, Robertus JD. Analysis of several key active site residues of ricin A chain by mutagenesis and X-ray crystallography. *Protein Eng*. 1992 Dec;5(8):775-9.

25. Hudak KA, Parikh BA, Di R, Baricevic M, Santana M, Sesar M, et al. Generation of pokeweed antiviral protein mutations in *saccharomyces cerevisiae*: Evidence that

ribosome depurination is not sufficient for cytotoxicity. *Nucleic Acids Res.* 2004 Aug 10;32(14):4244-56.

26. Li XP, Baricevic M, Saidasan H, Tumer NE. Ribosome depurination is not sufficient for ricin-mediated cell death in *saccharomyces cerevisiae*. *Infect Immun.* 2007 Jan;75(1):417-28.

27. Shen X, Zhang K, Kaufman RJ. The unfolded protein response--a stress signaling pathway of the endoplasmic reticulum. *J Chem Neuroanat.* 2004 Sep;28(1-2):79-92.

28. Parikh BA, Tortora A, Li XP, Tumer NE. Ricin inhibits activation of the unfolded protein response by preventing splicing of the HAC1 mRNA. *J Biol Chem.* 2008 Jan 7.

29. Kimata Y, Kimata YI, Shimizu Y, Abe H, Farcasanu IC, Takeuchi M, et al. Genetic evidence for a role of BiP/Kar2 that regulates Ire1 in response to accumulation of unfolded proteins. *Mol Biol Cell.* 2003 Jun;14(6):2559-69.

30. Alder NN, Shen Y, Brodsky JL, Hendershot LM, Johnson AE. The molecular mechanisms underlying BiP-mediated gating of the Sec61 translocon of the endoplasmic reticulum. *J Cell Biol.* 2005 Jan 31;168(3):389-99.

31. Iordanov MS, Pribnow D, Magun JL, Dinh TH, Pearson JA, Chen SL, et al. Ribotoxic stress response: Activation of the stress-activated protein kinase JNK1 by inhibitors of the peptidyl transferase reaction and by sequence-specific RNA damage to the alpha-sarcin/ricin loop in the 28S rRNA. *Mol Cell Biol.* 1997 Jun;17(6):3373-81.

32. Urano F, Bertolotti A, Ron D. IRE1 and efferent signaling from the endoplasmic reticulum. *J Cell Sci.* 2000 Nov;113 Pt 21:3697-702.

33. Harding HP, Zhang Y, Bertolotti A, Zeng H, Ron D. Perk is essential for translational regulation and cell survival during the unfolded protein response. *Mol Cell.* 2000 May;5(5):897-904.

34. Audi J, Belson M, Patel M, Schier J, Osterloh J. Ricin poisoning: A comprehensive review. *JAMA.* 2005 Nov 9;294(18):2342-51.

35. Soler-Rodriguez AM, Ghetie MA, Oppenheimer-Marks N, Uhr JW, Vitetta ES. Ricin A-chain and ricin A-chain immunotoxins rapidly damage human endothelial cells: Implications for vascular leak syndrome. *Exp Cell Res.* 1993 Jun;206(2):227-34.

36. Baluna R, Coleman E, Jones C, Ghetie V, Vitetta ES. The effect of a monoclonal antibody coupled to ricin A chain-derived peptides on endothelial cells in vitro: Insights into toxin-mediated vascular damage. *Exp Cell Res.* 2000 Aug 1;258(2):417-24.

37. Challoner KR, McCarron MM. Castor bean intoxication. *Ann Emerg Med.* 1990 Oct;19(10):1177-83.

38. Bigalke H, Rummel A. Medical aspects of toxin weapons. *Toxicology*. 2005 Oct 30;214(3):210-20.
39. Griffiths GD, Lindsay CD, Allenby AC, Bailey SC, Scawin JW, Rice P, et al. Protection against inhalation toxicity of ricin and abrin by immunisation. *Hum Exp Toxicol*. 1995 Feb;14(2):155-64.
40. Roy CJ, Hale M, Hartings JM, Pitt L, Duniho S. Impact of inhalation exposure modality and particle size on the respiratory deposition of ricin in BALB/c mice. *Inhal Toxicol*. 2003 May;15(6):619-38.
41. Fodstad O, Johannessen JV, Schjerven L, Phil A. Toxicity of abrin and ricin in mice and dogs. *J Toxicol Environ Health*. 1979(5):1073-84.
42. Godal A, Fodstad O, Ingebrigtsen K, Pihl A. Pharmacological studies of ricin in mice and humans. *Cancer Chemother Pharmacol*. 1984;13(3):157-63.
43. Fine DR, Shepherd HA, Griffiths GD, Green M. Sub-lethal poisoning by self-injection with ricin. *Med Sci Law*. 1992 Jan;32(1):70-2.
44. Griffiths GD, Bailey SC, Hambrook JL, Keyte MP. Local and systemic responses against ricin toxin promoted by toxoid or peptide vaccines alone or in liposomal formulations. *Vaccine*. 1998 Mar;16(5):530-5.
45. Kende M, Yan C, Hewetson J, Frick MA, Rill WL, Tammariello R. Oral immunization of mice with ricin toxoid vaccine encapsulated in polymeric microspheres against aerosol challenge. *Vaccine*. 2002 Feb 22;20(11-12):1681-91.
46. Kende M, Del Giudice G, Rivera N, Hewetson J. Enhancement of intranasal vaccination in mice with deglycosylated chain A ricin by LTR72, a novel mucosal adjuvant. *Vaccine*. 2006 Mar 15;24(12):2213-21.
47. Lemley PV, Wright DC. Mice are actively immunized after passive monoclonal antibody prophylaxis and ricin toxin challenge. *Immunology*. 1992 Jul;76(3):511-3.
48. Wang Y, Guo L, Zhao K, Chen J, Feng J, Sun Y, et al. Novel chimeric anti-ricin antibody C4C13 with neutralizing activity against ricin toxicity. *Biotechnol Lett*. 2007 Dec;29(12):1811-6.
49. Smallshaw JE, Richardson JA, Vitetta ES. RiVax, a recombinant ricin subunit vaccine, protects mice against ricin delivered by gavage or aerosol. *Vaccine*. 2007 Oct 16;25(42):7459-69.
50. Vitetta ES, Smallshaw JE, Coleman E, Jafri H, Foster C, Munford R, et al. A pilot clinical trial of a recombinant ricin vaccine in normal humans. *Proc Natl Acad Sci U S A*. 2006 Feb 14;103(7):2268-73.

51. Allen SC, Byron A, Lord JM, Davey J, Roberts LM, Ladds G. Utilisation of the budding yeast *saccharomyces cerevisiae* for the generation and isolation of non-lethal ricin A chain variants. *Yeast*. 2005 Dec;22(16):1287-97.
52. Kitaoka Y. Involvement of the amino acids outside the active-site cleft in the catalysis of ricin A chain. *Eur J Biochem*. 1998 Oct 1;257(1):255-62.
53. O'Hare M, Roberts LM, Thorpe PE, Watson GJ, Prior B, Lord JM. Expression of ricin A chain in *escherichia coli*. *FEBS Lett*. 1987 May 25;216(1):73-8.
54. Munishkin A, Wool IG. Systematic deletion analysis of ricin A-chain function. single amino acid deletions. *J Biol Chem*. 1995 Dec 22;270(51):30581-7.
55. Frankel A, Welsh P, Richardson J, Robertus JD. Role of arginine 180 and glutamic acid 177 of ricin toxin A chain in enzymatic inactivation of ribosomes. *Mol Cell Biol*. 1990 Dec;10(12):6257-63.
56. Morris KN, Wool IG. Determination by systematic deletion of the amino acids essential for catalysis by ricin A chain. *Proc Natl Acad Sci U S A*. 1992 Jun 1;89(11):4869-73.
57. Morris KN, Wool IG. Analysis of the contribution of an amphiphilic alpha-helix to the structure and to the function of ricin A chain. *Proc Natl Acad Sci U S A*. 1994 Aug 2;91(16):7530-3.
58. Hudak KA, Hammell AB, Yasenchak J, Tumer NE, Dinman JD. A C-terminal deletion mutant of pokeweed antiviral protein inhibits programmed +1 ribosomal frameshifting and Ty1 retrotransposition without depurinating the sarcin/ricin loop of rRNA. *Virology*. 2001 Jan 5;279(1):292-301.
59. Baykal U, Tumer NE. The C-terminus of pokeweed antiviral protein has distinct roles in transport to the cytosol, ribosome depurination and cytotoxicity. *Plant J*. 2007 Mar;49(6):995-1007.
60. Meusser B, Hirsch C, Jarosch E, Sommer T. ERAD: The long road to destruction. *Nat Cell Biol*. 2005 Aug;7(8):766-72.
61. Nishikawa SI, Fewell SW, Kato Y, Brodsky JL, Endo T. Molecular chaperones in the yeast endoplasmic reticulum maintain the solubility of proteins for retrotranslocation and degradation. *J Cell Biol*. 2001 May 28;153(5):1061-70.
62. Romisch K. Surfing the Sec61 channel: Bidirectional protein translocation across the ER membrane. *J Cell Sci*. 1999 Dec;112:4185-91.
63. Lenk U, Yu H, Walter J, Gelman MS, Hartmann E, Kopito RR, et al. A role for mammalian Ubc6 homologues in ER-associated protein degradation. *J Cell Sci*. 2002 Jul 15;115(Pt 14):3007-14.

64. Hirsch C, Jarosch E, Sommer T, Wolf DH. Endoplasmic reticulum-associated protein degradation--one model fits all? *Biochim Biophys Acta*. 2004 Nov 29;1695(1-3):215-23.
65. Wilkinson BM, Critchley AJ, Stirling CJ. Determination of the transmembrane topology of yeast Sec61p, an essential component of the endoplasmic reticulum translocation complex. *J Biol Chem*. 1996 Oct 11;271(41):25590-7.
66. Heinemeyer W, Gruhler A, Mohrle V, Mahe Y, Wolf DH. PRE2, highly homologous to the human major histocompatibility complex-linked RING10 gene, codes for a yeast proteasome subunit necessary for chymotryptic activity and degradation of ubiquitinated proteins. *J Biol Chem*. 1993 Mar 5;268(7):5115-20.
67. Simpson JC, Roberts LM, Romisch K, Davey J, Wolf DH, Lord JM. Ricin A chain utilises the endoplasmic reticulum-associated protein degradation pathway to enter the cytosol of yeast. *FEBS Lett*. 1999 Oct 1;459(1):80-4.
68. Lord JM, Deeks E, Marsden CJ, Moore K, Pateman C, Smith DC, et al. Retrograde transport of toxins across the endoplasmic reticulum membrane. *Biochem Soc Trans*. 2003 Dec;31(Pt 6):1260-2.
69. Baykal U, Tumer NE. The C-terminus of pokeweed antiviral protein has distinct roles in transport to the cytosol, ribosome depurination and cytotoxicity. *Plant J*. 2007 Mar;49(6):995-1007.
70. Suhan ML, Hovde CJ. Disruption of an internal membrane-spanning region in shiga toxin 1 reduces cytotoxicity. *Infect Immun*. 1998 Nov;66(11):5252-9.
71. LaPointe P, Wei X, Garipey J. A role for the protease-sensitive loop region of shiga-like toxin 1 in the retrotranslocation of its a domain from the endoplasmic reticulum lumen. *JBC*. 2005 June 17;280(24):23310-23318.
72. Simpson JC, Lord JM, Roberts LM. Point mutations in the hydrophobic C-terminal region of ricin A chain indicate that Pro250 plays a key role in membrane translocation. *Eur J Biochem*. 1995 Sep 1;232(2):458-63.
73. Chaddock JA, Roberts LM, Jungnickel B, Lord JM. A hydrophobic region of ricin A chain which may have a role in membrane translocation can function as an efficient noncleaved signal peptide. *Biochem Biophys Res Commun*. 1995 Dec 5;217(1):68-73.
74. Parikh BA, Baykal U, Di R, Tumer NE. Evidence for retro-translocation of pokeweed antiviral protein from endoplasmic reticulum into cytosol and separation of its activity on ribosomes from its activity on capped RNA. *Biochemistry*. 2005 Feb 22;44(7):2478-90.
75. Lin JH, Li H, Yasumura D, Cohen HR, Zhang C, Panning B, et al. IRE1 signaling affects cell fate during the unfolded protein response. *Science*. 2007 Nov 9;318(5852):944-9.

Curriculum Vitae

Education

Graduate School, Rutgers University, New Brunswick, NJ	2002-2008
Ph.D. candidate, Microbiology and Molecular Genetics	
 Rutgers College, Rutgers University, New Brunswick, NJ	 1998-2002
B.S. Genetics	

Research Positions

Graduate Student	2002-2008
Rutgers University, New Brunswick, NJ	
 Undergraduate Research Assistant	 2000-2002
Rutgers University, New Brunswick, NJ	
 Clinical Research Documenter	 1997-1998
Novartis Pharmaceuticals, East Hanover, NJ	

Teaching Experience

Teaching Assistant-Rutgers University	fall 2007
<i>Instruct laboratory exercises in Methods in Recombination DNA Technology (5 contact hours/week)</i>	
 Douglass Project Graduate Fellow /Advisor	 2007-2008
<i>Provide Douglass Residential College students with general advising in STEM fields at Rutgers University.</i>	
 Douglass Summer Institute Instructor	 2007
<i>Taught a variety of science lessons for high school girls, including dissections, forensics and the cardiovascular system.</i>	
 Douglass Weekend Academy	 2007
<i>Instructed high school girls on the methods of DNA isolation and forensics.</i>	
 NSF GK-12 Fellow	 2004-2007
<i>Developed and implemented hands-on enrichment lessons for earth, life and physical sciences, and mathematics, pre-algebra and algebra at the middle school level. Also served as an instructor for middle school students aboard the Rutgers Science Explorer, a mobile science laboratory serving the state of NJ. Trained other graduate student fellows to present activities on the Rutgers Science Explorer .</i>	

Mad Science Presenter**1998-1999**

Presented science experiments for local boy-scout troops.

Publications

Baricevic, M and Tumer, NE. 2007. *The C-terminus of ricin A chain is essential for cytotoxicity.* Northeast Biodefense Center Fourth Annual Retreat. West Point, New York.

Baricevic M, Li XP, Saidasan H and Tumer NE. 2007. *Ribosome depurination is not sufficient for ricin mediated cell death.* Infect Immun. 75(1):417-28

Baricevic M, Li XP, Parikh B, Saidasan H and Tumer NE. 2006. *Ribosome depurination and translation inhibition are not sufficient for ricin mediated cell death.* Northeast Biodefense Center Third Annual Retreat, program p 83. Lake George, New York.

Cohick W, Jetzt A, Cheng J, Leibowitz B, Baricevic M and Tumer N. 2006. *Molecular mechanisms of ricin-induced apoptosis in mammalian cells.* Northeast Biodefense Center Third Annual Retreat, program p 83. Lake George, New York.

Baricevic M and Tumer NE. *Analysis of the cytotoxicity of ricin A chain in yeast.* 2005 American Society for Virology 24th Annual Meeting, program p211. The Pennsylvania State University, University Park, Pennsylvania.

Hudak KA, Parikh BA, Di R, Baricevic M, Santana M, Seskar M and Tumer NE. 2004. *Generation of pokeweed antiviral protein mutations in Saccharomyces cerevisiae: evidence that ribosome depurination is not sufficient for cytotoxicity.* Nucleic Acids Research. 32(14):4244-56.